Master's thesis

NTNU
Norwegian University of Science and Technology
Faculty of Information Technology and Electrical Engineering
Department of Electric Energy

Mohammed Abdulkadir Younas Aljahaf

Study of rail potential and earth current for the BTRC and AT systems

Master's thesis in Electric Power Engineering
Supervisor: Hans Kristian Høidalen, IEL
Co-supervisor: Bente Langeland Roheim, Bane NOR SF
June 2023

NTNU
Norwegian University of Science and Technology

BANE NOR

Mohammed Abdulkadir Younas Aljahaf

Study of rail potential and earth current for the BTRC and AT systems

Master's thesis in Electric Power Engineering
Supervisor: Hans Kristian Høidalen, IEL
Co-supervisor: Bente Langeland Roheim, Bane NOR SF
June 2023

Norwegian University of Science and Technology
Faculty of Information Technology and Electrical Engineering
Department of Electric Energy

NTNU
Norwegian University of
Science and Technology

Problem Description

AC traction feeding systems as the booster transformer (BT) and the autotransformer (AT) systems, were introduced early in Norway. In addition to the benefits of the BT and AT systems, such as protection against the induction effect and voltage stability, these systems also have some challenges. The rail potential and earth current levels in the return circuit are one of these challenges. These voltages and currents can be dangerous for people or cause damage to neighbouring equipment or material if they are not according to the relevant standards.

The main goal of this thesis is to study the rail potential and earth current levels in the return circuit for the BT and AT systems. This thesis will study the effect of rail-to-earth leakage conductance (gE), train position on the track line, and transformer spacing between BTs and ATs on the rail potential and earth current levels. The ATPDraw program will be used to simulate these systems during normal operation and short-circuit conditions. It will also carry out a comparison between the BT and AT systems, with a focus on the levels of rail potential and earth current.

For verification purposes, the results of this thesis will be compared to other studies' results. The results will also be verified with the relevant regulations and standards.

Hypotheses:

- BT system: maximum rail potential and earth current levels occur when the load (train or short circuit) is at the first or last booster transformer (BT) nearest the feeding station.
- AT system: maximum rail potential and earth current levels occur when the load (train or short circuit) is in the middle of the track line between two autotransformers (ATs).
- Rail-to-earth leakage conductance (gE) affects the rail potential and earth current levels. Increased rail-to-earth leakage conductance (gE) decreases the rail potential and increases the earth current.
- Increased spacing between booster transformers (BTs) for the BT system and autotransformers (ATs) for the AT system increases the rail potential and earth current levels.
- The rail potential and earth current levels for the BT and AT systems are not identical.

Abstract

This master's thesis studied AC traction feeding systems in Norway and compared the BTRC and AT systems. Particularly, rail potential and earth current levels in the return circuit were studied since these can be dangerous for people or cause damage to neighbouring equipment.

This thesis used the ATPDraw program to simulate the BTRC and AT systems. In preparation for the simulation, the necessary values of series impedances were calculated and verified in the ATPDraw program. Four models were simulated in this thesis: two for the BTRC system with 3 km and 6 km spacing between booster transformers and two for the AT system with 12 km and 14 km spacing between autotransformers. The parameters of the models were the levels of rail-to-earth leakage conductance (gE), train position on the track line, and the spacing between booster transformers (BTs) and autotransformers (ATs). The study was divided into three case studies: Case Study 1 was conducted during normal operation and had the train position and gE (0.05 S/km - 2 S/km) as parameters. The transformer spacing in Case Study 1 is 3 km for the BTRC system and 12 km for the AT system. Case Study 2 is varied transformer spacing between BTs to 6 km and ATs to 14 km. Case Study 3 was during short-circuit conditions and had gE and spacing between BTs (3 km and 6 km) and ATs (12 km and 14 km) as parameters.

For the BTRC system, it was observed that the maximum levels of rail potential and earth current occur when the train is at the first or last booster transformer, while for the AT system, they occur when the train is in the middle of the track line between two ATs. It was also observed that the rail potential levels decreased while the earth current levels increased when the gE levels varied from 0.05 S/km to 2 S/km. Further, increased spacing between BTs and ATs increases the rail potential and earth current levels. For example, during normal operation, the rail potential levels of AT system (12 km) decreased by a factor of 0.29, while the earth current levels increased by 6.75 when gE varied from 0.05 S/km to 2 S/km. The rail potential and earth current levels increased by a factor of 1.1 when the spacing between autotransformers increased from 12 km to 14 km.

Varju has many studies on the Norwegian feeding systems, such as comparisons of the BTRR, BRTC, and AT systems and investigations of the AT system and the combination of the BT and AT systems. Therefore, the thesis results were compared to Varju's results for verification purposes. The comparison shows that the thesis results agreed with these, with some variations due to the different simulation methods and data used in this thesis.

Furthermore, the results of the rail potential were verified by the EN 50122-1 standard. Most of the rail potential results met the EN 50122-1 requirements except for some values at low levels of gE, especially at 0.05 S/km. For earth current levels, there is no requirement for the permissible levels of current in the return circuit. Earth current results can be useful for other studies, such as EMC management plan and induction effects on neighbouring lines and systems.

The results showed that levels of gE, train position, and transformer spacing have a significant effect on the rail potential and earth current levels. It also showed that transformer spacing can be increased from the recommended spacing by Bane NOR's technical regulations, which is 3 km for the BT system and 10 km for the AT system (single-track line).

Finally, the ATPDraw program provided a good possibility to simulate the AC traction feeding systems, but it was necessary to assume some simulation methods and values. For example, it was assumed that the gE and rail impedance were constant values for the whole system.

Abstract (Norwegian)

Denne oppgaven studerte AC forsyningssystemer i Norge og sammenlignet BTRC- og AT-systemene. Spesifikt ble skinnepotensialet og strømmen i jordsmonnet i returkretsen studert siden disse kan være farlige for mennesker eller forårsake skade på utstyr.

Denne oppgaven brukte ATPDraw-programmet til å simulere BTRC- og AT-systemene. Som forberedelse til simuleringen ble de nødvendige serieimpedanser beregnet og verifisert i ATPDraw-programmet. Fire modeller ble simulert i denne oppgaven: to for BTRC-systemet med 3 km og 6 km avstand mellom sugetransformatorer og to for AT-systemet med 12 km og 14 km avstand mellom autotransformatorer. Parameterne til modellene var nivåene for avledningskonduktansen (gE), togets posisjon på strekningen og avstanden mellom sugetransformatorer (BT-er) og autotransformatorer (AT-er). Studien ble delt inn i tre deler: Del 1 var ved driftsstrøm og hadde togets posisjon og gE (0.05 S/km - 2 S/km) som parametere. Avstanden mellom transformatorene for del 1 er 3 km for BTRC-systemet og 12 km for AT-systemet. Del 2 varierte dessuten økt avstand mellom BT-er til 6 km og AT-er til 14 km. Del 3 var ved kortslutningsstrøm og hadde gE og avstand mellom BT-er (3 km og 6 km) og AT-er (12 km og 14 km) som parametere.

For BTRC-systemet ble det observert at de maksimale skinnepotensialet og strømmen i jordsmonnet oppstår når toget er ved den første eller siste sugetransformatoren, mens de for AT-systemet oppstår når toget er på midt av strekningen mellom to autotransformatorer. Det ble også observert at skinnepotensialet reduserte mens strømmen i jordsmonnet økte når avledningskonduktansen (gE) varierte fra 0.05 S/km til 2 S/km. Videre økning av avstanden mellom BT-er og AT-er gir økt skinnepotensialet og strømmen i jordsmonnet nivåer. For eksempel, ved driftsstrøm, skinnepotensialet til AT-systemet (12 km) reduserte med en faktor på 0.29, mens strømmen i jordsmonnet økte med 6.75 når gE varierte fra 0.05 S/km til 2 S/km. Skinnepotensialet og strømmen i jordsmonnet økte med en faktor på 1.1 når avstanden mellom autotransformatorene økte fra 12 km til 14 km.

Varju har mange studier på de norske forsyningssystemene som sammenligner mellom BTRR-, BTRC- og AT-systemene og undersøkelser av AT-systemet og kombinasjon av BT- og AT-systemene. Derfor sammenlignet oppgavens resultater med Varjus resultater for verifikasjonsformål. Sammenligningen viser at oppgavens resultater hadde et godt samsvar med disse, med en viss variasjon på grunn av de forskjellige simuleringsmetodene og data som ble brukt i denne oppgaven.

Videre ble resultatene av skinnepotensialet verifisert i samsvar med EN 50122-1 standarden. De fleste resultatene av skinnepotensialet oppfylte EN 50122-1 kravene bortsett fra noen verdier ved lave nivåer av gE, spesielt ved 0.05 S/km. For strømmen i jordsmonnet, er det ingen krav til nivåer av strømmen i returkretsen. Resultatene av strømmen i jordsmonnet kan være nyttige for andre studier som for eksempel EMC-plan og induksjonseffekt på nabolinjer og systemer.

Resultatene viste at gE nivåer, togets posisjon og avstanden mellom transformatorene har en betydelig effekt på nivåene av skinnepotensialet og strømmen i jordsmonnet. De viste også at avstanden mellom transformatorene kan økes fra anbefalte avstander i Bane NORs tekniske regelverk, som er 3 km for BT-systemet og 10 km for AT-systemet (enkeltspor).

Til slutt, ga ATPDraw-programmet en god mulighet til å simulere AC forsyningssystemene, men det var nødvendig å anta noen simuleringsmetoder og verdier. For eksempel, ble det antatt at gE og skinneimpedansen var konstante verdier for hele systemet.

Preface

This master's thesis was written at the Department of Electric Energy at the Norwegian University of Science and Technology (NTNU), Trondheim. The master's thesis was carried out during the spring semester of 2023 in collaboration with Bane NOR SF to study the rail potential and earth current in the return circuit for the BTRC and AT systems.

I wish to thank my supervisor, Professor Hans Kristian Høidalen from NTNU, for his guidance and relevant literature. Thank you for sharing your knowledge about railway systems and the ATPDraw software program. I would like to thank my co-supervisor, Bente Langeland Roheim from Bane NOR SF, for her feedback, sharing of her knowledge, and relevant documentation.

I wish to thank my colleagues at Bane NOR SF for their support throughout this master's program.

I would like to thank my family for supporting me throughout my educational journey. Thank you for supporting me through good and bad days.

Finally, I dedicate this thesis to my father, who taught me and always influenced me in his short time here on earth.

Mohammed Abdulkadir Younas Aljahaf

Trondheim, June 2023

Table of Contents

List of Figures

List of Tables

List of Abbreviations

AC	Alternating Current
AT	Autotransformer
ATBT	Combined of AT system and BT system
ATP	Alternative Transient Program
BCTRAN	Transformer model in ATPDraw program
BT	Booster Transformer
BTRC	Booster Transformer with Return Conductor
BTRR	Booster Transformer Rial Return
CUS	Current Unbalance Suppression
DC	Direct Current
EMC	Electromagnetic compatibility
FEF	Regulations on electrical supply facilities
GUI	Graphical User Interface
LCC analysis	Life Cycle Cost analysis
LCC component	Line Constant or Cable Constants/Parameter component
NF	Negative Feeder
NEK	Norwegian Electrotechnical Committee
OCL/CL	Overhead Contact Line
PF	Positive Feeder
R	Running Rail
RC	Return Conductor
RR	Rail Return
RMS	Root Mean Square
TRV	Bane NOR's technical regulations
TSI	Technical Specification for Interoperability

1 Introduction

1.1 Background and Motivation

Electrification of the railway helps to get high-speed trains, reduces noise pollution, and reduces CO2 emissions. These advantages will develop the railway infrastructure, but electrification also has disadvantages, such as the induction effect and dangerous voltages for people and equipment. Therefore, it is crucial to select the appropriate traction feeding system according to the relevant technical regulations and requirements.

In Norway, the booster transformer (BT) system was introduced due to its good protection against the induction effect [1]. An alternative system called the autotransformer (AT) system was also introduced later in 2011 on the Ofoten Line (Ofotbanen). The AT system provides better voltage stability and has the capability to supply heavy and high-speed trains [1].

BT and AT systems have many challenges, such as levels of rail potential and earth current in the return circuit, which can cause an induction effect on neighbouring lines such as signalling and telecommunications (S&T) lines. These voltages and currents can also affect the track line's touch voltage level. The touch voltage might be dangerous to the equipment and people near the track line if it is higher than the permissible levels that are given in the relevant standards.

Rail potential and earth current levels depend on earth resistivity, rail-to-earth leakage conductance (gE), series impedance of the return circuit, load current, and the spacing between booster transformers (BTs) in the BT system and between autotransformers (ATs) in the AT system. Train position on the track line also affects the level of these voltages and currents. Therefore, this study will investigate the effects of rail-to-earth leakage conductance (gE), train position on the track line, and the spacing between BTs and between ATs. It is also necessary to ensure that the rail potential and earth current results in accordance with the relevant regulations and standards.

There are some studies, such as Høidalen's study [2] and Svendsen's master thesis [3] used the ATPDraw program to simulate AC traction feeding systems. Høidalen studied the current distribution in the AT system and induced voltages in the parallel cables. Svendsen studied the rail potential and earth current levels during normal operation for the BTRC and AT systems. This thesis will also use the ATPDraw program to simulate the AC traction feeding systems.

There are also other studies by Varju [1, 4, 5] for AC traction feeding systems. Varju studied the spacing of booster transformers, the levels of rail potential and earth current, the induction effect, and other studies about the AT system or the combination of the BT and AT systems in Norway. The results of this thesis will be compared to Varju's study results for verification purposes.

1.2 Summary of the specialization project

Section 1.2 is based on the specialization project [6]. In the autumn of 2022, I worked on the specialization project as part of the master's program in Electric Power Engineering. The project aimed to compare the rotary and static frequency converter stations in the Norwegian railway system. The comparison was in two parts. The first part was about how to dimension the frequency converter stations, while the other part was about the technical and economic factors that affect the procurement of frequency converter stations [6].

The project began with an introduction to the history of AC railway electrification, traction feeding systems, and frequency converter technologies. Relevant theories, regulations, and requirements for the dimension and procurement of frequency converter stations were also introduced.

Rotary and static frequency converter stations were simulated using the ATPDraw program. In the project, a load flow analysis was introduced to verify the operation of frequency converter stations.

The results of dimensioning the rotary and static frequency converter stations were satisfactory when there was no load (train) on the track line. In the case of load (train) on the track line, the load distribution between the frequency converter stations was not optimal because the overhead contact line (OCL) system was introduced into the model as an impedance, and the harmonic effect was negligible. The results can be improved by detailing the OCL model and modelling the regulation of the amplitude and phase angle of output voltage for the frequency converter stations.

The technical and economic factors of frequency converter station procurement were evaluated by using literature, Bane NOR's technical reports, and an LCC analysis.

According to the technical evaluation results rotary converter station can manage a higher overload and provide a higher short-circuit current than the static converter station. According to the economic evaluation results, the investment and renewal costs of rotary converter stations

are less costly than static converter stations. The cost of operation and maintenance depends on the number of frequency converter units at the frequency converter station. The evaluation shows that operation and maintenance costs for one or three units at a rotary converter station are higher than for one or three units at a static converter station. On the other hand, the operation and maintenance costs for a static converter station with two units are higher than for a rotary converter station with two units. Further, the results show that electric losses and their costs are higher for rotary converter stations due to the high losses of rotary units such as motors and generators.

The power requirement of the track line between two stations also affects the procurement or selection of frequency converter technology. As a result, the static frequency converter is the recommended technology for track lines with high power requirements (above 10 MVA). Table 1-1 summarizes the results of technical and economic factors.

Table 1-1: Results of the technical and economic factors [6].

	Rotary converter station	**Static converter station**
Overload	Can manage higher overload than static converter station	Can manage lower overload than rotary converter station
Short circuit	High	Low
Investment costs	Low	High
Renewal costs	Low	High
Operation, and Maintenance Costs	One converter unit: High Two converter units: Low Three converter units: High	One converter unit: Low Two converter units: High Three converter units: Low
Electric losses and costs	High	Low

1.3 Software used in this thesis

This section is based on [7]. In 1999, the Norwegian University of Science and Technology (NTNU) developed the Alternative Transient Program (ATP) program. Previous versions of ATP did not include a graphical user interface (GUI). In later years, Hans Kristian Høidalen, László Prikler, and Francisco Peñaloza renamed the software ATPDraw and introduced a graphical user interface (GUI). To conduct the simulations in the ATPDraw, the program, solver, and plotter should be installed. ATPDraw latest version is 7.3, published in 2021.

ATPDraw can start the simulations from a steady state, as it will be used in this thesis. It also predicts the variables for the electric power networks as functions of time. In the time domain, the trapezoidal rule of integration is used to solve the differential equations of system components. For simpler components, non-zero initial conditions can be specified by the user

or determined automatically using the steady-state solution. ATP has several models, including cables, transmission lines, AC/DC sources, transformers, etc.

1.4 Structure of the report

Chapter 1 Introduction, describes the background and motivation of this master's thesis and summarizes the specialization project with a brief description of its aims, simulations, evaluations, and results. Further, it provides a presentation of the software used in this thesis.

Chapter 2 Technical Regulations and Requirements, describes the requirements to design the AC traction feeding systems in Norway and the requirements for permissible levels of rail potential. Further, it introduces other standards for which the levels of earth current can be beneficial.

Chapter 3 AC Traction Feeding Systems, presents the types of AC traction feeding systems that are introduced in Norway and provides an explanation of the effect of rail-to-earth leakage conductance, train position, and transformer spacing on the levels of rail potential and earth current.

Chapter 4 Conductor Arrangement of the BTRC and AT Systems, explains the earth resistivity and rail-to-earth leakage conductance. Further, it presents a method to calculate the series impedance of AC traction feeding system parameters.

Chapter 5 Simulation of AC Traction Feeding Systems, shows the method of representing the BTRC and AT systems in the ATPDraw program. Further, it introduces three case studies that are performed during normal operation and short-circuit conditions.

Chapter 6 Results of ATPDraw, presents the rail potential and earth current results for the BTRC and AT systems during normal operation and short circuit conditions.

Chapter 7 Discussion, provides a discussion for the findings of Chapter 6, compares the thesis results to Varju's results, and verifies the results in accordance with the relevant standards.

Chapter 8 Conclusion and Further Work, presents the most important conclusions and suggests further work for this thesis.

2 Technical Regulations and Requirements

Bane NOR's technical regulations [8], which are also known in Norwegian (Teknisk regelverk- "TRV"), are the tool that is used to design, construct, and dimension the state railway network in Norway. TRV is also used to ensure that maintenance is implemented correctly. TRV provides regulations to infrastructure such as low voltage and 22 kV, overhead contact line (OCL) systems, superstructure, telecommunications, signalling, etc. The following sections will provide an overview of the relevant requirements for designing an AC traction feeding system in Norway. It will additionally introduce rail potential and earth current requirements in the return circuit.

2.1 System requirements

The following system requirements are according to Bane NOR's technical regulations [8]:

- Nominal voltage and nominal frequency of traction feeding system: 15 000 V and 16.7 Hz, which is in accordance with NEK EN 50163:2004 Clause 4 [9] as referred by Energy Technical Specification for Interoperability, (ENE TSI) point 4.2.3 [10].

- Overhead contact line (OCL) systems: AT systems (2 x 15 000 V) and conventional systems (15 000 V) with or without booster transformers and return conductors are permitted.

- Spacing between booster transformers for the booster transformer (BT) system is approximately 3 km.

- Spacing between autotransformers for the autotransformer (AT) system can always be chosen up to 10 km for a single-track line and 15 km for a double-track line. The spacing can be increased if the levels of rail potential in the return circuit and the induced voltage of parallel lines are according to the relevant standards. Standards will be given in Section 2.2.

2.2 Return circuit of AC feeding systems

The AC railway feeding systems are dimensioned according to regulations on electrical supply facilities (FEF) [11], and the earthing system of the railway is dimensioned according to FEF § 8-6.

FEF § 8-6: *'' Installations must be designed so that available potential differences, touch voltages and currents in earth and earth conductors do not represent a danger to persons or the risk of damage to equipment or material.''*

Generally, a return circuit includes rails and other electrical conductors that handle return currents for trains between a source (feeding station) and a load (train or short circuit). Moreover, the return circuit is also the earth potential to which conductive parts, foundations, and earth electrodes near the track lines are connected. Therefore, it is necessary to ensure that rail potential is within specified limits to protect people and equipment from dangerously high touch voltages [12].

2.2.1 Touch voltage

NEK EN 50122-1 (Fixed installations, Electrical safety, earthing, and the return circuit, Part 1: Protective provisions against electric shock) is part of NEK 900: 2023 [13] and is applied to protect people from electric shock due to contact with exposed conductive parts in the railway infrastructure. NEK EN 50122-1 gives the requirements of the return circuit design in Clause 9. The requirements specify the permissible levels of touch voltage caused by the rail potential in the return circuit. Clause 9 also provides provisions to reduce the risks from touch voltages.

EN 50122-1 specifies the maximum permissible body voltages ($U_{b,\,max}$) as a function of time duration and the maximum permissible effective touch voltage ($U_{te,max}$) for long-term conditions ($t \geq 0.7$ s) and for short-term conditions ($t \leq 0.7$ s). According to the standard, the permissible effective touch voltage ($U_{te,\,max}$) during normal operation for a time up to 300 s is 65 V. For long-term (more than 300 s) loads such as train heating systems, the permissible effective touch voltage ($U_{te,\,max}$) is 60 V. The long-term value is not the design value because these loads have a lower current compared to the design train load.

In the case of a short circuit, Figure 2-1 shows typical characteristics of a short circuit near a feeding station with two-sided feeding. Until time t_1, the feeding stations (frequency converter stations) feed the short circuit from both sides. At t_1, the protective equipment of the nearest feeding station is disconnected. After t_1, the farthest away feeding station feeds the short circuit, and the protective equipment near this station has a delayed disconnection time to ensure

selectivity (discrimination). Therefore, a smaller short circuit current (I_2) remains connected until the disconnection time t_2 [14].

Since the Norwegian railway system has two-sided feeding, one will get a sequential disconnection of the fault current depending on the fault location [8]. The fastest disconnection of the highest current can be less than 0.1 s (t_1). The disconnection time can be longer in some cases, so the latest disconnection time of the lowest current contribution can be up to 0.3 s (t_2).

Typically, the disconnection time of 0.1 s is assumed for touch voltage calculations during short circuit conditions. The disconnection time of 0.3 s is also assumed for touch voltage calculations as a conservative assumption. The short circuit current of 0.3 s is assumed to be 33% of the design short circuit current. This assumption can be high and lead to oversizing [8]. More details about the short circuit current will be introduced in Section 5.1.

As shown in Table 2-1, EN 50122-1 standard specifies the permissible levels of $U_{te,\,max}$, and $U_{b,\,max}$ that shall not exceed at time of 0.1 s and 0.3 s. The body voltage requirements are met also if touch voltage is less than $U_{te,\,max}$ permissible levels. Table 2-1 assumes that the current path through the body is from one hand to both feet, including the additional resistance of shoes.

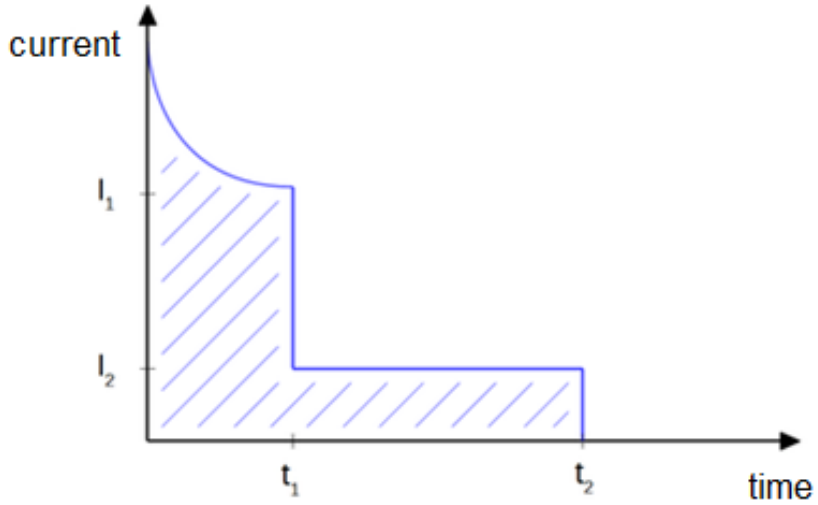

$t_1 = 0.1\ s \qquad t_2 = 0.3\ s$

Figure 2-1: Typical characteristics of a short circuit near a feeding station with two-sided feeding [8].

Table 2-1: $U_{te,\,max}$ and $U_{b,\,max}$ during normal operation and short circuit conditions [13].

Case	Requirements
During normal operation at t up to 300 s	$U_{te,\,max}$ = 65 V
During normal operation at t > 300 s	$U_{te,\,max}$ = 60 V
Short circuit at t = 0.1 s	$U_{b,\,max}$ = 345 V $U_{te,\,max}$ = 785 V
Short circuit at t = 0.3 s	$U_{b,\,max}$ = 230 V $U_{te,\,max}$ = 480 V

According to EN 50122-1 standard Annex D, the relation between rail potential (U_{RE}) and the voltage between the running rail and measuring point (U_{RP}) depends on the earth resistivity of the area and the distance between the exposed conductive parts and the measuring point. Figure 2-2 and Table 2-2 show the rail potential gradient measured for homogenous earth resistivity at an OCL pole where the running rails are directly earthed.

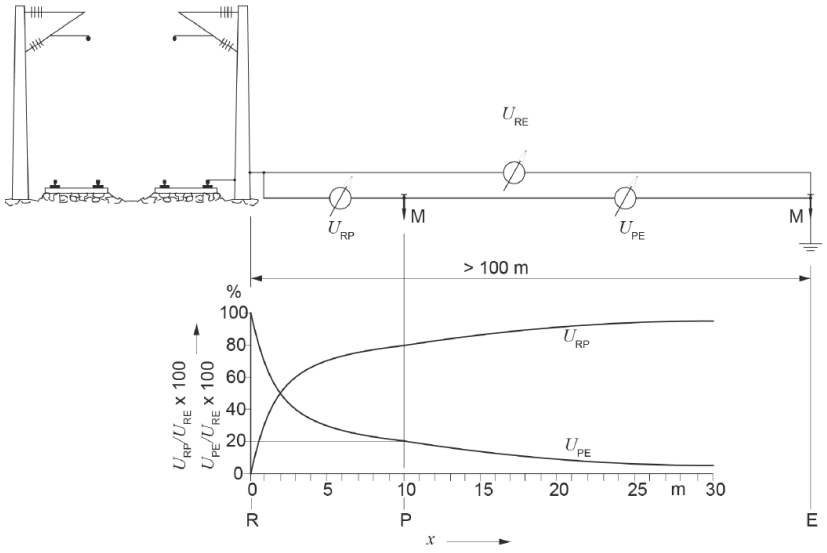

Figure 2-2: Rail potential gradient measured at an OCL pole [13].

X: Distance between running rail and measuring point.

E: Earth

R: Rail

M: Measuring electrode

P: Measuring point

U_{PE}: Voltage between measuring point and earth

U_{RP}: Voltage between the running rail and measuring point.

Table 2-2: Values for the rail potential gradient [13].

Distance to the expose conductive part	1 m	2 m	5 m	10 m	20 m	50 m	100 m
U_{RP} /U_{RE} x 100 (%)	30	50	70	80	90	95	100

2.3 Other Standards

There are standards about the impacts between various systems and equipment in the railway environment, such as EN 50121 (5 parts) [15]. However, the EN 50121 series of Electromagnetic Compatibility (EMC) do not provide satisfactory performance because of the moving sources of electromagnetic energy and the complexity of the railway systems. The list below gives the scope of each part of the EN 50121 standard:

- EN 50121 Part 1, General: The most important requirements in this part are EMC management plan. EMC-plan identifies the source of noise in the railway system and methods for reducing it. One of the challenges that EMC management plan handles is the current level in the return circuit.

- EN 50121 Part 2, Emission of the whole railway system to the outside world: This part outlines the whole railway system's emission limits to the outside world. It defines the EMC environment, including light rail and mass transit systems. Additionally, it includes the cartographic values for the most frequently encountered fields.

- EN 50121 Part 3-1, Rolling stock Train and complete vehicle: This part specifies the emission limit of all types of rolling stock to the outside world.

- EN 50121 Part 3-2, Rolling stock Apparatus: This part specifies limits and test methods for emission and immunity aspects of EMC for rolling stock. It gives the test requirements to conducted and radiated disturbances. Part 3-2 also specifies the requirements of signalling and telecommunications (S&T) apparatus mounted in vehicles.

- EN 50121 Part 4, Emission and immunity of the signalling and telecommunications apparatus: This part specifies the emission and immunity limitations of S&T apparatus placed inside the railway environment. It also applies to performance criteria for S&T apparatus that may raise total emissions for the railway environment or with other systems inside this environment.

The requirements for equipment, such as interlocking or command and control, are given in this part. EN 50121 Part 4 applies to equipment inside the 3 m zone, equipment inside the 10 m zone with a cable length of more than 30 m, and equipment inside the 10 m zone that is connected to other equipment inside the 3 m zone.

- EN 50121 Part 5, Emission and immunity of fixed power supply installations and apparatus: This part specifies emission and immunity limitations for electronic and electrical equipment that use in railway fixed installations, including power supply to the equipment, the equipment with its protective control circuits, and other equipment, such as switching stations, booster transformers, and power switchgear to supplies and substations.

3 AC Traction Feeding Systems

Chapter 3 introduces the design and components of the booster transformer (BT) and autotransformer (AT) systems. This chapter is based on my specialization project [6], Bane NOR's textbooks [12, 16], and Contact Lines for Electric Railways [17].

The Norwegian railway system consists of a power generation system (three-phase, 50 Hz) that supplies the feeding stations (frequency converter stations, single/two-phase, 16.7 Hz). The feeding stations feed the overhead contact line (OCL) with a rated voltage of 15 kV and a frequency of 16.7 Hz. The train gets its energy from the locomotive's pantograph, which is in contact with the overhead contact line (OCL). AC traction feeding systems are usually classified based on electrical and mechanical designs [6].

The traction feeding systems are classified depending on the type of transformer, such as booster transformers (BT) and autotransformers (AT). The selection between the BT and AT systems depends on some factors, such as the track line type (single or double), voltage stability, power capability, and induction effect on neighbouring lines (S&T lines) [1, 6].

The BT and AT systems have many electrical designs depending on how their components are designed and connected. In Norway, the electric systems classify as systems A, B, C, D, E, and F. There is also a combination of booster transformer and autotransformer (ATBT) systems.

The mechanical systems classify into many designs, such as systems S20, S25, and S35. The selection of these designs depends on speed, track line class, and the locomotive's pantograph configuration [6].

3.1 Booster Transformer (BT) system

Design of BT system

Booster transformer system has been introduced for single- and double-track lines in Norway. The main advantage of the BT system is that it protects against the high induction effect and coupling/mutual impedance caused by high earth resistivity. On the other hand, the BT system has a high equivalent impedance, which raises the voltage drop in the feed section. The series connection of booster transformers with contact lines is the reason for such high impedance.

For simulation purposes, Booster Transformer Return Conductor (BTRC) – Design C system is briefly presented in this section. For complementation, Design A[1], B, and D are also presented in Appendix 1.

As shown in Figure 3-1, the BTRC system Design C consists of a contact line (CL) and return conductors (RC). The contact line (CL) consists of a contact wire and a catenary wire. In this system, the return conductors are along the track line and connected to the rails at the midpoint between each two booster transformers. This connection between the return conductor and rails is called a bond. The return circuit of this system consists of earth, rails, booster transformers, and return conductors. The red arrows in Figure 3-1 indicate the path of the return current.

More details about the BTRC system conductors and their arrangement will be introduced in Chapter 4.

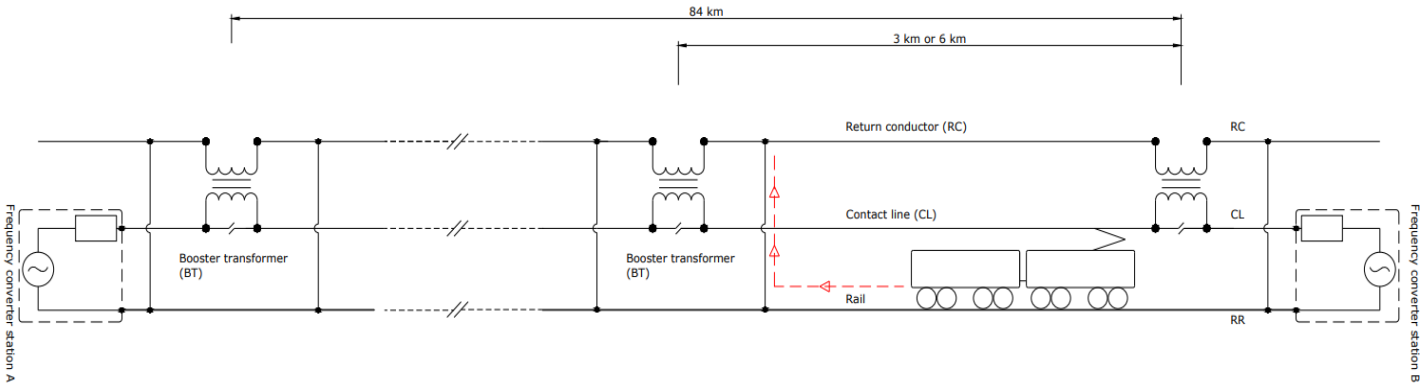

Figure 3-1: Booster Transformer system Design C. Figure adapted from [1].

Booster Transformer (BT)

The function of booster transformers in a BT system is to take the return current from the earth and the rails to the return conductors. It guarantees that all the return current flows in the return conductors. The booster transformer also reduces the voltage drop of the return circuit in the BT system. In other words, the booster transformer decreases the potential in the return circuit and the induced voltage in parallel telecommunications cables (if there are telecommunications cables along the track line).

Booster transformers are single-phase transformers with a ratio of 1:1. The rated voltage of BT is 15 kV which is the nominal voltage of the BT system. In Norway, 55 kVA (600 A nominal current) and 95 kVA (800 A nominal current) booster transformers are used. Appendix 2 shows

[1] Electric system Design A is without booster transformers.

the parameters data of a 95 kVA booster transformer. Figure 3-2 shows a simplified diagram of a booster transformer.

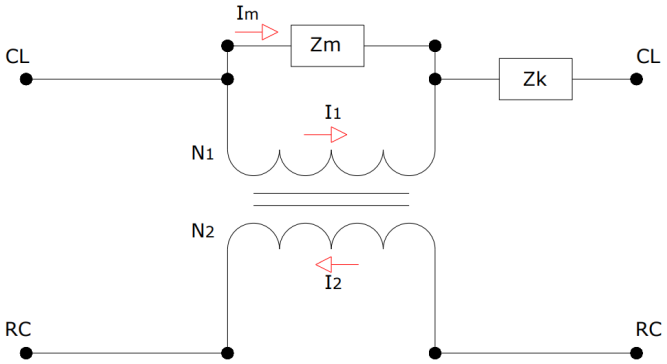

Figure 3-2: Simplified diagram of a booster transformer. Figure adapted from [12].

Parameter of Figure 3-2:

- N_1: Number of turns in the primary winding.
- N_2: Number of turns in the secondary winding.
- I_1: Current in the primary winding.
- I_2: Current in the secondary winding.
- I_m: Transformer magnetization current.
- Z_m: Transformer magnetization impedance.
- Z_k: Transformer short circuit impedance.

For BTRC system Design C, as shown in Figure 3-1, the primary winding of the booster transformer is connected in series with the contact line (CL), whereas the secondary winding is in series with the return conductors (RC). In Design D as shown in Appendix 1, there is a return conductor and zero-field point of the booster transformer. The midpoint of the secondary winding of the booster transformer is connected to the zero-rail point (the nearest rail). In other systems without return conductors, such as Design B as shown in Appendix 1, the secondary winding is connected in series to the rails over filter impedances.

The booster transformers are typically located outdoors on a platform between two overhead contact line poles. It can also be in a tunnel or a kiosk on the ground.

3.2 Autotransformer (AT) system

Design of AT system

AT system is the preferred system for the newly electrified track lines. The rated voltage level of the AT system, 30 kV doubles the rated voltage level of the BT system, 15 kV [6].

AT system has many advantages, such as voltage stability due to the high rated voltage level, enables long feed section, and thus will reduce the number of frequency converter stations. It can supply heavy trains and high-speed lines. AT system can have low induction levels if the distance between the autotransformers is selected appropriately. The AT system has a lower equivalent impedance than the BT system.

There are many designs of AT system, such as Design E using both negative and positive feeders (NF and PF), Design F using just negative feeder (NF), design using autotransformers system with power lines (established in Ofoten Line), and design using double negative feeders (2 x NF). Design E and F are the preferred systems according to Bane NOR's technical regulations [8]. For simulation purposes, AT system Design E is briefly presented in this section, while Design F is presented in Appendix 1.

The AT system Design E, as shown in Figure 3-3 consists of a contact line (CL), a positive feeder wire (PF), and a negative feeder wire (NF). The contact line (CL) consists of a contact wire and a catenary wire. The red arrows in Figure 3-3 indicate the path of the return current.

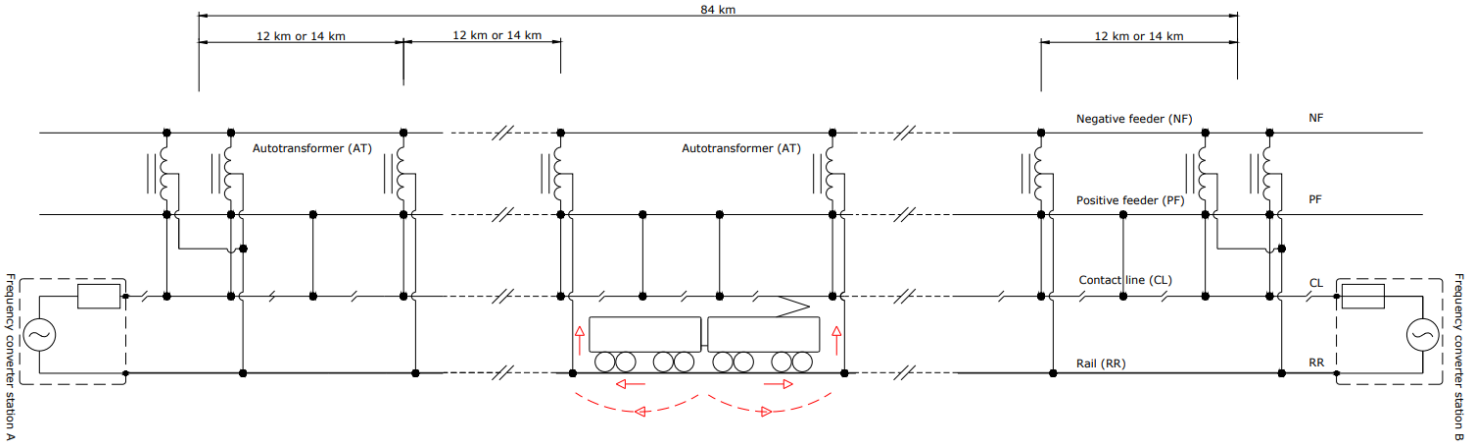

Figure 3-3: Autotransformer system Design E. Figure adapted from [5].

The benefit of Design E is that it enables continuous supply in a section while the catenary is out of operation due to maintenance or damage. However, due to the short circuit impedance of the autotransformer, the current is unbalanced in the PF-NF loop, and thus part of the current

is also flowing through the earth. This current can be reduced using the Current Unbalance Suppression (CUS) unit. In other words, the CUS unit reduces the noise on neighbouring parallel lines. Another alternative method proposed by Frank Martinsen, Bane NOR [16], is the AT system with a sectioned overhead contact line, as shown in Figure 3-3. The sectioning method gives the same function as the CUS unit, so there is no need for the CUS unit for Design E.

Other advantages of the AT system Design E according to [12]:

1. It provides better EMC conditions than the double negative feeder (2 x NF) system.
2. Provides satisfactory EMC conditions even if PF and NF feeders are placed differently than the preferred location on the top of overhead contact line poles.
3. Supply future train traffic using manageable conductor cross-sections.
4. Less complex than other systems with CUS units or booster transformers.
5. The costs are relatively low because there is no need for extra expensive components such as CUS units.

More details about the AT system conductors and their arrangement will be introduced in Chapter 4.

Autotransformer (AT)

The purpose of single-phase autotransformers in AC railways is to balance the voltage and current between the catenary and the earth. In other words, due to the low short circuit impedance of the autotransformer, the voltage between the positive feeder (PF) and the mid-point ("0- the return" in Figure 3-4) is equal to the voltage between the negative feeder (NF) and the mid-point ("0- the return" in Figure 3-4). The autotransformer takes the return current from the rails and earth to the negative feeder (NF), but it is not efficient as the booster transformer to take all the current. Therefore, part of the return current flows through the rails.

Figure 3-4 shows a simplified diagram of an autotransformer. The output voltage between the positive feeder/contact line (PF/CL) terminals and the negative feeder (NF) terminal is 30 kV, while the voltage between the PF/CL terminals and the midpoint (0- the return) is 15 kV. As shown in Figure 3-3, the terminals PF/CL are connected to the contact line (CL) and the positive feeder (PF), while terminal NF is connected to the negative feeder (NF). The 0-the return terminal is connected to the rails. The load (train) connects at the terminals PF/CL and the midpoint (0- the return).

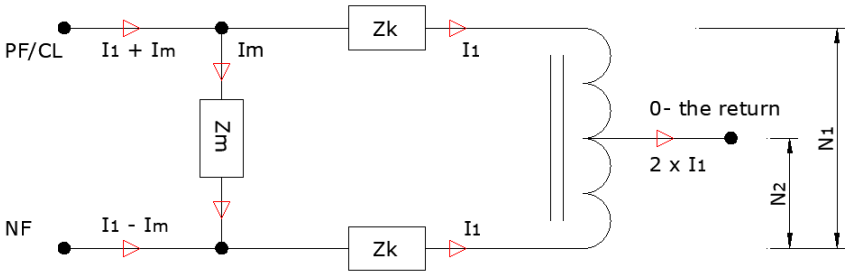

Figure 3-4: Simplified diagram of an autotransformer. Figure adapted from [18].

Parameter of Figure 3-4:

- N_1: Number of turns in the primary winding ($N_1 = 2 \times N_2$).
- N_2: Number of turns in the secondary winding.
- I_1: Current in the primary winding.
- I_2: Current in the centre terminal of the transformer ($2 \times I_1$).
- I_m: Transformer magnetization current.
- Z_m: Transformer magnetization impedance.
- Z_k: Transformer short circuit impedance.

The turn ratio (n) of the autotransformer is N_1/N_2:

$$n = \frac{N_1}{N_2} = \frac{I_2}{I_1} = \frac{2 \cdot I_1}{I_1} \qquad (3\text{-}1)$$

From equation (3-1), one can observe that the current between the PF/CL and NF terminals is always the same (I_1), while the current through terminal 0-the return is ($I_2 = 2 \times I_1$). In Norway, 5 MVA autotransformers are typically used. Appendix 2 shows the parameter data of 5 MVA autotransformers.

3.3 Rail potential and Earth current

3.3.1 Rail potential and earth current of BTRC system

The principle of the return circuit of the BTRC system depends on the train on the track line. If the train is on the track line at the booster transformer between two bonds, as shown in Figure 3-1, the return current will flow through the rail and the earth to the nearest bond. The return current will flow back to the feeding station (frequency converter station) through the return conductors. If there is no train on the track line between two bonds, most of the return current will flow back to the return conductors, and the rest will flow in the rails. This current consists of an induction current and magnetizing current. The rail potential occurs due to the current that

leaves the rails through the rail-to-earth leakage conductance [1, 12]. Moreover, the current flows through the booster transformers, which are located between the feeding stations and the load (train). When a train passes on the track, the pantograph momentarily short circuits the primary winding of the booster transformer. At the same time, the train's wheels short-circuit the secondary winding of the booster transformer. It is important to mention that the train's wheels should always short-circuit the secondary winding before the primary winding to avoid dangerous voltages (rail potential) at the insulation rail joints [12]. As a consequence, the rail potential is highest when the train is at the booster transformer near the feeding station.

For BTRC Design C, the increase in distance between booster transformers leads to a rise in rail-to-earth leakage conductance (gE), and thus increases the earth current. This earth current becomes the highest between two booster transformers. Therefore, the spacing between booster transformers cannot be decided until the rail-to-earth leakage conductance (gE) on the track line is measured [19]. It is also critical to ensure that the booster transformer is disconnected without any dangerous voltages arising along the track line. These increased voltages depend on rail potential, which is again determined by the series impedance of the return circuit and load current or short circuit current [12].

3.3.2 Rail potential and earth current of AT system

For the AT system, when the load (train) is between two autotransformers, as shown in Figure 3-3, the current through the rail-to-earth leakage conductance is taken by these two autotransformers. This current produce rail potential at the autotransformer location. When the train is located near an autotransformer, the rail potential will be reduced because the autotransformer will take most of the current that leaks through the earth. As a consequence, the rail potential is highest when the train is in the middle between two autotransformers.

The rail potential is affected by the spacing between autotransformers. Therefore, it is important to ensure that the rail potential (touch voltages) is according to standards in the case of increasing the spacing between the autotransformers.

For both the BT and AT systems, rail potential in the return circuit depends on:

- Train current or short circuit current.
- Earth resistivity
- Series impedance of the return circuit (rails and return conductors)
- Train position
- Rail-to-earth leakage conductance (gE), and transformer spacing between BTs and ATs

4 Conductor Arrangement of the BTRC and AT Systems

Electrical conductors in overhead contact line (OCL) systems are arranged in parallel with a common earth return. These parameters are represented by a complex matrix of series impedance (*Z*) and parallel admittance (*Y*):

$$Z = R + j X \tag{4-1}$$

$$Y = G + j B \tag{4-2}$$

R is the matrix of series resistance in (Ω/km), *X* is the matrix of series reactance in (Ω/km), *G* is the matrix of parallel conductance in (S/km), and *B* is the parallel matrix of susceptance in (S/km).

Earth resistivity and its effects on the OCL systems will be presented in Section 4.1. Admittance matrix (*Y*) will be introduced in Section 4.2 as a rail-to-earth leakage conductance (gE). Further, series impedance matrix (*Z*) of OCL parameters will be calculated in Section 4.3.

4.1 Earth resistivity

This section is based on literature [17, 20, 21]. Earth resistivity describes the earth's conductivity and depends on the earth's physical and chemical properties. Earth resistivity is a significant aspect of earthing installation design since it determines the earth resistance for foundations, earth electrodes, and earth systems. Earth resistivity is measured in Ωm.

The touch voltage is calculated using earth resistivity and the design values of the operating and short circuit currents. As described in Section 2.2, touch voltage levels should be within permissible limits to protect people from dangerous voltages. Moreover, the series impedance of OCL parameters is affected by earth resistivity because part of the return current flows through the earth, and the series impedance of conductor/earth loops depends on the depth of the earth current, which depends on earth resistivity as shown in the equations below:

$$D_e = 1.31 \cdot \sqrt{\frac{2\rho_e}{\omega \cdot \mu_0}} \quad (4\text{-}3)$$

$$D_e = 660\sqrt{\rho_e / f} \quad (4\text{-}4)$$

D_e is the penetration depth in m, ρ_e is earth resistivity in Ωm, f is the frequency (16.7 Hz), μ_0 is the permeability of free space ($4\pi \cdot 10^{-7}$ H/m), and $\omega = 2\pi f$.

The resistance and the resistivity of materials can be easily investigated, but it is more complex for earth due to its dimensions and the variety of its characteristics. There are some methods to measure earth resistivity, and the most frequent method is the four-point method, also called Wenner's method. Figure 4-1 shows the arrangement to measure earth resistivity according to Wenner's method. This method uses four rods arranged with the same spacing (a) and the rods depth (d) should be lower than 10% of the spacing (a). To measure the earth resistance (R_E), a current (I) is injected between the rods C1 and C2 then the voltage (V) can be measured between P1 and P2. Further, earth resistivity (ρ_e) can be calculated by the following equation:

$$\rho_e = 2\pi \cdot a \cdot R_E \quad (4\text{-}5)$$

a is the spacing between rods and R_E is the measured resistance as (V/I).

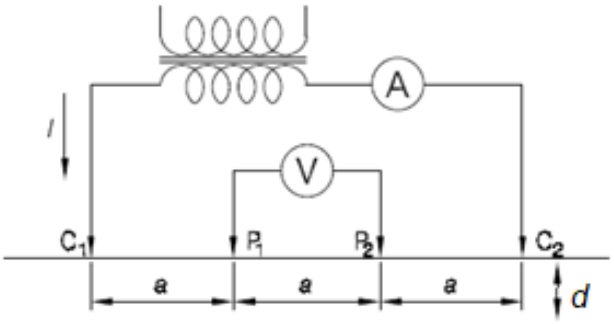

Figure 4-1: Arrangement to measure earth resistivity according to Wenner's method. Figure adapted from [17].

The earth resistance of foundations and earth electrodes such as strips, rings, or rods can be determined if one assumes that the earth is homogenous. EN 50522, Annex J [22] provides equations for each type of earth electrode to calculate the approximate earth resistance.

Resistance to earth of a meshed earth electrode:

$$R_E = \frac{\rho_e}{2D} \tag{4-6}$$

D is the diameter of the meshed earth electrode, and ρ_e is the earth resistivity in Ωm.

Resistance to earth of ring and strips earth electrode:

$$R_E = \frac{\rho_e}{\pi L} \ln \frac{2\,L}{d} \tag{4-7}$$

L is the length of the ring/strip in m and *d* is the diameter of ring in m. For strip, *d* is specified to half width of the strip. ρ_e is the earth resistivity in Ωm.

Resistance to earth of earth rods:

$$R_E = \frac{\rho_e}{2\pi L} \ln \frac{4L}{d} \tag{4-8}$$

L is the length of the rod in m, *d* is the diameter of the earth rod in m, and ρ_e is the earth resistivity in Ωm.

Table 4-1 shows the resistivity of different types of homogeneous soil. Earth resistivity depends on the soil type and decreases at high humidity, but this effect depends on the temperature. For example, the resistivity of humus-containing sand is approximately 100 Ωm at 20 °C to 3000 Ωm at -10 °C [20].

Table 4-1: Earth resistivities [22].

Type of soil	**Earth resistivity (ρ_e) in Ωm**
Marshy soil	5-40
Loam, clay, humus	20-200
Sand	200-2500
Gravel	2000-3000
Weathered rock	Mostly below 1000
Sandstone	2000-3000
Granite	Up to 50000
Moraine	Up to 30000

Section 4.3 will provide calculations of the series impedance for OCL parameters for earth resistivities of 100 Ωm, 2600 Ωm, and 5000 Ωm to show the effect of earth resistivity on the series impedance.

4.2 Rail-to-earth leakage conductance

As shown in equation (4-2), the parallel admittance matrix (Y) consists of the real part (G, the conductance) and the imaginary part (B, the susceptance). The susceptance (B) is the capacitive effect between the conductors and between the conductor and the earth, which is often negligible. B is frequency-dependent, as shown in the following equation:

$$B = \omega \cdot C \tag{4-9}$$

ω is the angular frequency of the voltage ($2\pi \cdot f$), and C is the capacitance matrix.

The conductance (G) is a diagonal matrix representing the connection between the conductors and the earth. The conductance (G) primarily represents the connection between the rails and the earth. This value is called rail-to-earth leakage conductance (gE).

Rail-to-earth leakage conductance (gE) reduces the dangerous voltage levels in the return circuit during normal operation and short-circuit conditions, and this contributes to keeping the touch voltage according to the requirements that are described in Section 2.2. gE is measured in S/km and depends on the surrounding earth (earth type and its resistivity), earth electrodes, and the design of foundations. The components and foundations that are connected to the track line increase the rail-to-earth leakage conductance (gE). Several works of literature, like [17, 21] and Bane NOR's literature study [8], shows that (gE) depends on:

- Components and their foundations that are connected to rails, such as OCL poles, low voltage components, signal components, tunnels, and station buildings.
- The along-track earth wires that are installed directly on the earth.
- Resistance to earth or earth resistivity and weather conditions (frost, humidity).
- Degree of pollution and type of superstructure such as sleepers (concrete or wood), track fasteners, track ballast, and insulating pads between rails and sleepers.

The equations (4-6), (4-7), and (4-8) can be utilized to estimate the resistance to earth (R_E) of earth electrodes. The resistance to earth value can be used to calculate the rail-to-earth leakage conductance (gE) of an exposed conductive part that is connected to rails such as OCL poles using the following equation:

$$\mathrm{gE} = \sum_{i=1}^{n} \frac{1}{R_E} \tag{4-10}$$

Several works of literature have focused on the rail-to-earth leakage conductance (gE) for foundations of components and especially foundations of OCL poles because OCL poles have the majority effect on rail admittance. There are several measurements of rail-to-earth leakage conductance (gE) shown in Kiessling [17] and Sture [19]. According to Sture [19], measurements show that gE in Norway is from 0.0004 S/km to 0.143 S/km, and in the case of an OCL pole connected to rails, gE was between 0.02 S/km and 2.86 S/km. Sture also described that another measurement shows that gE is 0.03 S/km at -20 ℃, while it is 2 S/km for soil moisture at high temperatures. Kiessling [17] also shows some measurements of gE in Germany. It is worth mentioning that rail-to-earth leakage conductance (gE) measurements in Germany are higher than in Norway due to the high resistivity in Norway. Sture and Kiessling conclude that (gE) is 0.1 S/km at temperatures under 0 ℃, while it is 0.5 S/km at temperatures over 0 ℃.

Varju [4] used the following values of gE in his study: 0.05 S/km as a minimum value, 0.25 S/km as the design value, and 0.75 S/km as the maximum value.

For the simulation, this report will use the following values of rail-to-earth leakage conductance (gE): 0.05 S/km, 0.25 S/km, 0.75 S/km, 1 S/km, and 2 S/km.

4.3 Carson's equations

This section is based on literature [20, 23]. J. R. Carson's method is the way to solve the problem of wave propagation on an overhead conductor line with returns in the earth. It provides expressions to calculate the series impedance (self and mutual) of overhead conductors. J. R. Carson's original expressions are in integral form, but in later years, some literature like [20] presents the expressions in the differential form for a lower frequency (16.7 Hz). These expressions/formulations have some assumptions for the surrounding medium and the conductors:

- The earth is assumed to be flat.
- The conductors are parallel to the earth.
- The earth is homogenous, and the resistivity is constant.
- Neglected the non-linearity effect and magnetic permeability.

According to [20], the formulations of self- and mutual series impedance are:

The series impedance is:

$$Z' \approx Z'_{in} + Z'_{ex} \tag{4-11}$$

The inner self-impedance is:

$$Z'_{in} \approx R_{dc} + j \cdot \frac{f \cdot \mu}{4} \tag{4-12}$$

$$R_{dc} = R' = \frac{1}{A \cdot \sigma} = \frac{1}{\pi \cdot a^2 \cdot \sigma} \tag{4-13}$$

$$Z'_{in} \approx \frac{1}{\pi \cdot a^2 \cdot \sigma} + \frac{j \cdot \omega \cdot \mu}{8\pi} \tag{4-14}$$

$R' = R_{dc}$: Resistance of wires and conductors in Ω/m.

f: The frequency, 16.7 Hz.

μ: Permeability ($\mu_0 \cdot \mu_r$). Where the magnetic space constant is $\mu_0 = 4\pi \cdot 10^{-7}\ H/m$ and μ_r is the relative permeability. For copper material $\mu_0 \approx \mu_r$ and for steel μ_r is higher and nonlinear.

A: Cross-section area in mm^2.

a: Radius of wires and conductors in mm.

σ: Specific conductivity in 1/Ωm.

ω: The angular frequency of the voltage ($2\pi \cdot f$).

The external self-impedance is:

$$Z'_{ex} \approx R'_E + j \cdot f \cdot \mu_0 \cdot ln(\frac{D_e}{a}) \tag{4-15}$$

$$R'_E = \left(\frac{\pi}{4}\right) \cdot \mu \cdot f \tag{4-16}$$

$$Z'_{ex} \approx \frac{\omega \cdot \mu_0}{8} + \frac{j\omega \cdot \mu_0}{2\pi} \cdot ln(\frac{D_e}{a}) \tag{4-17}$$

R'_E: The resistance of the earth return path in Ω/m.

f: The frequency, 16.7 Hz.

μ_0: The permeability of free space ($4\pi \cdot 10^{-7}$ H/m).

D_e: The penetration depth. See equation (4-4).

a: Radius of wires and conductors in mm.

ω: The angular frequency of the voltage ($2\pi \cdot f$).

By inserting equations (4-14) and (4-17) in equation (4-18) one gets the following:

Self-impedance:

$$Z'_{ii} = R' + R'_E + j \cdot f \cdot \mu_0 \cdot ln\,(\frac{D_e}{a}) \qquad (4\text{-}18)$$

$$Z'_{ii} = \frac{1}{\pi \cdot a^2 \cdot \sigma} + \left(\frac{\pi}{4}\right) \cdot \mu \cdot f + j \cdot f \cdot \mu_0 \cdot ln\,(\frac{D_e}{g}) \qquad (4\text{-}19)$$

g: The geometric mean distance and equal to (0.7788 · a).

Mutual/coupling impedance:

$$Z'_{ik} \approx \frac{\pi \cdot f \cdot \mu_0}{4} + j \cdot f \cdot \mu_0 \cdot ln(\frac{D_e}{D}) \qquad (4\text{-}20)$$

D: The distance between conductors/wires.

The following sections provide calculations of self- and mutual impedances for AC traction feeding system parameters. Table 4-2 shows the parameter arrangements of the BTRC and AT systems. These values are for system S20A and are based on the figures in Appendix 3.

Table 4-2: Parameter arrangement of BTRC and AT systems.

Parameter	X-coordinate in m	Y-coordinate in m
Catenary wire (No.1)	0	7.2
Contact wire (No.2)	0	5.6
Return conductor (RC 1)	-3.7	7.55
Return conductor (RC 2)	-3.7	7.05
Rail 1 (R1)	-0.7175	0.2
Rail 2 (R2)	0.7175	0.2
Negative feeder (NF)	-4	10
Positive feeder (PF)	-3	10

4.3.1 Catenary wire and Contact wire

Catenary wire (No.1):

The catenary wire consists of copper, bronze, or copper-steel wire and is located above the contact wire, as shown in Figure 4-2.

According to the technical report [24] and standard EN 50149 [25], the type of catenary wire is DIN 48201 – 50 – BzII, the cross-section area is 50 mm^2, and the diameter is 9 mm. The conductivity is $3.6 \cdot 10^7\ S/m$, according to Kiessling [17].

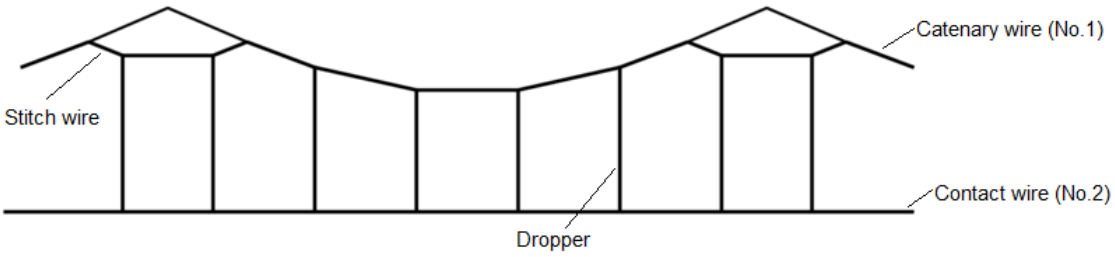

Figure 4-2: Mechanical system of S20A. Figure adapted from [8].

Contact wire (No.2):

The contact wire (No.2) with catenary wires (No.1), droppers, and stitch wires together represents the overhead contact line (OCL), as shown in Figure 4-2. Contact wires glide toward the collectors on the locomotive's pantograph to transfer the electrical energy from the source (feeding station) to the load (train). Standard EN 50149 [25] provides the electrical and mechanical characteristics and requirements of contact wires.

According to the technical report [24] and standard EN 50149 [25], the type of contact wires for mechanical system S20A is AC -100 - CuAg0,1. The cross-section area is 100 mm^2, and the diameter is 12 mm. According to Bane NOR's technical specifications [18], the conductivity of this type is $5.68 \cdot 10^7\ S/m$. The contact wire height for this system is 5600 mm. The distance between the contact wires and catenary wires of the S20A system is 1600 mm, as shown in Appendix 3.

Self- and mutual impedances of contact wire and catenary wire are calculated for earth resistivities of 100 Ωm, 2600 Ωm, and 5000 Ωm by equations (4-19) and (4-20), as shown in Table 4-5.

4.3.2 Running rails (R)

As mentioned before, running rails are part of the return circuit, and therefore it is important to determine their series impedances. Running rails are also part of the train detection system, which is not part of this thesis.

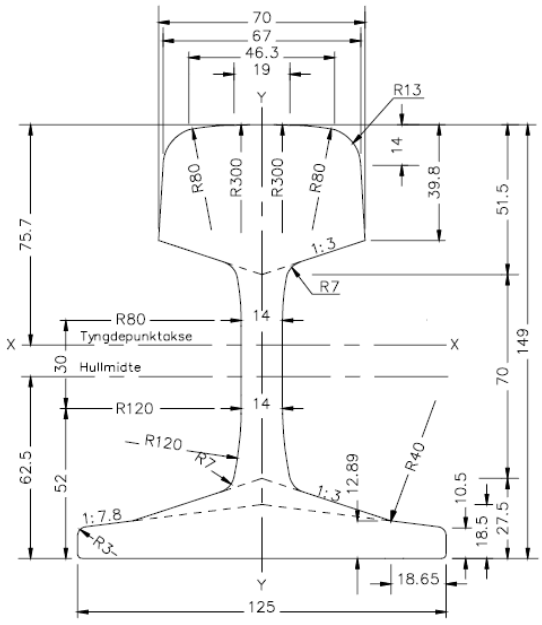

Figure 4-3: Running rail S49 [8].

Rail profiles and grades can be specified in accordance with standard EN 13674-1 [26]. In Norway, several types of rails have been used, such as S49, S54, and S60 [18].

The self-impedance of rails cannot be determined in the same way as other conductors by equation (4-19) for the following reasons: Rails are not circular, as shown in Figure 4-3, and Rails are close to the earth and have large dimensions.

Kiessling [17] recommended measuring the self-impedance of rails and provided approximation expressions to calculate it. There are some measurements for the inner self-impedance of running rails in literature. The measurement results can be different due to the different types of materials and the measurement arrangement. The self-impedance of rails is current-dependent, as shown in Table 4-3.

Table 4-3: Measurements of inner self-impedance for one rail.

Ref. Sture [19]	**Current [A]**			
	200 A	300 A	400 A	500 A
Inner self-impedance of 50 kg/m [Ω/km]	0.098 + j0.078	0.126 + j0.087	0.146 + j0.095	0.158 + j0.098
Inner self-impedance of 41 kg/m [Ω/km]	0.108 + j0.085	0.140 + j0.096	0.162 + j0.102	0.171 + j0.105
Ref. Storset [27] as referred in Høidalen [20]				
Inner self-impedance of S49 [Ω/km] - used	0.111 + j0.111	0.138 + j0.138	0.158 + j0.158	0.173 + j0.172
Inner self-impedance of S49 [Ω/km] - unused	0.065 + j0.065	0.080 + j0.080	0.110 + j0.101	0.128 + j0.120
Inner self-impedance of S54 [Ω/km]	0.067 + j0.067	0.078 + j0.084	0.107 + j0.104	0.123 + j0.123

To calculate the inner self-impedance, Kiessling [17] supposed that the inner self-impedance of rails for the 50 Hz system is 0.12 + j0.15 Ω/km at 100 A and 0.25 + j0.22 Ω/km at 1000 A. Kiessling assumed that the inner self-impedance of the 16.7 Hz system is half of the 50 Hz system inner self-impedance. Therefore, the inner self-impedance of the 16.7 Hz system is 0.06 + j0.075 Ω/km at 100 A and 0.125 + j0.11 Ω/km at 1000 A. Varju in his study [4], used the inner self-impedance of 0.06 + j0.0658 Ω/km at 500 A.

Table 4-4 shows the calculated self-impedance of S49, S54, and S60 for earth resistivities of 100 Ωm, 2600 Ωm, and 5000 Ωm. The inner self-impedance of Varju and Kiessling is used, while the external self-impedance is calculated using equation (4-17).

The calculated self-impedance and mutual impedance of running rails are shown in Table 4-5. The mutual impedance of rails is calculated by equation (4-20). The distance between running rails is 1435 mm, as shown in Appendix 3.

In the simulations, the self-impedance of rails for earth resistivity of 2600 Ωm for type S49 will be used. It is marked in bold in Table 4-4 and Table 4-5.

Table 4-4 Calculations of rail self-impedance for one rail.

Rail type	**Radius (a) in mm**	**Earth resistivity (ρ_e) [Ωm]**	**Self-impedance (Z'_{ii}) [Ω/km] [17]**	**Self-impedance (Z'_{ii}) [Ω/km] [4]**
S49	44.77	100	0.076 + j0.295	0.076 + j0.286
		2600	0.076 + j0.329	**0.076 + j0.320**
		5000	0.076 + j0.336	0.076 + j0.327
S54	47.03	100	0.076 + j0.295	0.076 + j0.286
		2600	0.076 + j0.328	0.076 + j0.320
		5000	0.076 + j0.335	0.076 + j0.326
S60	49.35	100	0.076 + j0.286	0.076 + j0.276
		2600	0.076 + j0.327	0.076 + j0.318
		5000	0.076 + j0.334	0.076 + j0.324

4.3.3 Return conductor (RC)

For the BTRC system, the return conductors transfer the electrical energy from the load (train) back to the source (feeding station). The return conductors can be laid parallel to the running rails and connected to them. Return conductors can also be suspended on the OCL poles. The purpose of the suspended return conductors is to reduce the longitudinal rail voltage and rail potential [12, 17]. In this report, it is assumed that there are two parallel return conductors suspended on the OCL poles, as shown in Appendix 3. The purpose of using two parallel return conductors is to ensure the continuity of the return current path in case of faults or damage to one of them. Typically, the distance between return conductors is 500 mm.

According to Bane NOR's technical specifications [18] and standard EN 50149 [25], the type of return conductor is 240 mm^2 Al. The cross-section area is 240 mm^2, and the diameter is 20 mm. According to Kiessling [17], the conductivity of this type is $3.54 \cdot 10^7\ S/m$.

Self- and mutual impedances of return conductors are calculated for earth resistivities of 100 Ωm, 2600 Ωm, and 5000 Ωm by equations (4-19) and (4-20), as shown in Table 4-5.

4.3.4 Positive feeder (PF) and Negative feeder (NF)

For the AT system, the PF and NF transfer electrical energy at a voltage level of 30 kV. PF and NF conductors are commonly installed on top of the OCL poles, as shown in Appendix 3. The distance between them is 1000 mm.

According to Bane NOR's technical specifications [18] and EN 50182:2001 [28], table F.22, the PF and NF conductor type is 381-AL-1, which is often used in Norway. The cross-section area is 380.8 mm^2, and the diameter is 25.3 mm. According to Kiessling [17], the conductivity is $3.54 \cdot 10^7\ S/m$ for this type of conductor.

Self- and mutual impedances of PF and NF feeders are calculated for earth resistivities of 100 Ωm, 2600 Ωm, and 5000 Ωm by equations (4-19) and (4-20), as shown in Table 4-5.

Values marked in bold in Table 4-5 refer to values that will be used in the simulation at the ATPDraw program.

Table 4-5: Results of self- and mutual impedance.

Parameter	Earth resistivity (ρ_e) [Ωm]	Self-impedance (Z'_{ii}) [Ω/km]	Mutual impedance (Z'_{ik}) [Ω/km]
Catenary wire (No.1)	100	0.572 + j0.274	
	2600	**0.572 + j0.308**	0.0164 + j0.145
	5000	0.572 + j0.315	0.0164 + j0.179
Contact wire (No.2)	100	0.192 + j0.268	0.0164 + j0.186
	2600	**0.192 + j0.302**	
	5000	0.192 + j0.309	
Return conductor (RC)	100	0.134 + j0.257	0.0164 + j0.170
	2600	**0.134 + j0.291**	0.0164 + j0.204
	5000	0.134 + j0.298	0.0164 + j0.210
Running rails (R)	100	0.076 + j0.286	0.0164 + j0.147
	2600	**0.076 + j0.320**	0.0164 + j0.182
	5000	0.076 + j0.327	0.0164 + j0.188
Positive feeder (PF) and Negative feeder (NF)	100	0.0905 + j0.252	0.0164 + j0.155
	2600	**0.0905 + j0.286**	0.0164 + j0.189
	5000	0.0905 + j0.293	0.0164 + j0.196

5 Simulation of AC Traction Feeding Systems

5.1 Components of traction feeding systems in ATPDraw

AC traction feeding systems are simulated in the ATPDraw program. Appendix 4 shows the BTRC system Design C model based on Figure 3-1, and Appendix 5 shows the AT system Design E model based on Figure 3-3. The track line length of each system is 84 km. It is the same length that Varju investigated. The reason for using 84 km is for comparison and verification purposes. The following sections detail the ATPDraw simulation method for each component of traction feeding systems.

5.1.1 Frequency converter station

The frequency converter station is represented as an AC voltage source with a short-circuit impedance (*Zk*). The rated voltage of the voltage source is 16.5 kV, and the frequency is 16.7 Hz. The short circuit impedance (*Zk*) is 1.344 + j3.55, which corresponds to the short circuit impedance of a 10 MVA single-phase transformer. The phase angle of the converter station is assumed to be 0˚. It is also assumed that there is a resistance to earth (R) of 10 Ω at the converter station. Figure 5-1 shows the converter station model in ATPDraw.

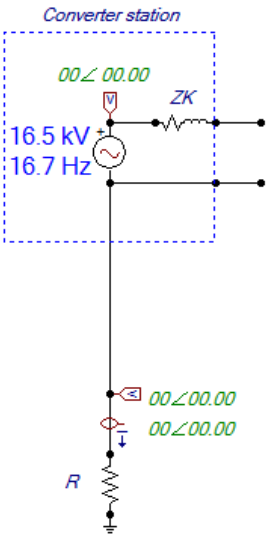

Figure 5-1: Converter station model in ATPDraw.

5.1.2 Booster and Auto-transformers

In ATPDraw, booster and auto-transformer models can be found under *Selection* ➔ *Transformers* ➔ *BCTRAN.* In the *BCTRAN* model, the user can specify the type of transformer (booster or auto). In the BTRC system, 95 kVA booster transformers are used, while 5 MVA autotransformers are used in the AT system. Appendix 2 provides the input data for transformers. Figure 5-2 shows the model of the booster and auto-transformer in ATPDraw. As mentioned in Section 3.1, the booster transformer's primary winding is connected in series with the contact line (CL), whereas the secondary winding is connected in series with the return conductor (RC).

As mentioned in Section 3.2, the autotransformer's terminal PF/CL is connected to the contact line (CL) and the positive feeder (PF), while the terminal NF is connected to the negative feeder (NF). The midpoint (0-the return) terminal is connected to the running rails.

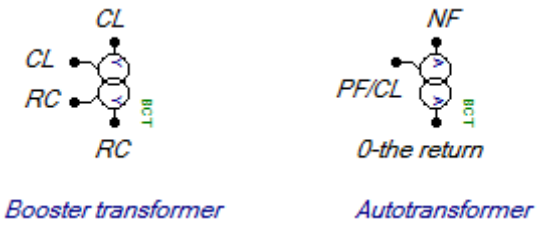

Figure 5-2: Booster and auto-transformer model in ATPDraw.

5.1.3 Overhead contact line (OCL)

The overhead contact line is simulated using the *Line Constant or Cable Constants/Parameter component (LCC)*. LCC components can be found under *Selection* ➔ *Line/Cables*.

LCC component:

The model of OCL is simulated using two LCC components: the first one is the *LCC template* (see Figure 5-3), and the second one is the *LCC section* (see Figure 5-3).

In the *LCC template* ➔ *Model*, the following data is specified:

Name: Can be specified by the user.

System type: Overhead line

Number of phases: 6

Frequency: 16.7 Hz

Earth resistivity: 2600 Ωm (constant value)

Model type: PI

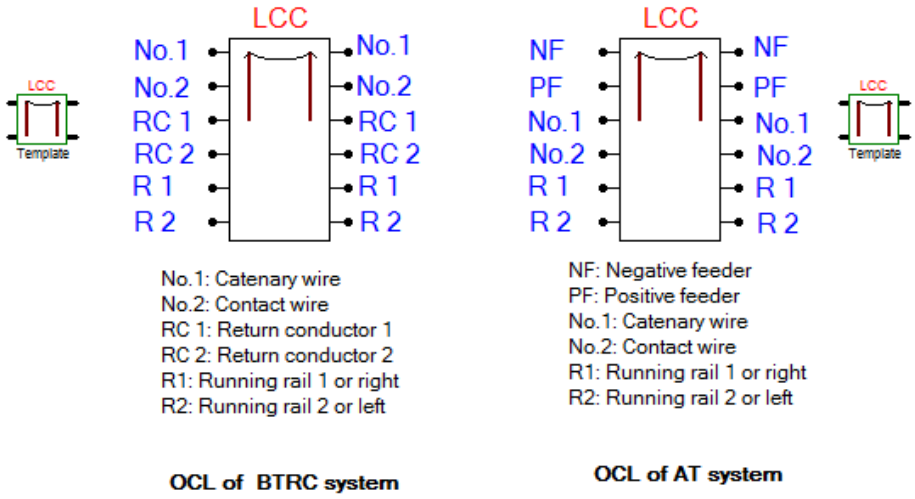

Figure 5-3: Model of the OCL in the ATPDraw.

In the *LCC template* ➔ *Data,* the following data is specified:

Input data are the geometry values of each wire/conductor and the values of series impedances that are shown in Table 4-2 and Table 4-5, respectively. Appendix 6 shows the input data of overhead contact lines for the BTRC and AT systems. It is worth mentioning that the user needs to adjust the values of *React*, *Rout*, and *Resis* in ATPDraw to match the given value of series impedance. The series impedance of each wire/conductor is simulated in ATPDraw to verify the calculated series impedance. Appendix 7 shows the verification method and the series impedance values that are used in ATPDraw.

LCC section component data are:

Length: 3 km or 6 km for the BTRC system and 12 km or 14 km for the AT system

Frequency: 16.7 Hz

Earth resistivity: 2600 Ωm (constant value)

Template and name: This should match the name of the *LCC template.*

Number of LCC components:

The number of LCC components between the transformers can be specified by the user. In this report, the BTRC and AT models are tested with 4, 6, and 8 LCC components between transformers (booster or auto). The test is carried out for rail-to-earth leakage conductance (gE), 0.25 S/km. The results in Appendix 8 shows that there is a difference of 1 V in the levels of rail potential and 1 A in the levels of earth current between the 4, 6, and 8 models of the BTRC and AT systems.

From the results, one can conclude that the number of LCC components has no significant effect on the levels of rail potential and earth current. To obtain more accurate results and study the systems under the same conditions, it will use 8 LCC components between transformers in this thesis. In the AT system model with 14 km spacing, 10 LCC components between autotransformers are used to make the manual sectioning of the overhead contact line (OCL) even.

Bond and Sectioning

For the BTRC system, a connection is created between the running rails and the return conductors. This connection is called Bond. The booster transformer is located between two bonds for Design C.

For the AT system Design E, the overhead contact line (OCL) is manually sectioned every 3 km for a 12 km spacing between the autotransformers, while it is sectioned every 2.8 km for a 14 km spacing between the autotransformers.

5.1.4 Rail-to-earth leakage conductance model

The rail-to-earth leakage conductance is represented as concentrated resistances between running rails and earth according to:

$$R_E = \frac{1}{gE \cdot \frac{L}{n}} \tag{5-1}$$

R_E: The resistance to earth in **Ω**

gE: Rail-to-earth leakage conductance in S/km

L: Spacing between BTs or ATs (3 km or 6 km for the BTRC system and 12 km or 14 km for the AT system)

n: Number of rail-to-earth leakage conductance branches between each two BTs or ATs. The number of rail-to-earth leakage conductance branches is selected to be equal to the number of LCC components between transformers +1 at each booster- or auto-transformer.

5.1.5 Load

Train: The load is simulated as an impedance that is connected between running rails (R) and contact lines (CL). The train of 500 A is represented in the model as an impedance of 25.5 + j15.8 **Ω** at a rated voltage of 15 kV and a cos φ of 0.85.

Short circuit:

Bane NOR's technical regulations [8] and COWI report [14] provide the requirements for the calculated RMS values of the alternating current (the maximum permissible short circuit current for the track lines) in accordance with the geographical area.

Table 5-1 shows the RMS value of alternating current that can be used to calculate the touch voltage at a disconnection time of 0.1 s and 0.3 s. These values are calculated based on a short circuit near the feeding station at two-sided feeding, as shown in Figure 2-1.

As mentioned in Section 2.2, the short-circuit current of 0.3 s is 33% of the design short-circuit current (I_{rms}). This assumption refers to the assumed (ca. 33%) contribution from the neighbouring frequency converter station. According to [14], the short-circuit current of 0.3 s is:

$$I_{rms,0.3\,s} = \sqrt{\frac{1}{0.3}\left[(I_k)^2 \cdot 0.1 + \left(\frac{1}{3} \cdot I_k\right)^2 \cdot 0.2\right]} \tag{5-2}$$

$$I_{rms,0.3} = 0.64 \cdot I_k \tag{5-3}$$

Table 5-1: Calculated values of short circuit current based on Figure 2-1 [8].

Geographical area	**Design short circuit current (I_k) [kA]**	**Alternating current (I_{rms}) [kA]**	
		t = 0.1 s	**t = 0.3 s***
Oslo S switching station	31.5	31.5	20.2
Within Oslo area	25.0	25.0	16.0
Ofoten Line (Narvik)	20.0	20.0	12.8
Outer of Oslo area	16.0	16.0	10.3
The rest of the country	12.5	12.5	8.0

* I_{rms} of 0.3 s calculated by equation (5-3).

The track line in this report is assumed to be in "the rest of the country," which means the maximum short circuit current is 12.5 kA for t = 0.1 s and 8 kA for t = 0.3 s. In ATPDraw, the fault is represented as an impedance, which is adjusted to obtain the fault of 12.5 kA for t = 0.1 s, and adjusted again to obtain the fault of 8 kA for t = 0.3 s.

5.1.6 Group

A *group* object is used to reduce the visual complexity of traction feeding models. The idea of a *group* object is to compress several components that the user specifies into a simple icon. In this thesis, the *group* object is modified to represent the LCC components and rail-to-earth leakage conductance branches between every two transformers. Figure 5-4 shows the OCL modified group object of the BTRC and AT systems.

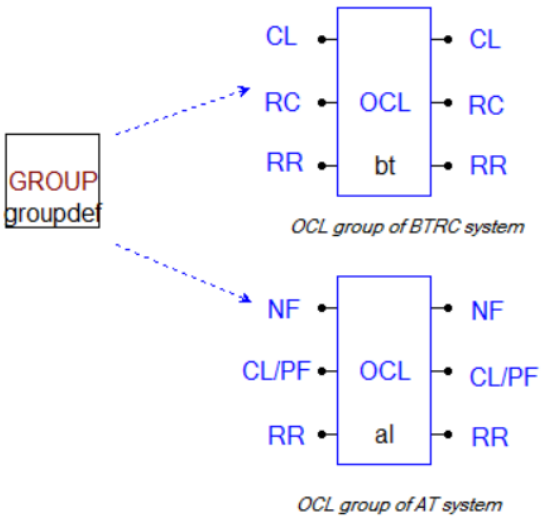

Figure 5-4: OCL modified group of BTRC and AT systems.

5.1.7 Results from the ATPDraw program

Probes of voltage and current are used on the rail-to-earth leakage conductance branches to get the results of rail potential in Volt (V) and earth current in Ampere (A). Figure 5-5 shows the probes of voltage and current in the ATPDraw program. It is worth mentioning that the probs of current and voltage are specified to ($\sqrt{2}$) in the *scale* function to get the RMS values.

The results can manually import from the probes or using the *Write Max/Min* object. In this thesis, the results are imported into the Excel program to plot the results of rail potential and earth current versus train position in km.

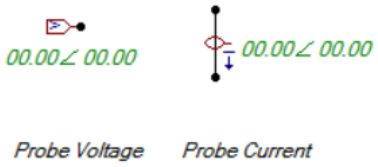

Figure 5-5: Probes of voltage and current in ATPDraw.

5.2 Study of Rail potential and Earth current

This section presents the scenarios and specifications to study the rail potential and earth current in the return circuit using ATPDraw models. Appendix 4 and Appendix 5 show the models that are used. The results of the case studies will be introduced in Chapter 6. In addition, ATPDraw files (acp.) for the BTRC and AT models are also attached as external files.

5.2.1 Case Study 1: Effect of train position and gE during normal operation

This case aims to study the effects of train position and rail-to-earth leakage conductance (gE) on the levels of rail potential and earth current during normal operation.

Case 1 specifications:

- **Spacing:** 3 km between booster transformers for the BTRC system, which is according to Bane NOR's technical regulations [8]. For the AT system, the spacing is 12 km between autotransformers (12 km is almost equal to 10 km spacing for a single-track line, according to Bane NOR's technical regulations [8]). In this case, 12 km of spacing is used to verify if the case study results are in accordance with Varju's results [4, 5].
- **Train position:** at the first or last transformer (the first or last transformer is the nearest AT or BT transformer to the converter station) and in the middle of the track line between two BTs or ATs.
- **Rail-to-earth leakage conductance (gE)**: 0.05 S/km, 0.25 S/km, 0.75 S/km, 1 S/km, and 2 S/km.

5.2.2 Case Study 2: Effect of transformer spacing, train position, and gE during normal operation

This case aims to study the effects of spacing between ATs and BTs, train position, and rail-to-earth leakage conductance (gE) on the levels of rail potential and earth current during normal operation.

Case 2 specifications:

- **Spacing:** 6 km between booster transformers for the BTRC system and 14 km between autotransformers for the AT system
- **Train position:** at the first or last transformer (the first or last transformer is the nearest AT or BT transformer to the converter station) and in the middle of the track line between two BTs or ATs.

- **Rail-to-earth leakage conductance (gE)**: 0.05 S/km, 0.25 S/km, 0.75 S/km, 1 S/km, and 2 S/km.

5.2.3 Case Study 3: Effect of transformer spacing and gE during short circuit

This case aims to study the effects of rail-to-earth leakage conductance (gE) and spacing between ATs and BTs on the levels of rail potential and earth current during a short circuit. The short circuit will be tested for time t = 0.1 s and t = 0.3 s. The EN 50122-1 standard [13] recommended that there is no need to evaluate the multiple faults that occur at the same time to study the touch voltage during short circuit conditions. Therefore, Case Study 3 does not evaluate these types of faults.

Case 3 specifications:

- **Spacing:** 3 km or 6 km between booster transformers for the BTRC system. 12 km or 14 km between autotransformers for the AT system.
- **Load position:** at the first or last booster transformer (the nearest booster transformer to the converter station) for the BTRC system and in the middle of the track line between two autotransformers for the AT system.
- **Rail-to-earth leakage conductance (gE)**: 0.05 S/km, 0.25 S/km, 0.75 S/km, 1 S/km, and 2 S/km.

6 Results of ATPDraw

Chapter 6 presents the results of the case studies that are described in Section 5.2. The results are presented as plots of rail potential and earth current versus load position during normal operation and short-circuit conditions. The results are also introduced as tables to show the maximum levels of rail potential and earth current for traction feeding systems. The results will be discussed and verified in Chapter 7.

6.1 Results of Case Study 1

Case study 1 investigates the effect of rail-to-earth leakage conductance (gE) and train position during normal operation. The transformer spacing is 3 km for the BTRC system and 12 km for the AT system.

6.1.1 Rail potential of BTRC system (3 km) during normal operation

The levels of rail potential for the BTRC system with 3 km spacing during normal operation are shown in Figure 6-1 and Figure 6-2.

Figure 6-1 shows the levels of rail potential when the train is at the first or last booster transformer. Since the highest levels of rail potential from 0 km to 75 km are lower than 5 V, the results are studied from 75 km at BT26 to the train location at 84 km at BT29. The highest levels of rail potential from 75 km to 81 km are lower than 10 V. The rail potential levels increase at the connection between the contact line and running rails (Bond) at 82,5 km and decrease immediately behind the bond, then become the highest at the train location at 84 km. The rise in rail potential at the bond at 82,5 km can be noticed for gE levels of 0.75 S/km - 2 S/km.

Figure 6-2 shows the levels of rail potential when the train is almost in the middle of the track line between two BTs at 40.5 km. The results are studied from 36 km at BT13 to 45 km at BT16. The levels of rail potential gradually increase from 36 km and become the highest at 40.5 km (train location), then decrease after 40.5 km.

As shown in Table 6-1, the maximum values of rail potential when the train is at the first booster transformer are higher than the maximum values of rail potential, when the train is at 40.5 km. The results show that rail potential levels decrease when gE levels vary from 0.05 S/km to 2 S/km, where the $U_{RE,\,max}$ is 64.26 V at gE = 0.05 S/km and 41.59 V at gE = 2 S/km.

Table 6-1: Maximum rail potential of BTRC, train at 1st BT and 40.5 km for 3 km spacing.

Rail-to-earth leakage conductance (gE) [S/km]	**Maximum rail potential ($U_{RE, max}$) [V] at 1st BT**	**Maximum rail potential ($U_{RE, max}$) [V] at 40.5 km**
0.05	64.26	5.29
0.25	57.09	2.16
0.75	50.18	1.24
1	47.92	1.08
2	41.59	0.77

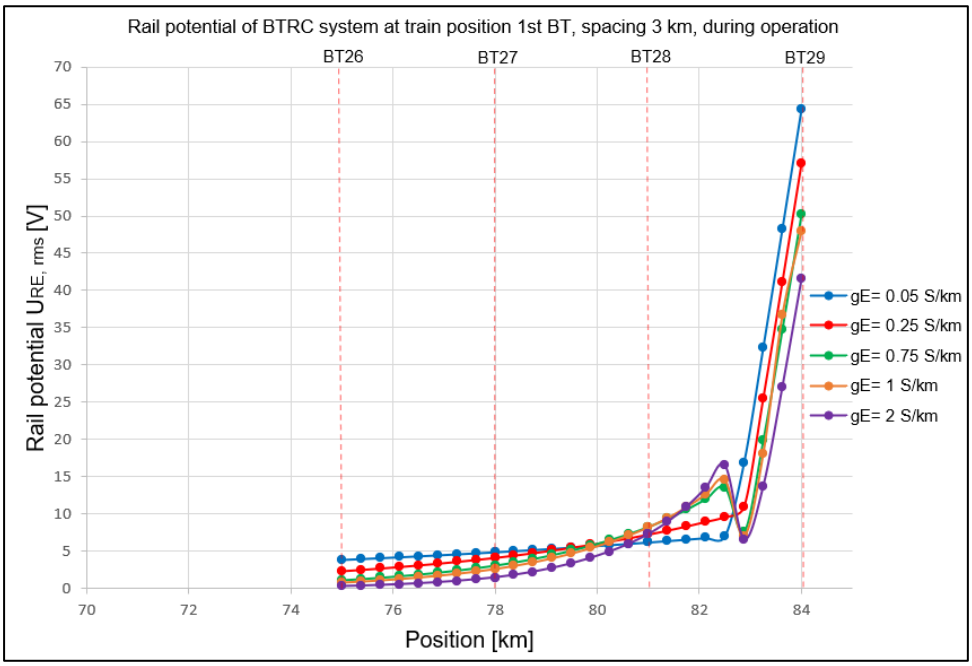

Figure 6-1: Rail potential at train position 1st BT, spacing 3 km, during normal operation.

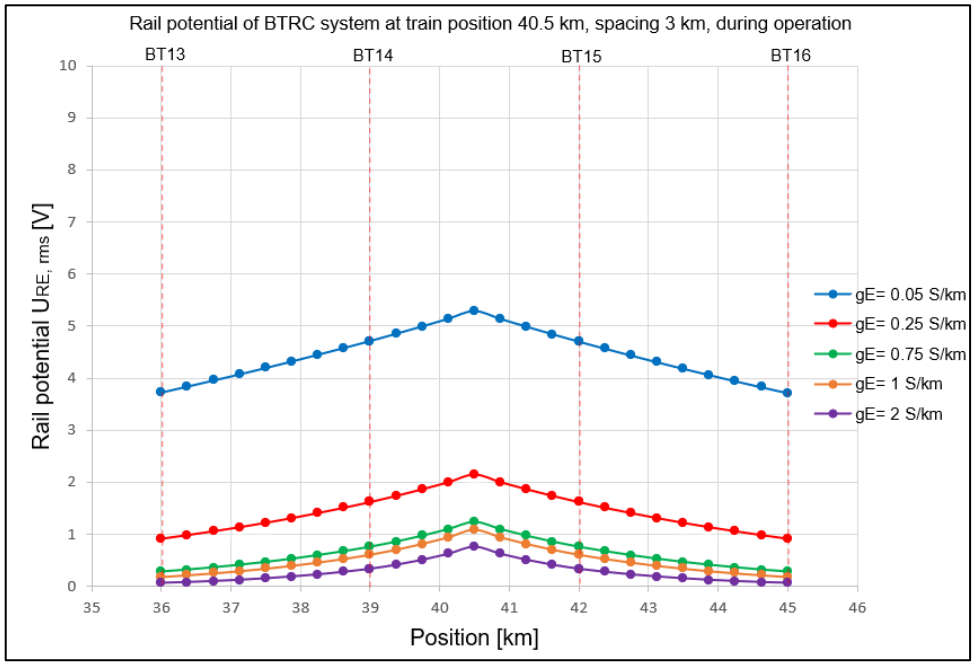

Figure 6-2: Rail potential at train position 40.5 km, spacing 3 km, during normal operation.

6.1.2 Earth current of BTRC system (3 km) during normal operation

The levels of earth current for the BTRC system with 3 km spacing during normal operation are shown in Figure 6-3 and Figure 6-4.

Figure 6-3 shows the levels of earth current when the train is at the first or last booster transformer. Since the highest levels of earth current from 0 km to 75 km are almost 0 A, the results are studied from 75 km at BT26 to the train location at 84 km at BT29. The highest levels of earth current from 75 km to 81 km are lower than 15 A, then increase and reach the highest level in the section between BT28 at 81 km and BT29 at 84 km.

Figure 6-4 shows the levels of earth current when the train is almost in the middle of the track line between two BTs at 40.5 km. The results are studied from 36 km at BT13 to 45 km at BT16. The maximum levels of earth current reach immediately ahead and immediately behind the train location (40.5 km).

As shown in Table 6-2, the maximum values of earth current when the train is at the first booster transformer are higher than the maximum values of earth current, when the train is at 40.5 km. The results show that the earth current levels increase when g_E levels vary from 0.05 S/km to 2 S/km, where the $I_{E,\,max}$ is 2.36 A at g_E = 0.05 S/km and 35.89 A at g_E = 2 S/km.

Table 6-2: Maximum earth current of BTRC, train at 1st BT and 40.5 km for 3 km spacing.

Rail-to-earth leakage conductance (g_E) [S/km]	**Maximum earth current ($I_{E,\,max}$) [A] at 1st BT**	**Maximum earth current ($I_{E,\,max}$) [A] at 40.5 km**
0.05	2.36	0.41
0.25	8.61	0.39
0.75	18.38	0.50
1	22.35	0.57
2	35.89	0.75

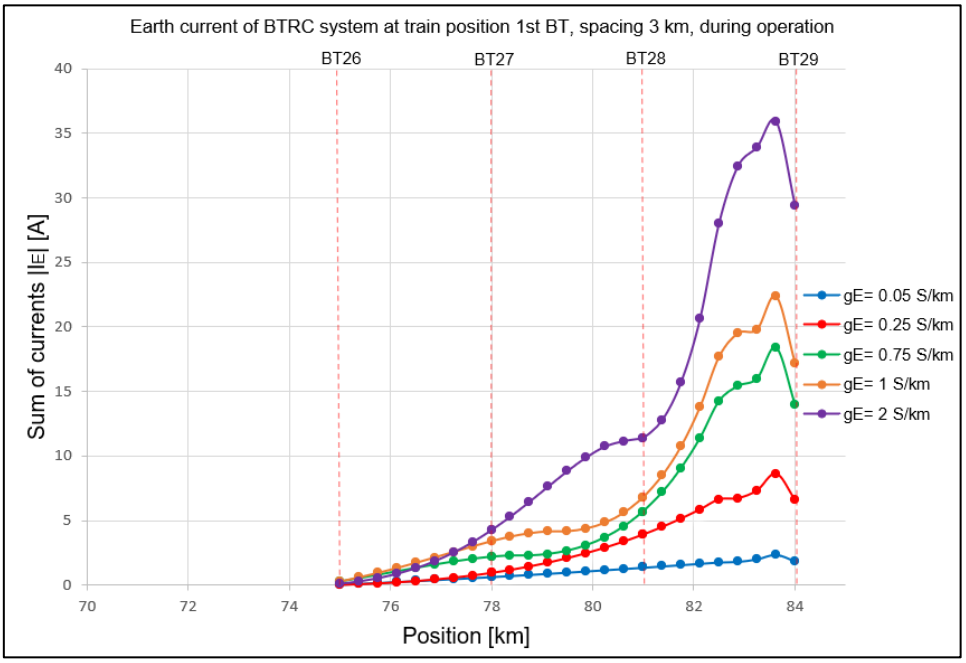

Figure 6-3: Earth current at train position 1st BT, spacing 3 km, during normal operation.

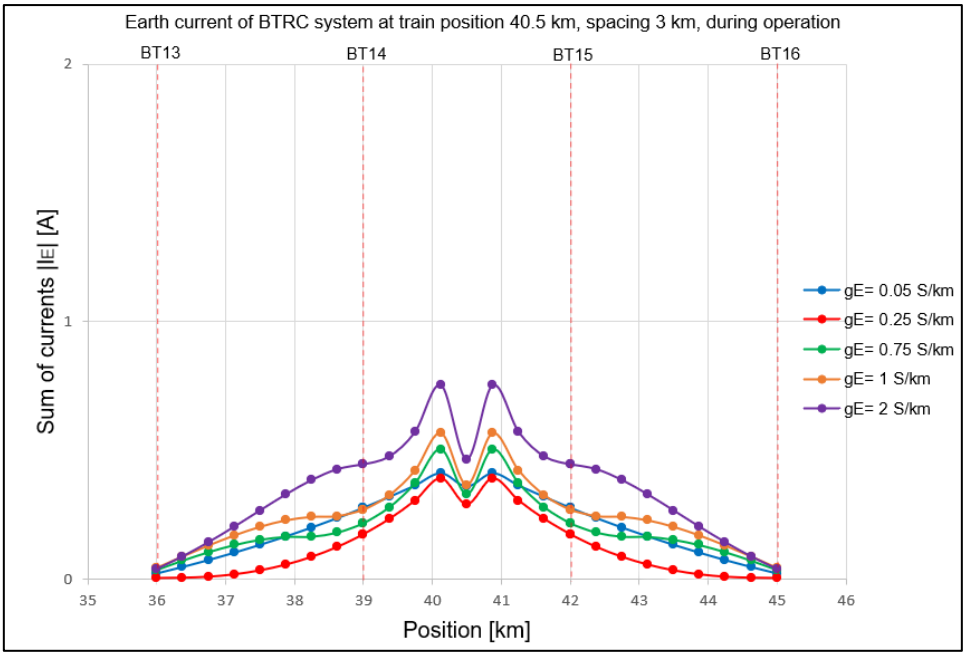

Figure 6-4: Earth current at train position 40.5 km, spacing 3 km, during normal operation.

6.1.3 Rail potential of AT system (12 km) during normal operation

The levels of rail potential for the AT system with 12 km spacing during normal operation are shown in Figure 6-5 and Figure 6-6.

Figure 6-5 shows the levels of rail potential when the train is at the first or last autotransformer. Since the highest levels of rail potential from 0 km to 48 km are lower than 1 V, the results are studied from 48 km at AT6 to the train location at 84 km at AT9. The levels of rail potential rise at 72 km (AT8), then decrease just after AT8 and rise again to reach the highest level at 84 km.

Figure 6-6 shows the levels of rail potential when the train is in the middle of the track line between two ATs at 42 km. The results are studied from 24 km at AT4 to 60 km at AT7. The peaks of rail potential occur at AT5 and AT7 and become the highest at the train location (42 km).

As shown in Table 6-3, the maximum values of rail potential, when the train is at 42 km are higher than the maximum values of rail potential when the train is at the first autotransformer. The results show that rail potential levels decrease when g_E levels vary from 0.05 S/km to 2 S/km, where the $U_{RE, max}$ is 117.74 V at g_E = 0.05 S/km and 33.74 V at g_E = 2 S/km.

Table 6-3: Maximum rail potential of AT, train at 1st AT and 42 km for 12 km spacing.

Rail-to-earth leakage conductance (g_E) [S/km]	**Maximum rail potential ($U_{RE, max}$) [V] at 1st AT**	**Maximum rail potential ($U_{RE, max}$) [V] at 42 km**
0.05	3.66	117.74
0.25	2.28	81.94
0.75	1.27	55.22
1	1.06	48.50
2	0.67	33.74

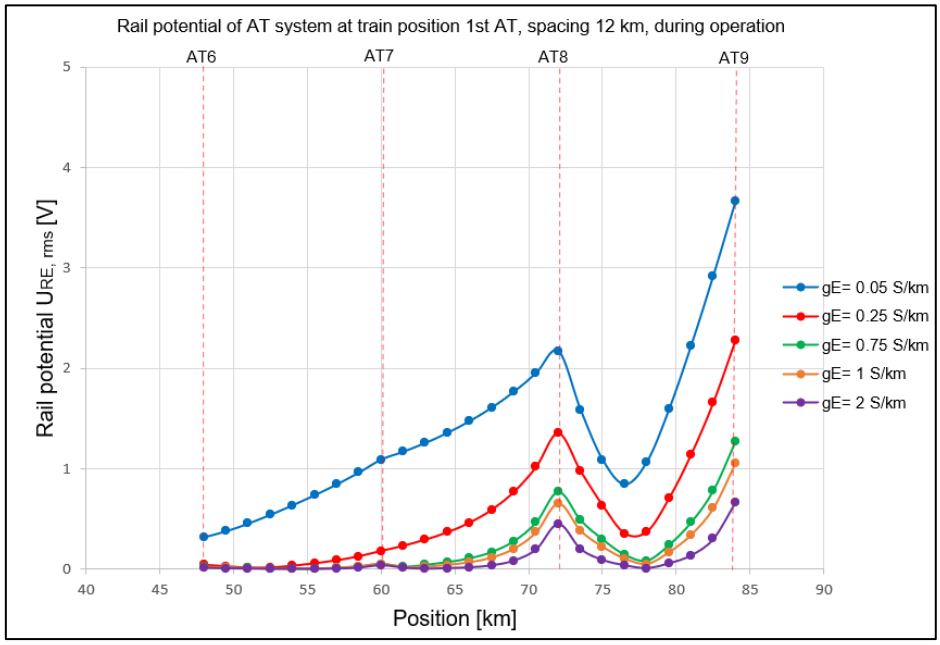

Figure 6-5: Rail potential at train position 1st AT, spacing 12 km, during normal operation.

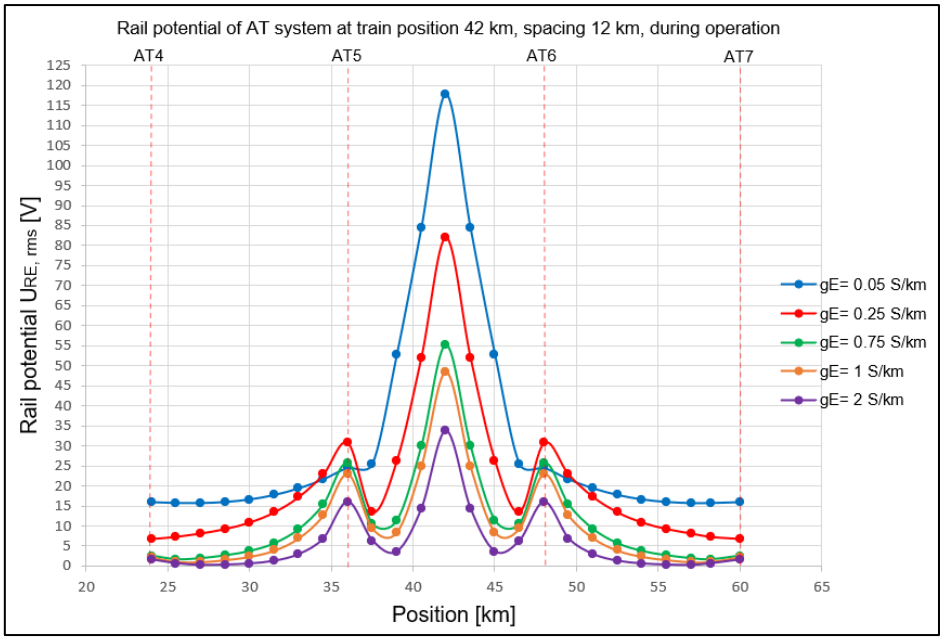

Figure 6-6: Rail potential at train position 42 km, spacing 12 km, during normal operation.

6.1.4 Earth current of AT system (12 km) during normal operation

The levels of earth current for the AT system with 12 km spacing during normal operation are shown in Figure 6-7 and Figure 6-8.

Figure 6-7 shows the levels of earth current when the train is at the first or last autotransformer. Since the highest levels of earth current from 0 km to 48 km are lower than 1 A, the results are studied from 48 km at AT6 to the train location at 84 km at AT9. The highest levels of earth current from 48 km to 72 km are lower than 2 A, then increase and reach the highest level in the section between AT8 at 72 km and AT9 at 84 km.

Figure 6-8 shows the levels of earth current when the train is in the middle of the track line between two ATs at 42 km. The results are studied from 24 km at AT4 to 60 km at AT7. The earth current levels increase from 24 km and reach the highest level immediately ahead and immediately behind the train location (42 km).

As shown in Table 6-4, the maximum values of earth current, when the train is at 42 km are higher than the maximum values of earth current when the train is at the first autotransformer. The results show that the earth current levels increase when g_E levels vary from 0.05 S/km to 2 S/km, where the $I_{E,\,max}$ is 11.62 A at g_E = 0.05 S/km and 78.47 A at g_E = 2 S/km.

Table 6-4: Maximum earth current of AT, train at 1st AT and 42 km for 12 km spacing.

Rail-to-earth leakage conductance (g_E) [S/km]	**Maximum earth current ($I_{E,\,max}$) [A] at 1st AT**	**Maximum earth current ($I_{E,\,max}$) [A] at 42 km**
0.05	0.75	11.62
0.25	1.78	28.74
0.75	2.75	57.11
1	3.00	61.95
2	3.20	78.47

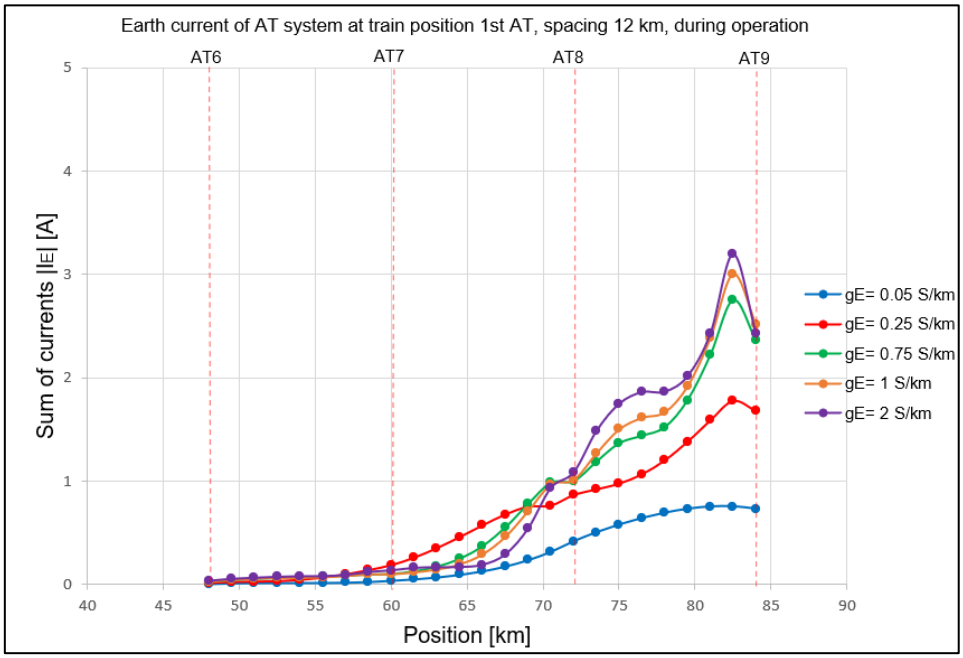

Figure 6-7: Earth current at train position 1st AT, spacing 12 km, during normal operation.

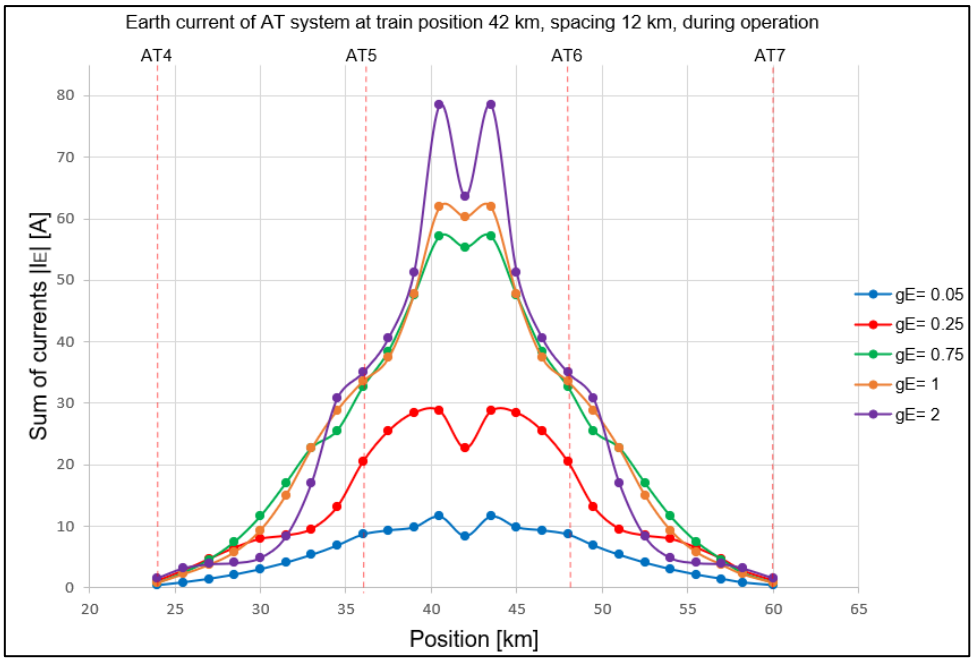

Figure 6-8: Earth current at train position 42 km, spacing 12 km, during normal operation.

6.2 Results of Case Study 2

Case Study 2 also investigates the effect of rail-to-earth leakage conductance (gE) and train position during normal operation, but the transformer spacing increases to 6 km for the BTRC system and 14 km for the AT system. Therefore, this case is introduced in the same way as Case Study 1.

6.2.1 Rail potential of BTRC system (6 km) during normal operation

The levels of rail potential for the BTRC system with 6 km spacing during normal operation are shown in Figure 6-9 and Figure 6-10.

Figure 6-9 shows the levels of rail potential when the train is at the first or last booster transformer. Since the highest levels of rail potential from 0 km to 66 km are lower than 6 V, the results are studied from 66 km at BT12 to the train location at 84 km at BT15. The highest levels of rail potential from 66 km to 78 km are lower than 17 V. The rail potential levels increase at the connection between the contact line and running rails (Bond) at 81 km and decrease immediately behind the bond, then become the highest at the train location at 84 km. The rise in rail potential at the bond at 81 km can be noticed for gE levels of 0.25 S/km - 2 S/km.

Figure 6-10 shows the levels of rail potential when the train is almost in the middle of the track line between two BTs at 39 km. The results are studied from 30 km at BT6 to 48 km at BT9. The levels of rail potential gradually increase from 30 km and become the highest at 39 km (train location), then decrease after 39 km.

As shown in Table 6-5, the maximum values of rail potential, when the train is at the first booster transformer are higher than the maximum values of rail potential when the train is at 39 km. The results show that rail potential levels decrease when gE levels vary from 0.05 S/km to 2 S/km, where the $U_{RE,\,max}$ is 121.39 V at gE = 0.05 S/km and 53.12 V at gE = 2 S/km.

Table 6-5: Maximum rail potential of BTRC, train at 1st BT and 39 km for 6 km spacing.

Rail-to-earth leakage conductance (gE) [S/km]	Maximum rail potential ($U_{RE,\,max}$) [V] at 1st BT	Maximum rail potential ($U_{RE,\,max}$) [V] at 39 km
0.05	121.39	5.21
0.25	97.92	2.06
0.75	75.73	1.21
1	69.12	1.10
2	53.12	0.76

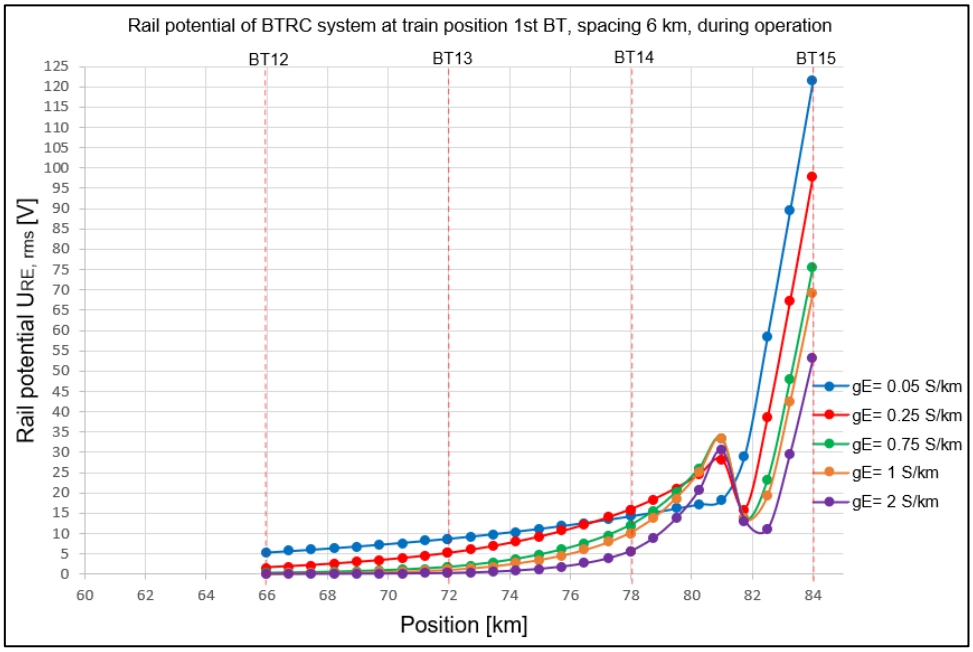

Figure 6-9: Rail potential at train position 1st BT, spacing 6 km, during normal operation.

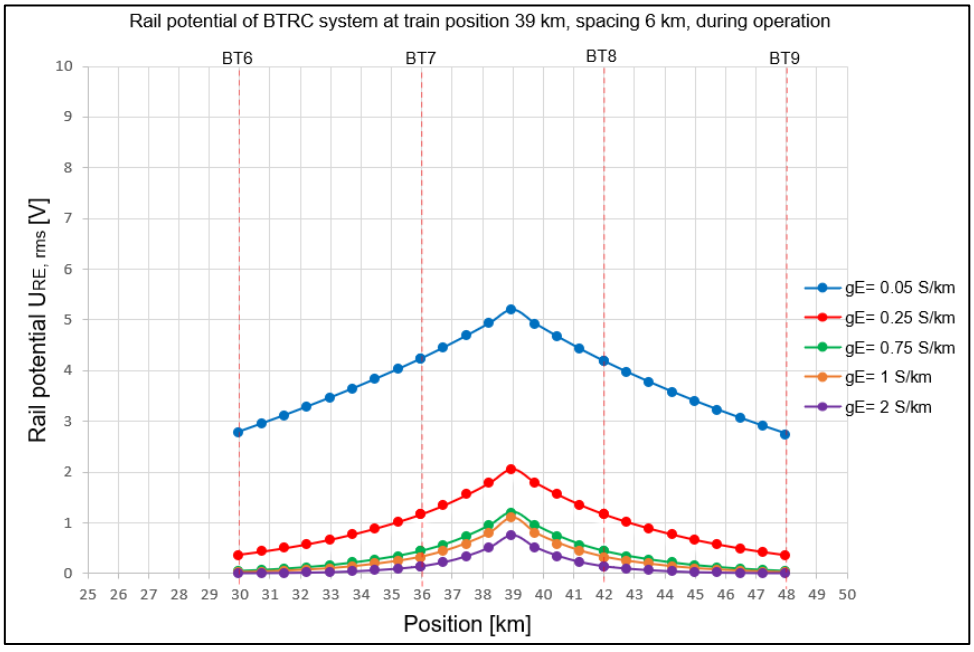

Figure 6-10: Rail potential at train position 39 km, spacing 6 km, during normal operation.

6.2.2 Earth current of BTRC system (6 km) during normal operation

The levels of earth current for the BTRC system with 6 km spacing during normal operation are shown in Figure 6-11 and Figure 6-12.

Figure 6-11 shows the levels of earth current when the train is at the first or last booster transformer. Since the highest levels of earth current from 0 km to 66 km are almost 0 A, the results are studied from 66 km at BT12 to the train location at 84 km at BT15. The highest levels of earth current from 66 km to 78 km are lower than 21 A, then increase and reach the highest level in the section between BT14 at 78 km and BT15 at 84 km.

Figure 6-12 shows the levels of earth current when the train is almost in the middle of the track line between two BTs at 39 km. The results are studied from 30 km at BT6 to 48 km at BT9. The maximum levels of earth current reach immediately ahead and immediately behind the train location (39 km).

As shown in Table 6-6, the maximum values of earth current, when the train is at the first booster transformer are higher than the maximum values of earth current when the train is at 39 km. The results show that the earth current levels increase when gE levels vary from 0.05 S/km to 2 S/km, where the $I_{E, max}$ is 8.45 A at gE = 0.05 S/km and 74.36 A at gE = 2 S/km.

Table 6-6: Maximum earth current of BTRC, train at 1st BT and 39 km for 6 km spacing.

Rail-to-earth leakage conductance (gE) [S/km]	**Maximum earth current ($I_{E, max}$) [A] at 1st BT**	**Maximum earth current ($I_{E, max}$) [A] at 39 km**
0.05	8.45	1.20
0.25	22.67	1.03
0.75	44.89	1.06
1	54.25	1.07
2	74.36	1.08

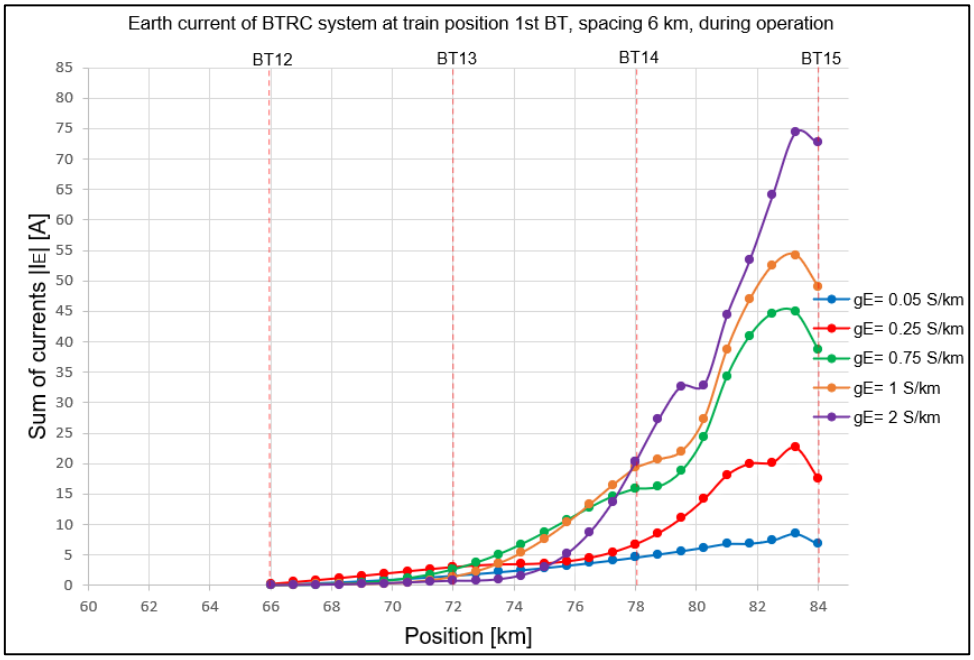

Figure 6-11: Earth current at train position 1st BT, spacing 6 km, during normal operation.

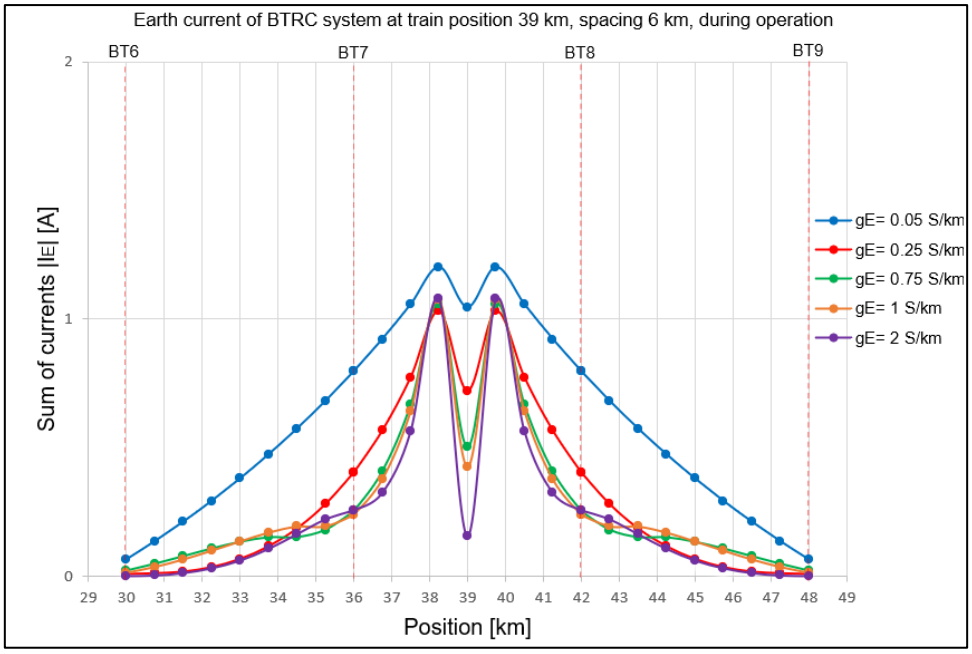

Figure 6-12: Earth current at train position 39 km, spacing 6 km, during normal operation.

6.2.3 Rail potential of AT system (14 km) during normal operation

The levels of rail potential for the AT system with 14 km spacing during normal operation are shown in Figure 6-13 and Figure 6-14.

Figure 6-13 shows the levels of rail potential when the train is at the first or last autotransformer. Since the highest levels of rail potential from 0 km to 42 km are lower than 1 V, the results are studied from 42 km at AT5 to the train location at 84 km at AT8. The levels of rail potential rise at 70 km (AT7), then decrease just after AT7 and rise again to reach the highest level at 84 km.

Figure 6-14 shows the levels of rail potential when the train is almost in the middle of the track line between two ATs at 35 km. The results are studied for the track line from 14 km at AT3 to 56 km at AT6. The peaks of rail potential reach at AT4 and AT5 and become the highest at the train location (35 km).

As shown in Table 6-7, the maximum values of rail potential, when the train is at 35 km are higher than the maximum values of rail potential when the train is at the first autotransformer. The results show that rail potential levels decrease when gE levels vary from 0.05 S/km to 2 S/km, where the $U_{RE, max}$ is 129.90 V at gE = 0.05 S/km and 33.70 V at gE = 2 S/km.

Table 6-7: Maximum rail potential of AT, train at 1st AT and 35 km for 14 km spacing.

Rail-to-earth leakage conductance (gE) [S/km]	**Maximum rail potential ($U_{RE, max}$) [V] at 1st AT**	**Maximum rail potential ($U_{RE, max}$) [V] at 35 km**
0.05	3.51	129.90
0.25	2.09	87.10
0.75	1.14	56.60
1	0.95	49.20
2	0.61	33.70

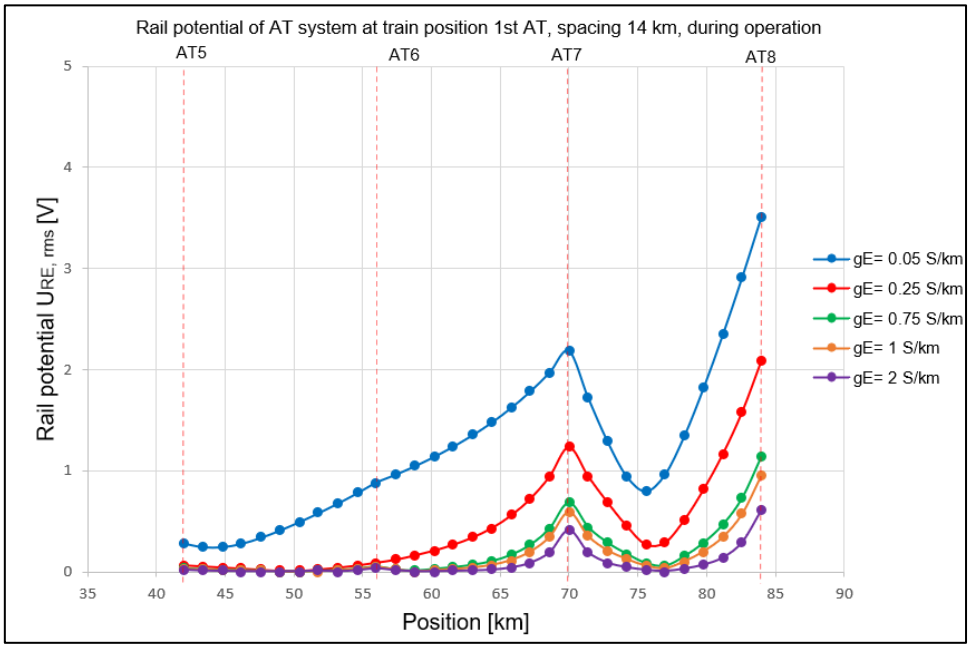

Figure 6-13: Rail potential at train position 1st AT, spacing 14 km, during normal operation.

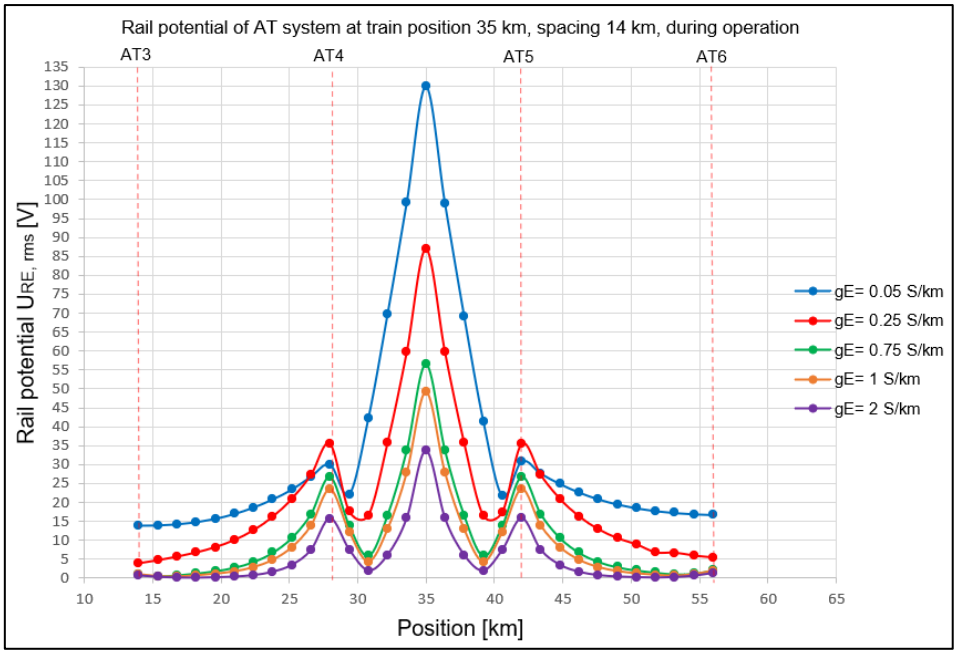

Figure 6-14: Rail potential at train position 35 km, spacing 14 km, during normal operation.

6.2.4 Earth current of AT system (14 km) during normal operation

The levels of earth current for the AT system with 14 km spacing during normal operation are shown in Figure 6-15 and Figure 6-16.

Figure 6-15 shows the levels of earth current when the train is at the first or last autotransformer. Since the highest levels of earth current from 0 km to 42 km are almost 0 A, the results are studied from 42 km at AT5 to the train location at 84 km at AT8. The highest levels of earth current from 42 km to 70 km are lower than 2 A, then increase and reach the highest level in the section between AT7 at 70 km and AT8 at 84 km.

Figure 6-16 shows the levels of earth current when the train is almost in the middle of the track line between two ATs at 35 km. The results are studied from 14 km at AT3 to 56 km at AT6. The levels of earth current increase from 14 km and reach the highest level immediately ahead and immediately behind the train location (35 km).

As shown in Table 6-8, the maximum values of earth current, when the train is at 35 km are higher than the maximum values of earth current when the train is at the first autotransformer. The results show that the earth current levels increase when g_E levels vary from 0.05 S/km to 2 S/km, where the $I_{E,\,max}$ is 12.71 A at g_E = 0.05 S/km and 89.11 A at g_E = 2 S/km.

Table 6-8: Maximum earth current of AT, train at 1st AT and 35 km for 14 km spacing.

Rail-to-earth leakage conductance (g_E) [S/km]	**Maximum earth current ($I_{E,\,max}$) [A] at 1st AT**	**Maximum earth current ($I_{E,\,max}$) [A] at 35 km**
0.05	0.83	12.71
0.25	1.61	34.43
0.75	2.47	61.46
1	2.54	65.20
2	2.35	89.11

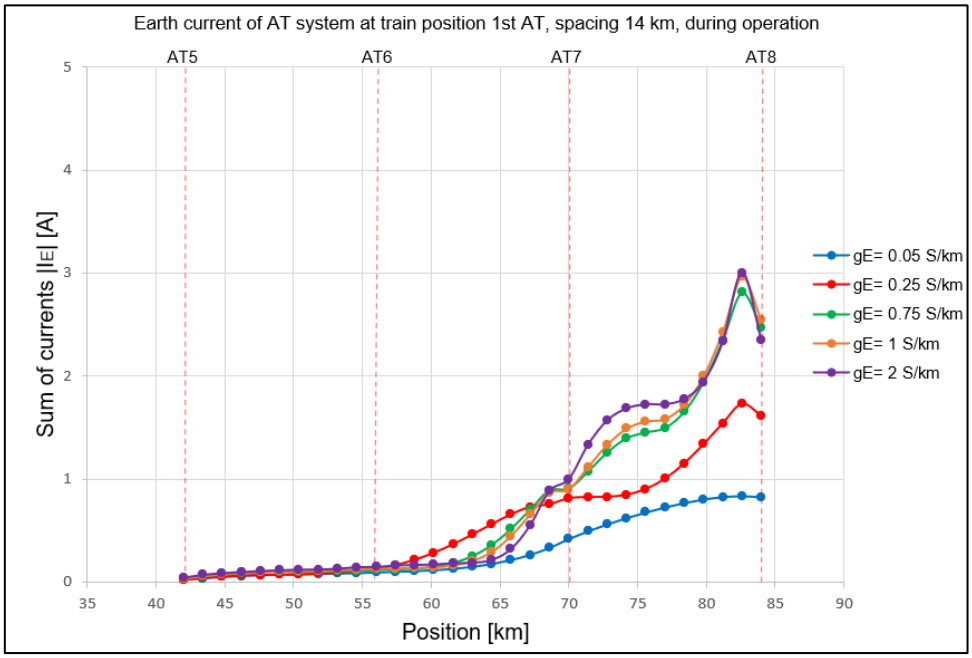

Figure 6-15: Earth current at train position 1st AT, spacing 14 km, during normal operation.

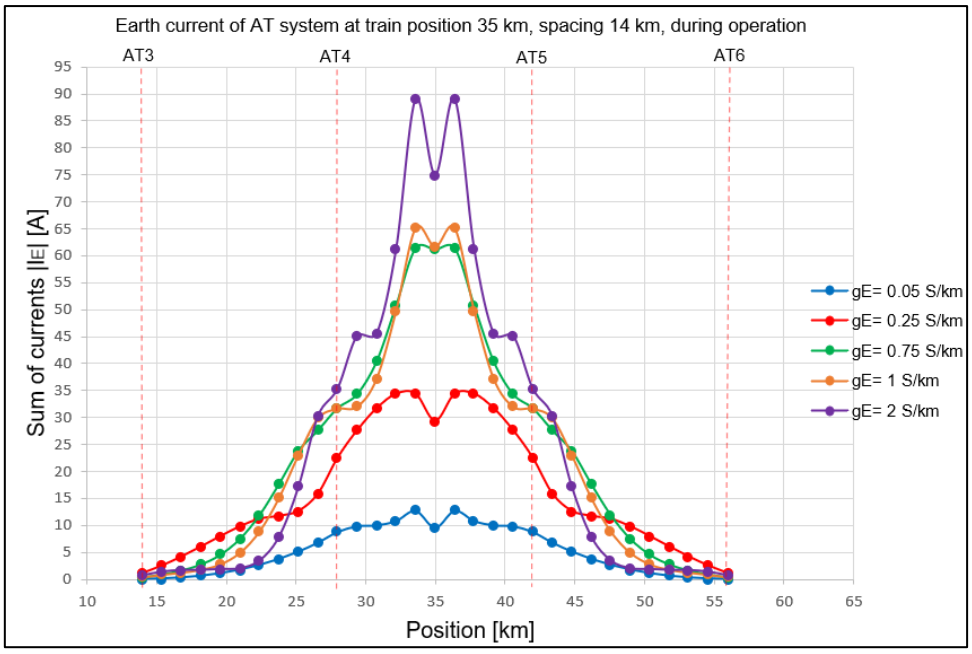

Figure 6-16: Earth current at train position 35 km, spacing 14 km, during normal operation.

6.3 Results of Case Study 3

Case Study 3 studies the effect of rail-to-earth leakage conductance (gE) during short circuit conditions. The transformer spacing is 3km, 6 km for the BTRC system, and 12 km, 14 km for the AT system. The results of the worst-case (12.5 kA) for t = 0.1 s will be introduced in this section, while the short-circuit (8 kA) results for t = 0.3 s will be in Appendix 9.

6.3.1 Rail potential and Earth current of BTRC system (3 km) during s.c. (t = 0.1 s)

The results of rail potential and earth current for the BTRC system with 3 km spacing during a short circuit (t = 0.1 s) are shown in Figure 6-17 and Figure 6-18, respectively. The load (short circuit) is at the first or last booster transformer between CL and RR. The rail potential and earth current are studied from 75 km at BT26 to the load (short circuit) location at 84 km at BT29.

The highest rail potential and earth current from 75 km to 81 km are lower than 210 V and 490 A, respectively. The rail potential levels increase at the connection between the contact line and running rails (Bond) at 82,5 km and decrease immediately behind the bond, then become the highest at the load (short circuit) location at 84 km. The rise in rail potential at the bond at 82,5 km can be noticed for gE levels of 0.75 S/km - 2 S/km. The levels of earth current reach their highest levels in the section between BT28 at 81 km and BT29 at 84 km.

As shown in Table 6-9, rail potential levels decrease while earth current levels increase when gE levels vary from 0.05 S/km to 2 S/km. The $U_{RE,\,max}$ is 1623 V and the $I_{E,\,max}$ is 49.04 A at gE = 0.05 S/km, while the $U_{RE,\,max}$ is 1042 V and the $I_{E,\,max}$ is 1052.93 A at gE = 2 S/km.

Table 6-9: Maximum rail potential and earth current of BTRC, load at 1st BT for 3 km spacing, s.c. (t = 0.1 s).

Rail-to-earth leakage conductance (gE) [S/km]	Maximum rail potential ($U_{RE,\,max}$) [V] at 1st BT	Maximum earth current ($I_{E,\,max}$) [A] at 1st BT
0.05	1623.00	49.04
0.25	1438.80	126.93
0.75	1262.10	409.84
1	1204.40	557.46
2	1042.00	1052.93

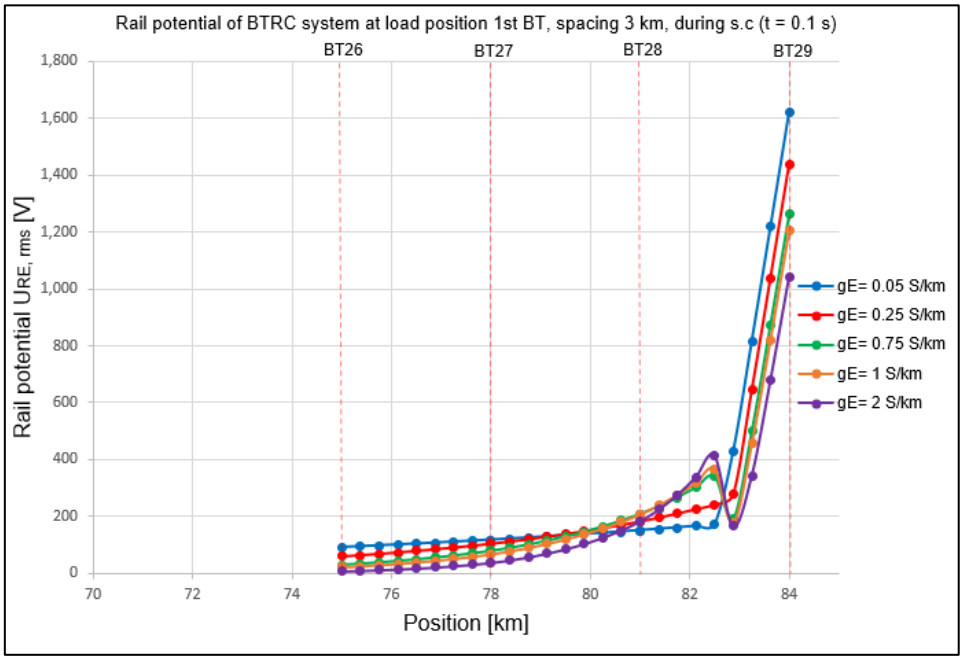

Figure 6-17: Rail potential at load position 1st BT, spacing 3 km, during s.c., t = 0.1 s.

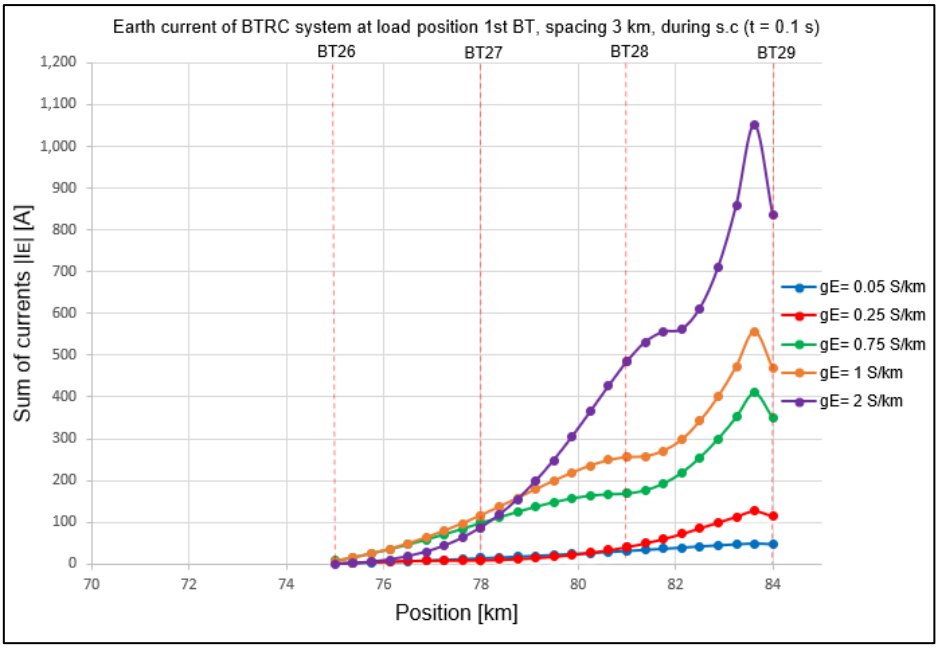

Figure 6-18: Earth current at load position 1st BT, spacing 3 km, during s.c., t = 0.1 s.

6.3.2 Rail potential and Earth current of BTRC system (6 km) during s.c. (t = 0.1 s)

The results of rail potential and earth current for the BTRC system with 6 km spacing during a short circuit (t = 0.1 s) are shown in Figure 6-19 and Figure 6-20, respectively. The load (short circuit) is at the first or last booster transformer. The levels of rail potential and earth current are studied for the track line from 66 km at BT12 to the load (short circuit) location at 84 km at BT15.

The highest rail potential and earth current from 66 km to 78 km are lower than 400 V and 610 A, respectively. The rail potential levels increase at the connection between the contact line and running rails (Bond) at 81 km and decrease immediately behind the bond, then become the highest at the load (short circuit) location at 84 km. The rise in rail potential at the bond at 81 km can be noticed for g_E levels of 0.25 S/km - 2 S/km. The levels of earth current reach their highest levels in the section between BT14 at 78 km and BT15 at 84 km.

As shown in Table 6-10, rail potential levels decrease while earth current levels increase when g_E levels vary from 0.05 S/km to 2 S/km. The $U_{RE,\,max}$ is 3033.7 V and the $I_{E,\,max}$ is 154.46 A at g_E = 0.05 S/km, while the $U_{RE,\,max}$ is 1370.8 V and the $I_{E,\,max}$ is 2693.82 A at g_E = 2 S/km.

Table 6-10: Maximum rail potential and earth current of BTRC, load at 1st BT for 6 km spacing, s.c. (t = 0.1 s).

Rail-to-earth leakage conductance (g_E) [S/km]	**Maximum rail potential ($U_{RE,\,max}$) [V] at 1st BT**	**Maximum earth current ($I_{E,\,max}$) [A] at 1st BT**
0.05	3033.70	154.46
0.25	2458.50	542.20
0.75	1921.40	1389.06
1	1763.00	1717.44
2	1370.80	2693.82

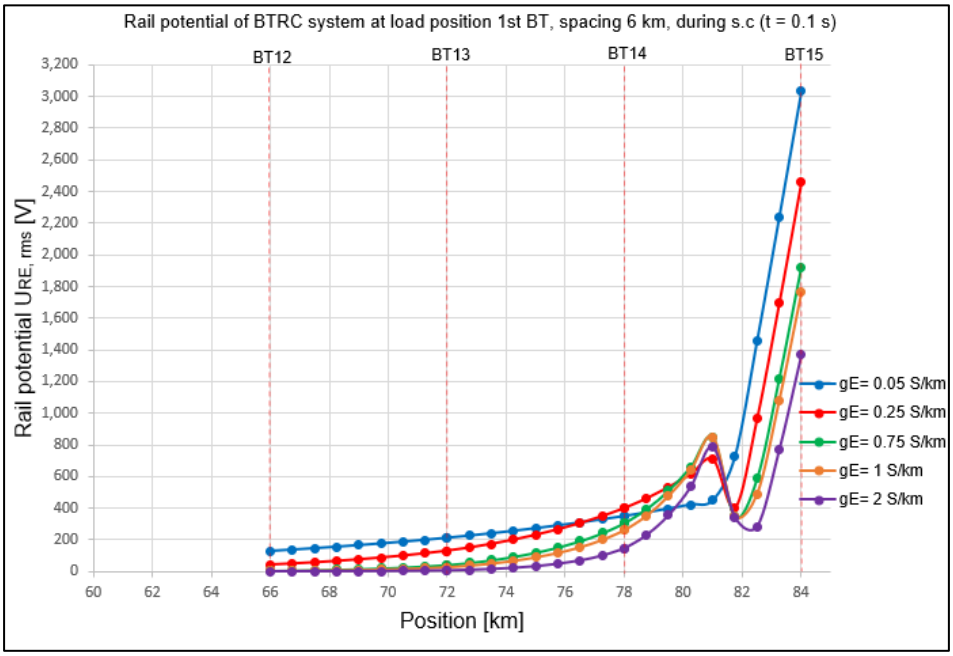

Figure 6-19: Rail potential at load position 1st BT, spacing 6 km, during s.c., t = 0.1 s.

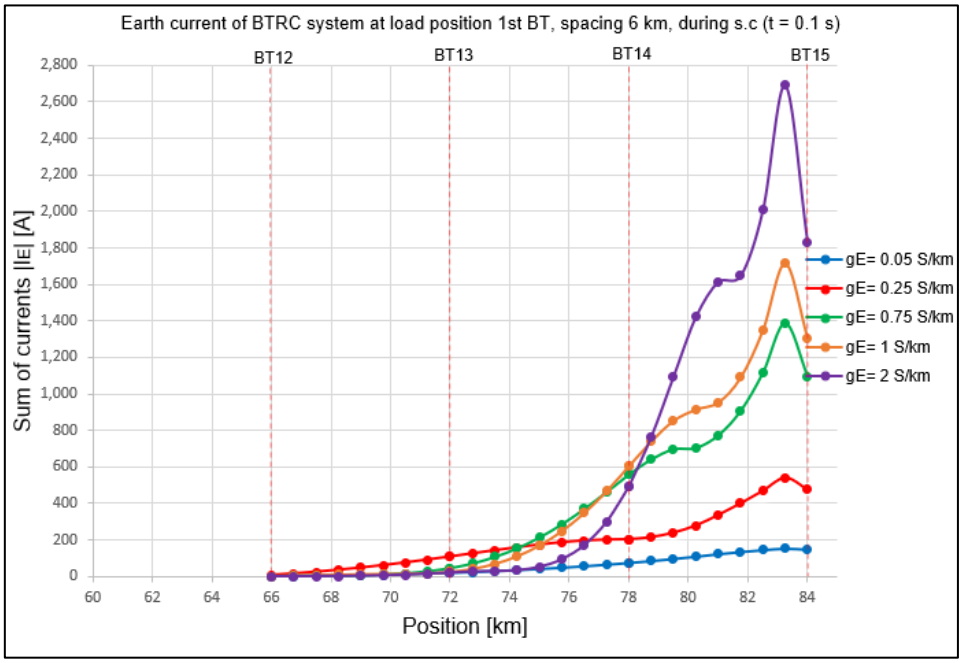

Figure 6-20: Earth current at load position 1st BT, spacing 6 km, during s.c., t = 0.1 s.

6.3.3 Rail potential and Earth current of AT system (12 km) during s.c. (t = 0.1 s)

The results of rail potential and earth current for the AT system with 12 km spacing during a short circuit (t = 0.1 s) are shown in Figure 6-21 and Figure 6-22, respectively. The load (short circuit) is in the middle of the track line between two ATs at 42 km. The results are studied for the track line from 24 km at AT4 to 60 km at AT7.

The peaks of rail potential reach at AT5 and AT6, then become the highest at the load (short circuit) location (42 km). The earth current levels increase from 24 km and reach their highest levels immediately ahead and immediately behind the load (short circuit) location (42 km).

As shown in Table 6-11, rail potential levels decrease while earth current levels increase when gE levels vary from 0.05 S/km to 2 S/km. The $U_{RE,\,max}$ is 2874.4 V and the $I_{E,\,max}$ is 362.26 A at gE = 0.05 S/km, while the $U_{RE,\,max}$ is 865.29 V and the $I_{E,\,max}$ is 3706.63 A at gE = 2 S/km.

Table 6-11: Maximum rail potential and earth current of AT, load at 42 km for 12 km spacing, s.c. (t = 0.1 s).

Rail-to-earth leakage conductance (gE) [S/km]	Maximum rail potential ($U_{RE,\,max}$) [V] at 42 km	Maximum earth current ($I_{E,\,max}$) [A] at 42 km
0.05	2874.40	362.26
0.25	2038.50	1668.82
0.75	1399.60	2935.66
1	1234.70	3246.19
2	865.29	3706.63

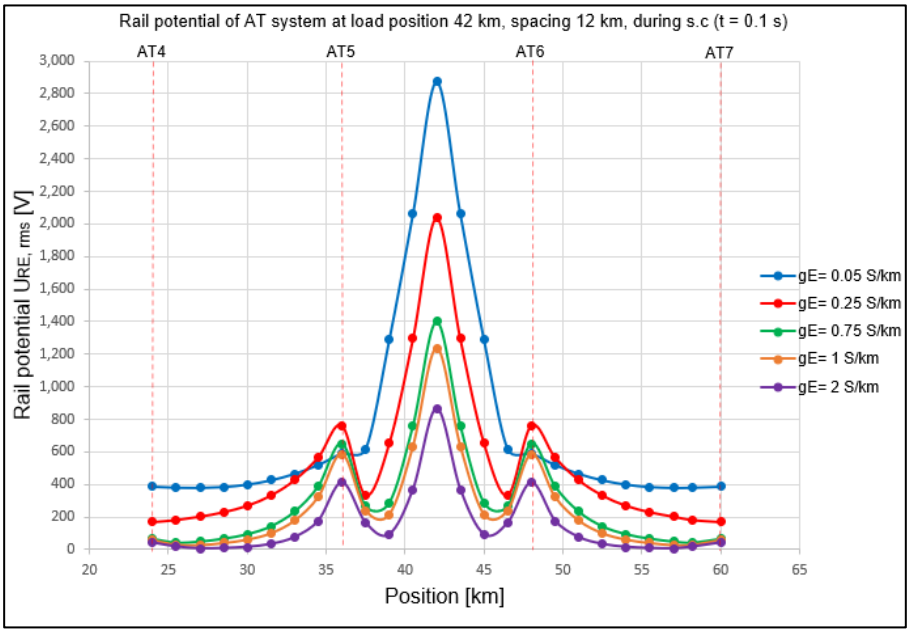

Figure 6-21: Rail potential at load position 42 km, spacing 12 km, during s.c., t = 0.1 s.

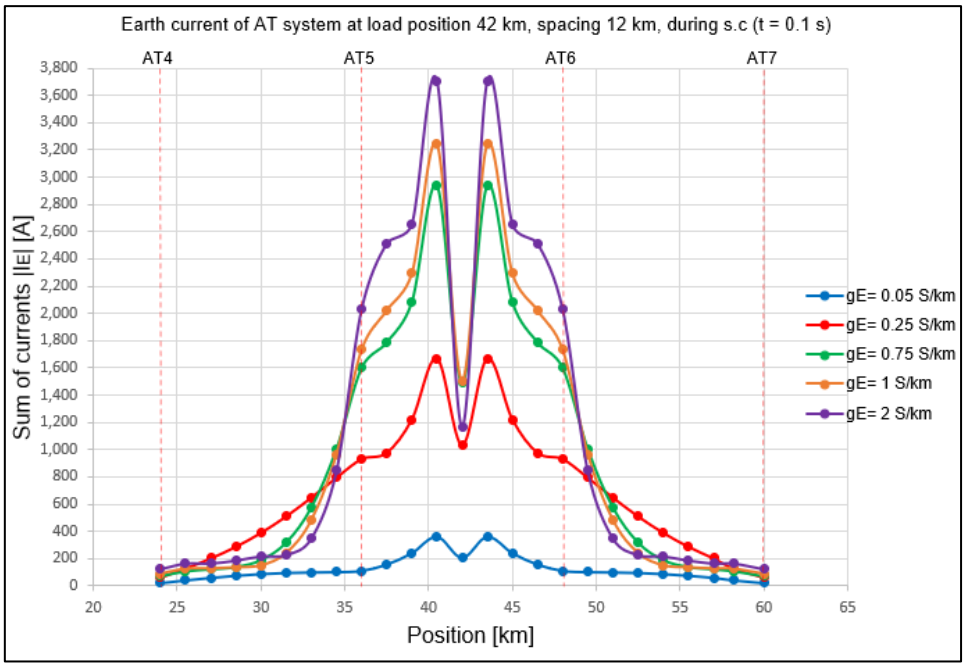

Figure 6-22: Earth current at load position 42 km, spacing 12 km, during s.c., t = 0.1 s.

6.3.4 Rail potential and Earth current of AT system (14 km) during s.c. (t = 0.1 s)

The results of rail potential and earth current for the AT system with 14 km spacing during a short circuit (t = 0.1 s) are shown in Figure 6-23 and Figure 6-24, respectively. The load (short circuit) is almost in the middle of the track line between two ATs at 35 km. The results are studied for the track line from 14 km at AT3 to 56 km at AT6.

The peaks of rail potential reach at AT4 and AT5, then become the highest at the load (short circuit) location (35 km). The earth current levels increase from 14 km and reach their highest levels immediately ahead and immediately behind the load (short circuit) location (35 km).

As shown in Table 6-12, rail potential levels decrease while earth current levels increase when gE levels vary from 0.05 S/km to 2 S/km. The $U_{RE,\,max}$ is 3358.1 V and the $I_{E,\,max}$ is 522.87 A at gE = 0.05 S/km, while the $U_{RE,\,max}$ is 853.42 V and the $I_{E,\,max}$ is 3910.79 A at gE = 2 S/km.

Table 6-12: Maximum rail potential and earth current of AT, load at 35 km for 14 km spacing, s.c. (t = 0.1 s).

Rail-to-earth leakage conductance (gE) [S/km]	**Maximum rail potential ($U_{RE,\,max}$) [V] at 35 km**	**Maximum earth current ($I_{E,\,max}$) [A] at 35 km**
0.05	3358.10	522.87
0.25	2311.10	2152.32
0.75	1534.30	3531.99
1	1339.40	3852.89
2	853.42	3910.79

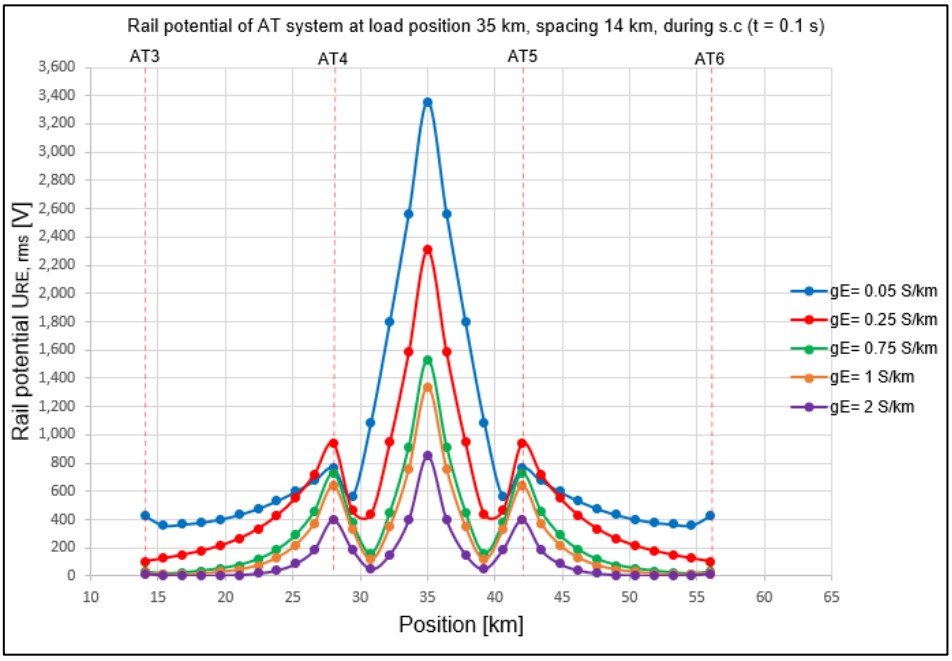

Figure 6-23: Rail potential at load position 35 km, spacing 14 km, during s.c., t = 0.1 s.

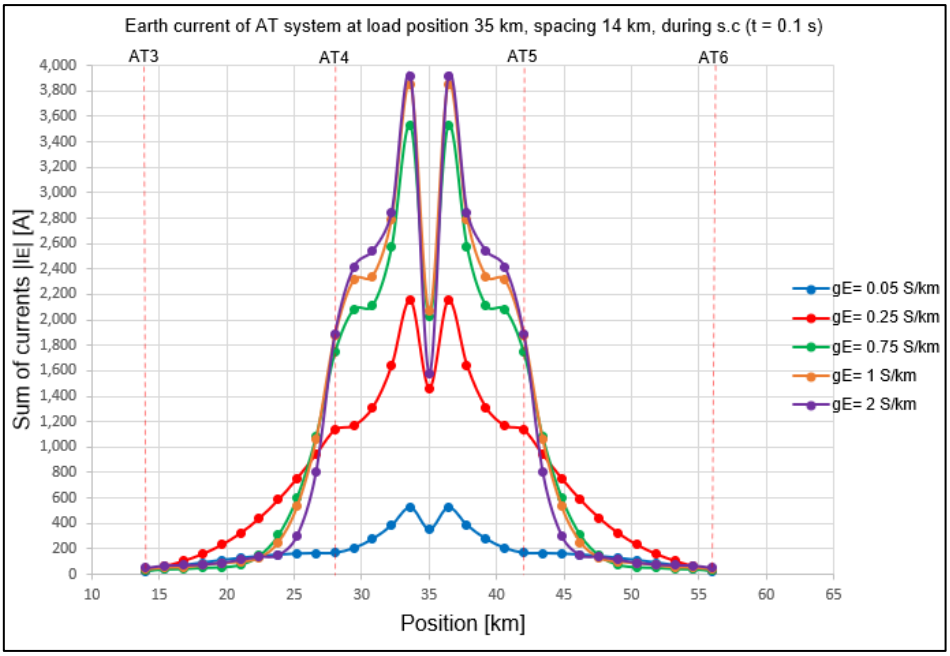

Figure 6-24: Earth current at load position 35 km, spacing 14 km, during s.c., t = 0.1 s.

7 Discussion

7.1 Discussion of ATPDraw models

Models of AC traction feeding systems are simulated in ATPDraw with some assumptions and approaches, such as:

- As shown in Appendix 8, the number of LCC components (PI-equivalent discretization) between BTs or ATs affects the accuracy of rail potential and earth current results by 1 V and 1 A, respectively. Increasing the number of LCC components will improve the accuracy of the results, but it will also increase the complexity and time required to simulate the feeding systems. The maximum discretization accuracy was applied in this thesis to study the BTRC and AT systems under the same conditions.

- Rail-to-earth leakage conductance (gE) levels and running rail impedance are assumed to be constant over the whole system. This assumption can affect the results since the impedance of running rails is current-dependent and gE depends on the weather conditions and soil resistivity.

- The frequency converter station is modelled as a voltage source with a short-circuit impedance (Z_K). The phase angle and voltage level of frequency converter stations are assumed to be 0˚ and 16.5 kV, respectively. These values are not constant and vary by the amplitude and phase angle of the output voltage regulation depending on the load on the track line, the traffic of trains, etc.

- The results of the rail potential and earth current versus train position in km are plotted using the Excel program because the PlotXY function in the ATPDraw program does not provide this possibility.

7.2 Discussion of ATPDraw results

7.2.1 During normal operation

Results of Case Study 1 of the BTRC and AT systems in Chapter 6 (Figure 6-1 to Figure 6-8) show that rail potential and earth current during normal operation are affected by the train position on the track line and rail-to-earth leakage conductance (gE) levels. The highest levels of rail potential and earth current are reached when the train is at the first or last booster transformer for the BTRC system, while they are the highest when the train is in the middle of the track line between two ATs for the AT system. The results also show that rail potential levels decrease while earth current levels increase when gE levels vary from 0.05 S/km to 2 S/km.

Rail potential:

Results of the BTRC system (3 km) and the AT system (12 km) (Figure 6-1, Figure 6-2, Figure 6-5, and Figure 6-6) show that the highest rail potential is reached at the train location. Further, the train current is injected into the running rails at the train location and through the rail-to-earth leakage conductance. Part of this current will flow to earth and cause a rail potential.

For the BTRC system, the current is forced by the booster transformer from the running rails and earth through the rail-to-earth leakage to the return conductor. Due to this process, the current through the booster transformer near the feeding station (at the train location) will be higher, which increases the rail potential. When the train is in the middle of the track line at or near the bond between two BTs, the current is forced through the bond, which minimizes the rail potential.

For the AT system, when the train is in the middle of the track line between two ATs, the current takes two opposite directions and is forced by these two ATs from the running rails and earth through the rail-to-earth leakage. This process will increase the level of rail potential at the train location. When the train is near the autotransformer, most of the current is forced directly by this autotransformer, which minimizes the rail potential.

As shown in Table 6-1 and Table 6-3, the highest rail potential at gE = 0.05 S/km is 64.26 V for the BTRC system and 117.74 V for the AT system. Levels of rail potential decrease by a factor of 0.65 for the BTRC system and 0.29 for the AT system when gE levels vary from 0.05 S/km to 2 S/km. The results are more even at higher levels of gE.

Earth current:

The results of earth current for the BTRC system (3 km) and the AT system (12 km) are shown in Figure 6-3, Figure 6-4, Figure 6-7 and Figure 6-8.

For the same reasons as for rail potential, the highest earth current is reached when the train is at the first or last booster transformer for the BTRC system. The highest earth current occurs in the section between the train location (at the first or last booster transformer) and the next booster transformer. For the AT system, the highest earth current is different from the BTRC system. When the train is in the middle of the track line between two autotransformers, the highest earth current occurs as two peaks of earth current immediately ahead and immediately behind the train location.

As shown in Table 6-2 and Table 6-4, the highest earth current at g_E = 0.05 S/km is 2.36 A for the BTRC system and 11.62 A for the AT system. Levels of earth current increase by a factor of 15.2 for the BTRC system and 6.75 for the AT system when g_E levels vary from 0.05 S/km to 2 S/km. The results are more even at higher levels of g_E.

Transformer spacing effect:

Results of Case Study 2 show that the level of rail potential and earth current is also affected by the spacing between BTs and ATs. By increasing the spacing for the BTRC system from 3 km to 6 km and from 12 km to 14 km for the AT system, the levels of rail potential and earth current are also increased. This effect occurs due to the voltage drop in the BTs and ATs.

For the BTRC system, the highest levels of rail potential and earth current increase by a factor of 1.89 – 1.28 and 3.6 – 2.07, respectively, when the train is at the first or last booster transformer. For the AT system, the highest rail potential and earth current increase by a factor of 1.1 when the train is in the middle of the track line between two autotransformers. Increasing the spacing by 2 km for the AT system does not have a great effect on the levels of rail potential and earth current, especially at g_E from 0.75 S/km to 2 S/km.

7.2.2 During short circuit

Results of Case Study 3 studied the rail potential and earth current for the BTRC and AT systems during short circuit conditions. The short circuit is represented as an impedance in the models of traction feeding systems. The simulation of a short circuit to determine the touch voltage is more complex because it needs to calculate the I_{rms} for each point on a track line if

one takes into consideration that the short circuit current varies when the short circuit moves toward the middle of the track line [12].

In Case Study 3, it is assumed that there is a short circuit between the contact line (CL) and the running rails (R). The short circuit is located at the first or last booster transformer for the BTRC system, while it is in the middle of the track line between two ATs for the AT system because these locations give the highest levels of rail potential and earth current, as discussed in Subsection 7.2.1. As for normal operation, short circuit results are affected by rail-to-earth leakage conductance (gE) and transformer spacing.

Rail potential and earth current:

For t = 0.1 s, Table 6-9 and Table 6-11 show that the highest rail potential and earth current at gE = 0.05 S/km are 1623 V and 49.04 A, respectively, for the BTRC system (3 km). The highest levels are 2874.4 V and 362.26 A, respectively, for the AT system (12 km). Levels of rail potential decrease by a factor of ca. 0.64 for the BTRC system and ca. 0.3 for the AT system when gE levels vary from 0.05 S/km to 2 S/km. Levels of earth current increase by a factor of 21.47 for the BTRC system and ca. 10.23 for the AT system when gE levels vary from 0.05 S/km to 2 S/km.

For t = 0.3 s, Table A9-10-1 and Table A9-10-3 show that the highest rail potential and earth current at gE = 0.05 S/km are 1062.8 V and 34.89 A, respectively, for the BTRC system (3 km). The highest levels are 1882.5 V and 153.6 A, respectively, for the AT system (12 km). Levels of rail potential decrease by a factor of ca. 0.65 for the BTRC system and ca. 0.3 for the AT system when gE levels vary from 0.05 S/km to 2 S/km. Levels of earth current increase by a factor of ca. 22.73 for the BTRC system and ca. 14.52 for the AT system when gE levels vary from 0.05 S/km to 2 S/km.

Transformer spacing effect:

Results of Case Study 3 show that levels of rail potential and earth current are increased by increasing the spacing between BTs or ATs due to the voltage drop in the BTs and ATs.

For the BTRC system, the highest levels of rail potential are increased by a factor of 1.87 – 1.3 for t = 0.1 s and 1.887 – 1.3 for t = 0.3 s. The highest levels of earth current are also increased by a factor of 3.15 – 2.55 for t = 0.1 s and 2.956 – 2.617 for t = 0.3 s.

For AT system, the highest levels of rail potential are increased by a factor of 1.168 at t= 0.1 s and 1.138 for t = 0.3 s. The highest levels of earth current are also increased by a factor of 1.44 – 1.055 for t = 0.1 s and ca. 1.356 – 1.078 for t = 0.3 s.

7.3 Comparison of the traction feeding systems

This section compares the traction feeding systems that are simulated in ATPDraw. The comparison will focus on the rail potential and earth current results that are discussed in Section 7.2.

- The highest rail potential and earth current levels for the BTRC system reach when the load (train or short circuit) is at the first or last booster transformer, while for the AT system, they reach when the load (train or short circuit) is in the middle of the track line between two ATs. The rail potential reaches its highest level at the load location for the BTRC and AT systems. For the BTRC system, the earth current reaches its highest level in the section between the nearest booster transformer and the load location (at the first BT), while for the AT system, it reaches immediately ahead and immediately behind the load location. The reason for this phenomenon is the injected train current, as discussed in Section 7.2.

- Rail-to-earth leakage conductance (gE) has a more significant effect on the levels of rail potential (U_{RE}) for the AT system than for the BTRC system during normal operation and short circuit conditions. For example, the rail potential during normal operation when gE varies from 0.05 S/km to 2 S/km decreases by a factor of 0.29 for the AT system (12 km spacing, train at 42 km), while it decreases by a factor of 0.65 for the BTRC system (3 km spacing, train at the first BT). Table 7-1 shows more about the U_{RE} values.

- Rail-to-earth leakage conductance (gE) has a more significant effect on the levels of earth current (I_E) for the BTRC system than for the AT system during normal operation and short circuit conditions. For example, the earth current during normal operation when gE varies from 0.05 S/km to 2 S/km increases by a factor of 15.2 for the BTRC system (3 km spacing, train at the first BT), while it increases by a factor of 6.75 for the AT system (12 km spacing, train at 42 km). Table 7-1 shows more about the I_E values.

- Spacing has a significant effect on the rail potential and earth current for the BTRC system during normal operation and short circuit conditions. For example, when the

train at the first BT and the spacing of the BTRC system are increased from 3 km to 6 km, the rail potential and earth current increase by a factor of 1.89 – 1.28 and 3.6 – 2.07, respectively. Increasing spacing from 12 km to 14 km for the AT system has a low effect because it was just increased by 2 km. Table 7-1 shows more about U_{RE} and I_E values.

- The earth current (I_E) of the AT system (12 km and 14 km) is higher than the earth current (I_E) of the BTRC system (3 km and 6 km) at gE 0.05 S/km to 2 S/km. The rail potential (U_{RE}) of the AT system (12 km and 14 km) is higher than the U_{RE} of the BTRC system (3 km) at gE 0.05 S/km to 1 S/km, but it is lower than the U_{RE} of the BTRC system (6 km) at gE 0.25 S/km to 2 S/km. The difference in spacing between the BTRC and AT systems, the short circuit impedance of transformers, and the series impedance of the system can be the reasons for this variation. Table 7-1 compares the maximum rail potential and earth current values.

Table 7-1: Comparison the maximum levels of the U_{RE} and I_E.

During normal operation								
gE [S/km]	**BTRC 3km**		**BTRC 6 km**		**AT 12 km**		**AT 14 km**	
	U_{RE}	**I_E**	**U_{RE}**	**I_E**	**U_{RE}**	**I_E**	**U_{RE}**	**I_E**
0.05	64.26	2.36	121.39	8.45	117.74	11.62	129.90	12.71
0.25	57.09	8.61	97.92	22.67	81.94	28.74	87.10	34.43
0.75	50.18	18.38	75.73	44.89	55.22	57.11	56.60	61.46
1	47.92	22.35	69.12	54.25	48.50	61.95	49.20	65.20
2	41.59	35.89	53.12	74.36	33.74	78.47	33.70	89.11
During short circuit (t = 0.1 s)								
0.05	1623.00	49.04	3033.70	154.46	2874.40	362.26	3358.10	522.87
0.25	1438.80	126.93	2458.50	542.20	2038.50	1668.82	2311.10	2152.32
0.75	1262.10	409.84	1921.40	1389.06	1399.60	2935.66	1534.30	3531.99
1	1204.40	557.46	1763.00	1717.44	1234.70	3246.19	1339.40	3852.89
2	1042.00	1052.93	1370.80	2693.82	865.29	3706.63	853.42	3910.79
During short circuit (t = 0.3 s)								
0.05	1062.80	34.89	2005.50	103.16	1882.50	153.60	2142.40	209.74
0.25	943.42	89.48	1623.40	400.38	1324.20	740.22	1458.10	920.01
0.75	830.06	307.98	1264.90	1040.18	904.38	1472.97	962.69	1814.26
1	793.20	417.87	1159.10	1316.16	797.39	1724.62	840.31	2039.11
2	689.80	793.00	897.43	2075.36	559.08	2229.65	553.09	2404.51

7.4 Comparison with Varju's results

To verify the results of Chapter 6, the maximum rail potential and earth current results will be compared to Varju's results [4, 5]. It is worth mentioning that Varju studied the rail potential and earth current during normal operation with 3 km and 6 km of transformer spacing for the BTRC system and 12 km of transformer spacing for the AT system. Varju's studies were investigated at g_Es of 0.05 S/km, 0.25 S/km, and 0.75 S/km. Therefore, part of the thesis results will be verified, as shown in the tables below.

Table 7-2: Verification of the BTRC system of 3 km transformer spacing.

	BTRC, 3 km			**BTRC, 3 km**		
Train [Km]	**1st BT**			**Middle (40.5 km)**		
g_E [S/km]	**0.05**	**0.25**	**0.75**	**0.05**	**0.25**	**0.75**
Thesis's U_{RE} [V]	64.26	57.09	50.18	5.29	2.16	1.24
Varju's U_{RE} [V]	62.00	57.00	51.00	3.30	2.30	1.20
Thesis's I_E [A]	2.36	8.61	18.38	0.41	0.39	0.50
Varju's I_E [A]	1.30	7.00	20.00	0.25	0.53	1.36

Table 7-3: Verification of the BTRC system of 6 km transformer spacing.

	BTRC, 6 km			**BTRC, 6 km**		
Train [Km]	**1st BT**			**Middle (39 km)**		
g_E [S/km]	**0.05**	**0.25**	**0.75**	**0.05**	**0.25**	**0.75**
Thesis's U_{RE} [V]	121.39	97.92	75.73	5.21	2.06	1.21
Varju's U_{RE} [V]	116.00	101.00	89.00	5.00	4.60	4.00
Thesis's I_E [A]	8.45	22.67	44.89	1.20	1.03	1.06
Varju's I_E [A]	4.20	20.00	49.50	0.30	1.36	4.50

Table 7-4: Verification of the AT system of 12 km transformer spacing.

	AT, 12 km			**AT, 12 km**		
Train [Km]	**1st AT**			**Middle (42 km)**		
g_E [S/km]	**0.05**	**0.25**	**0.75**	**0.05**	**0.25**	**0.75**
Thesis's U_{RE} [V]	3.66	2.28	1.27	117.74	81.94	55.22
Varju's U_{RE} [V]	*	*	*	93.88	65.31	44.44
Thesis's I_E [A]	0.75	1.78	2.75	11.62	28.74	57.11
Varju's I_E [A]	*	*	*	17.00	37.00	53.00

*This scenario was not studied by Varju in [5].

It is worth mentioning that part of Varju's results are obtained from graphs. This action can affect the accuracy of decimal numbers.

The results of the BTRC system (3 km) are in good agreement with Varju's results, with some variations in the rail potential result of 2 V to 2.26 V at g_E = 0.05 S/km and less than 2 A in

the earth current results. The BTRC (6 km) and AT (12 km) systems also have variations in results. For example, the difference between the rail potential results for the AT system (12 km) is about 23.86 V at g_E = 0.05 S/km. There are some factors that can be the reason for these variations, such as:

- Simulation methods: In this thesis, rail-to-earth leakage conductance (g_E) is represented as concentrated resistances to earth. The number of g_Es is assumed to be at each LCC component and transformer. The simulation method of g_E is not shown in Varju's studies [4, 5].
- Data: There are differences in the data of some components that are used in this thesis, such as the series impedance of conductors and wires, the single-phase transformers of frequency converter stations, and the short-circuit impedance of BTs and ATs.

7.5 NEK EN 50122-1 standard

As explained in Chapter 2, the levels of rail potential of traction feeding systems should be according to the EN 50122-1 standard. The permissible levels during normal operation and short-circuit conditions are given in Table 2-1. The voltage (U_{RP}) between the running rail and the measuring point (touch voltage) depends on the distance between the running rail and the measuring point. The relationship between distance and touch voltage is given in Table 2-2.

As recommended by the Bane NOR's technical regulations [8], it will assume a person is standing 1 m from the nearest electrode or fundament that is connected to the running rail to calculate the allowed touch voltage (permissible rail potential). As shown in Table 2-2, the U_{RP} for a 1 m distance is 30% of the rail potential ($0.3 \cdot U_{RE}$).

As shown in the tables below, most of the touch voltage levels for the BTRC and AT systems during normal operation and short-circuit conditions are according to EN 50122-1 requirements. Touch voltage levels that are not according to EN 50122-1 requirements, are marked in bold in the tables below. For the BTRC system, the deviation from EN 50122-1 occurs during short-circuit when the transformer spacing is increased from 3 km to 6 km at low g_E. For the AT system (12 km and 14 km), the deviation from EN 50122-1 occurs during short-circuit at g_E = 0.05 S/km. The source of deviation can be the spacing between BTs and ATs, g_E levels, or the series impedance of the return circuit.

The EN 50122-1 standard gives some requirements and provisions to reduce the touch voltage, such as increasing levels of g_E and reducing the spacing between BTs and ATs. The investigation of these provisions is not part of this thesis.

During normal operation:

Table 7-5: Touch voltage of the BTRC system during normal operation.

gE [S/km]	**$U_{RE, max}$ [V] BTRC (3 km)**	**U_{RP} [V] $U_{RE, max}$ < 65 V**	**$U_{RE, max}$ [V] BTRC (6 km)**	**U_{RP} [V] $U_{RE, max}$ < 65 V**
0.05	64.26	19.28	121.39	36.42
0.25	57.09	17.13	97.92	29.38
0.75	50.18	15.05	75.73	22.72
1	47.92	14.38	69.12	20.74
2	41.59	12.48	53.12	15.94

Table 7-6: Touch voltage of the AT system during normal operation.

gE [S/km]	**$U_{RE, max}$ [V] AT (12 km)**	**U_{RP} [V] $U_{RE, max}$ < 65 V**	**$U_{RE, max}$ [V] AT (14 km)**	**U_{RP} [V] $U_{RE, max}$ < 65 V**
0.05	117.74	35.32	129.90	38.97
0.25	81.94	24.58	87.10	26.13
0.75	55.22	16.57	56.60	16.98
1	48.50	14.55	49.20	14.76
2	33.74	10.12	33.70	10.11

During Short circuit:

Table 7-7: Touch voltage of the BTRC system during short-circuit.

gE [S/km]	**Switching time [s]**	**$U_{RE, max}$ [V] BTRC (3 km)**	**U_{RP} [V] $U_{RE, max}$ < $U_{te, max}$**	**$U_{RE, max}$ [V] BTRC (6 km)**	**U_{RP} [V] $U_{RE, max}$ < $U_{te, max}$**
0.05	0.1	1623.00	486.90	3033.70	**910.11**
0.25		1438.80	431.64	2458.50	737.55
0.75		1262.10	378.63	1921.40	576.42
1		1204.40	361.32	1763.00	528.90
2		1042.00	312.60	1370.80	411.24
0.05	0.3	1062.80	318.84	2005.50	**601.65**
0.25		943.42	283.03	1623.40	**487.02**
0.75		830.06	249.02	1264.90	379.47
1		793.20	237.96	1159.10	347.73
2		689.80	206.94	897.43	269.23

Table 7-8: Touch voltage of the AT system during short-circuit.

gE [S/km]	Switching time [s]	$U_{RE, max}$ [V] AT (12 km)	U_{RP} [V] $U_{RE, max} < U_{te, max}$	$U_{RE, max}$ [V] AT (14 km)	U_{RP} [V] $U_{RE, max} < U_{te, max}$
0.05	0.1	2874.40	**862.32**	3358.10	**1007.43**
0.25		2038.50	611.55	2311.10	693.33
0.75		1399.60	419.88	1534.30	460.29
1		1234.70	370.41	1339.40	401.82
2		865.29	259.59	853.42	256.03
0.05	0.3	1882.50	**564.75**	2142.40	**642.72**
0.25		1324.20	397.26	1458.10	437.43
0.75		904.38	271.31	962.69	288.81
1		797.39	239.22	840.31	252.09
2		559.08	167.72	553.09	165.93

7.6 NEK EN 50121 (5-parts) standards

In the EN 50121 series of Electromagnetic Compatibility (EMC) standards, there is no guide or requirement about the permissible levels of earth current in the AC traction feeding system. As mentioned in Chapter 2, EN 50121 standards provide requirements for emission and immunity limitations between the various systems and equipment of the railway infrastructure, such as electronic and electric apparatus, signalling and telecommunications (S&T) apparatus and lines, etc.

EN 50121 standards can use the levels of earth current to study the induced voltage effect on the S&T lines that are installed along the track line in parallel with the running rails. The levels of earth current can also be useful for other studies like EMC management plan, as specified in EN 50121 Part 1. The EMC management plan identifies the source of noise, such as the earth current on neighbouring systems. It is also providing methods to reduce these noises. To study the induction effect or earth current noise on neighbouring systems and lines, one needs information about these systems and lines. These types of studies are not part of this thesis.

8 Conclusion and Further Work

8.1 Conclusion

The levels of rail potential and earth current for the BTRC and AT systems during normal operation and short circuit conditions are studied in this thesis. The objectives were to analyse the effect of rail-to-earth leakage conductance (gE), train position, and spacing between BTs and ATs; compare the BTRC and AT systems; use ATPDraw for simulation of the BTRC and AT systems; verify if the thesis results are in accordance with Varju's results; and check if the thesis results are according to the relevant standards and regulations. In addition to the conclusion, hypotheses will be clarified in this chapter.

The following conclusions can be drawn from the results and discussion of Case Studies 1, 2, and 3:

- ATPDraw provides a good possibility to simulate AC traction feeding systems using diverse components such as energy sources, booster transformers, autotransformers, and LCC components. The LCC components are used to represent the overhead contact line (OCL) between transformers (BTs and ATs). The LCC component has an additional feature to specify the OCL type. In this thesis, an "Overhead line" was utilized. It can also be an ''Enclosing Pipe'' to simulate the OCL inside tunnels, as in Høidalen's study [2].

- There is no function in ATPDraw to simulate the continuous rail-to-earth leakage conductance (gE). Therefore, gEs were simulated as concentrated resistances to the earth along the track line.

- Rail impedance is not a constant value for the whole system because it is current-dependent. In the thesis, the rail impedance value is assumed to be constant for the whole system because ATPDraw does not provide the ability to study current-dependent rail impedances.

- The rail-to-earth leakage conductance (gE), train position, and spacing between BTs and ATs have a significant effect on the levels of rail potential (U_{RE}) and earth current (I_E).

- The measurement of rail-to-earth leakage conductance (gE) is important because of its effect on the levels of rail potential (U_{RE}) and earth current (I_E).

- The rail potential levels of the AT system (12 km and 14 km) were higher than the rail potential of the BTRC system (3 km) at gE up to 1 S/km, while they were lower than the rail potential of the BTRC system (6 km) at gE ≥ 0.25 S/km. The earth current levels of the AT system (12 km and 14 km) were higher than the levels of the BTRC system (3 km and 6 km) at gE 0.05 S/km to 2 S/km.

- The results of rail potential (U_{RE}) and earth current (I_E) at higher gE levels show that the transformer spacing for the BTRC and AT systems can be increased from the recommended spacing by Bane NOR's technical regulations.

- The comparison between the thesis results and Varju's results gives a good agreement, although there were some variations due to different simulation methods and data used in this thesis.

- The rail potential (U_{RE}) results met the EN 50122-1 requirements, except for some values at low gE levels.

- There is no standard to verify the permissible levels of earth current. Earth current (I_E) values can be used for other studies, such as the EMC management plan and the induction effect on neighbouring lines.

8.1.1 Hypothesis

- BTRC system: the rail potential and the earth current reached their maximum levels when the train was at the first or last booster transformer. AT system, the rail potential and earth current reached their maximum levels when the train was in the middle of the track line between two ATs.

- By increasing the level of rail-to-earth leakage conductance (gE) from 0.05 S/km to 2 S/km, the rail potential (U_{RE}) levels are decreased while the earth current (I_E) levels are increased, as shown in the table below.

Table 8-1: Rail-to-earth leakage conductance effect.

	Decreasing factor of $U_{RE, max}$		**Increasing factor of $I_{E, max}$**	
During operation				
BTRC system (3 km)	0.65		15.2	
AT system (12 km)	0.29		6.75	
During short-circuit	t = 0.1 s	t = 0.3 s	t = 0.1 s	t = 0.3 s
BTRC system (3 km)	ca. 0.64	ca. 0.65	21.47	ca. 22.73
AT system (12 km)	ca. 0.3	ca. 0.3	ca. 10.23	ca. 14.52

- By increasing the transformer spacing between BTs (3 km to 6 km) and ATs (12 km to 14 km), rail potential and earth current levels are increased during normal operation and short circuit conditions, as shown in the table below.

Table 8-2: Spacing between BTs and ATs effect.

	Increasing factor of $U_{RE, max}$		**Increasing factor of $I_{E, max}$**	
During operation	**-**		**-**	
BTRC system	1.89 – 1.28		3.6 – 2.07	
AT system	1.1		1.1	
During short-circuit	t = 0.1 s	t = 0.3 s	t = 0.1 s	t = 0.3 s
BTRC system	1.87 – 1.3	1.887 – 1.3	3.15 – 2.55	2.956 – 2.617
AT system	1.168	1.138	1.44 – 1.055	1.356 – 1.078

- The levels of rail potential (U_{RE}) and earth current (I_E) for the BTRC and AT systems are not identical. The rail potential levels of the AT system (12 km and 14 km) were higher than the rail potential of the BTRC system (3 km) at 0.05 S/km to 1 S/km, while they were lower than the rail potential of the BTRC system (6 km) at gE 0.25 S/km to 2 S/km. The earth current levels of the AT system (12 km and 14 km) were higher than the levels of the BTRC system (3 km and 6 km) at gE 0.05 S/km to 2 S/km.

8.2 Further work

This thesis provides the possibility of utilizing the AC traction feeding models that are simulated in ATPDraw and their results for future studies. The recommendations for further work are:

- Measure the rail-to-earth leakage conductance (gE) and rail impedance to use them as design values in the calculations and simulations.
- Study the effect of earth resistivity on rail potential (U_{RE}) and earth current (I_E). The calculated series impedances of conductors, wires, and running rails for earth resistivities of 100 Ωm, 2600 Ωm, and 5000 Ωm can be used.
- Study the levels of rail potential (U_{RE}) and earth current (I_E) by using the spacing between BTs and ATs as a parameter, for example, spacing of 3 km, 6 km, and 9 km for the BTRC system and 10 km, 15 km, and 20 km for the AT system.
- Investigate the economic consequences of increasing the transformer spacing for the AC traction feeding systems.
- The earth current (I_E) results can be investigated for an EMC management plan study or to study the induction effect on the signalling and telecommunication (S&T) lines.
- Study the recommended provisions in the EN 50122-1 standard to reduce the rail potential levels (U_{RE}) that exceed the permissible levels.
- Analyse the AC traction feeding systems by considering the practice values of phase shift and voltage amplitude for the frequency converter stations.
- In addition to the conductors, wires, and running rails of the BTRC and AT systems, simulate the along-track earth wires.
- Study and evaluate the levels of rail potential (U_{RE}) and earth current (I_E) during short-circuit conditions at different locations along the track line.
- Modify and further investigate Case Study 3 (during short-circuit conditions) to determine the short-circuit impedance that is seen by the protection relay. It can be investigated for different types of short circuits, such as at PL-NL, PL-RR, or CL-RC. This kind of study is useful for distance protection settings.

9 References

[1] Varju Gy., Sollerkvist F. J., Karlsson D. and Olofsson M., “Application of AT and AT/BT traction feeding systems in Norway Preliminary study,” STRI Report S01-238, 2001.

[2] Høidalen, H. Kr., “Calculation of current flow and induced voltages in AT system [Original title in Norwegian: Beregning av strømflyt og induserte spenninger i kontaktledningsanlegg (AT)],” NTNU - Norwegian University of Science and Technology, Trondheim, 2013.

[3] Svendsen, E. K., “Current and voltage levels in the return circuit of the BTRC and AT systems [Original title in Norwegian: Strøm- og spenningsnivåer i returkretsen til BTRC- og AT-systemet],” NTNU - Norwegian University of Science and Technology, Sandvika, 2016.

[4] Varju Gy., and Sollerkvist F. J. , “Comparison of the BTRR, BTRC and the AT Traction Feeding Systems in Norway,” STRI Report R02-100, 2003.

[5] Varju, Gy., “Further investigation of AT-system for the Norwegian Railway Part 2, EMC Study for ATPLNL system in Norway,” VARJU EMC Bt, Budapest, 2005.

[6] Aljahaf, M. A. Y., “Electric traction power supply for AT system and BTRC system in railways, Rotary and static converter stations [Original title in Norwegian: Banestrømforsyning mot AT-system og BTRC-system i jernbane, Roterende og statiske omformerstasjoner],” Project report in TET4510 - Electrical Energy and Power Systems, Department of Electric Energy, NTNU - Norwegian University of Science and Technology, Trondheim, Dec. 2022.

[7] Høidalen H. Kr., Prikler L., and Peñaloza F., ATPDRAW version 7.3 for windows, Users' Manual, 2021.

[8] Bane NOR, “Bane NOR's Technical regulations, [Original title in Norwegian: Bane NORs Tekniske regelverk],” 09 Feb. 2023. [Online]. Available: https://trv.banenor.no/wiki/Forside. [Accessed 12 Feb. 2023].

[9] NEK, “NEK EN 50163:2004, Railway applications, Supply voltages of traction systems,” Norwegian Electrotechnical Committee (NEK), 2004.

[10] LOVDATA, “Regulation on the implementation of Commission Regulation (EU) No. 1301/2014 of 18 November 2014 on the technical specifications for interoperability applicable to the subsystem "energy" in the European Union's railway system (TSI-ENE Regulation),” 19 Jun. 2015. [Online]. Available: https://lovdata.no/dokument/SF/forskrift/2015-06-19-720. [Accessed 20 Feb. 2023].

[11] LOVDATA, “Regulations on electrical supply facilities [Original title in Norwegian: Forskrift om elektriske forsyningsanlegg, FEF],” 20 Dec. 2005. [Online]. Available: https://lovdata.no/dokument/SF/forskrift/2005-12-20-1626. [Accessed 20 Feb. 2023].

[12] Bane NOR, “Textbooks in railway engineering: Contact lines [Original title in Norwegian: Lærebøker i jernbaneteknikk: Kontaktledningsanlegg],” 25 Mar. 2021. [Online]. Available: https://www.jernbanekompetanse.no/wiki/Kontaktledningsanlegg. [Accessed 15 Feb. 2023].

[13] NEK, “NEK 900:2023 Electric railway installations,” Norwegian Electrotechnical Committee (NEK), 2023.

[14] COWI, “Electric traction power supply, Short-circuit dimensioning for components connected to the 15 kV network [Original title in Norwegian: Banestrømforsyning, Kortslutningsdimensjonering for komponenter tilknyttet 15 kV nettet],” Bane NOR, 2007.

[15] NEK, “NEK EN 50121 (5 parts) Railway applications, Electromagnetic compatibility,” Norwegian Electrotechnical Committee (NEK), 2016-2017.

[16] Bane NOR, “Textbooks in railway engineering: Electric traction power supply [Original title in Norwegian: Lærebøker i jernbaneteknikk: Banestrømforsyning],” 03 Oct. 2018. [Online]. Available:

https://www.jernbanekompetanse.no/wiki/Banestr%C3%B8mforsyning. [Accessed 15 Feb. 2023].

[17] Kiessling F., Puschmann R., Schmieder A., and Schneider E., Contact Lines for Electric Railways: Planning, Design, Implementation, Maintenance, Third edition, Erlangen, 2018.

[18] Bane NOR, “Bane NOR's Technical specifications, Overhead Contact Lines [Original title in Norwegian: Bane NORs tekniske spesifikasjoner, Kontaktledning],” 16 Nov. 2021. [Online]. Available: https://trv.banenor.no/ts/Kontaktledning. [Accessed 17 Feb. 2023].

[19] Sture, P., Textbook for Overhead Contact Lines Engineers, Part 2 [Original title in Norwegian: Lærebok for Kontaktledningsingeniører, Del 2], Nesodden: NSB Baneteknisk kontor, 1993.

[20] Høidalen, H. Kr., Electromagnetic coexistence in railway facilities [Original title in Norwegian: Elektromagnetisk sameksistens i Jernbaneanlegg], Trondheim: NTNU - Norwegian University of Science and Technology, 2006.

[21] Ogunsola A. and Mariscotti A., Electromagnetic Compatibility in Railways, Analysis and Management, vol. 168, Berlin: Springer, 2013.

[22] NEK, “NEK EN 50522:2022, Earthing of power installations exceeding 1 kV a.c.,” Norwegian Electrotechnical Committee (NEK), 2022.

[23] Carson, J. R., “Wave Propagation in Overhead Wires with Ground Return,” Bell System Technical Journal 5, Page 539-554., 04 Oct. 1926. [Online]. Available: https://archive.org/details/bstj5-4-539/page/n3/mode/2up?view=theater. [Accessed 15 Mar. 2023].

[24] Bane NOR, “Technical report, Power supply, OCL Design S20 and S25, Verification of conformity with TSIs,” Bane NOR, 2016.

[25] NEK, “NEK EN 50149:2012, Railway applications, Fixed installations, Electric traction, Copper and copper alloy grooved contact wires,” Norwegian Electrotechnical Committee (NEK), First edition, 2012.

[26] NS, “NS-EN 13674-1, Railway applications – Track – Rails – Part 1:Vignole railway rails 46kg/m and above,” Norwegian Standard - NS, 2011.

[27] Storset, K., “Current distribution, impedance and field in NSB's overhead contact line system, [Original title in Norwegian: Strømfordeling, impedanser og felt i NSBs kontaktledningsanlegg],” NTH - The Norwegian Technical University, Trondheim, 1995.

[28] NEK, “NEK, EN 50182:2001, Conductors for overhead lines - Round wire concentric lay stranded conductors,” Norwegian Electrotechnical Committee (NEK), 2001.

10 Appendices

Appendix 1: Design of BT and AT systems

Appendix 2: Data of booster transformer and autotransformer

Appendix 3: Parameter arrangement of the BTRC and AT systems

Appendix 4: BTRC system model in ATPDraw

Appendix 5: AT system model in ATPDraw

Appendix 6: Data of LCC template for the BTRC and AT systems in ATPDraw

Appendix 7: Verification of series impedance of the BTRC and AT systems

Appendix 8: Results for the number of LCC components test

Appendix 9: Results of Case Study 3 during short circuit (t = 0.3 s)

Appendix 10: BTRC model_3km.acp [External file]

Appendix 11: BTRC model_6km.acp [External file]

Appendix 12: AT model_12km.acp [External file]

Appendix 13: AT model_14km.acp [External file]

Appendix 1: Design of BT and AT systems

System A: The overhead contact line with running rails as return conductors. This system is without booster transformers. The red arrows in the figure below indicate the path of the return current.

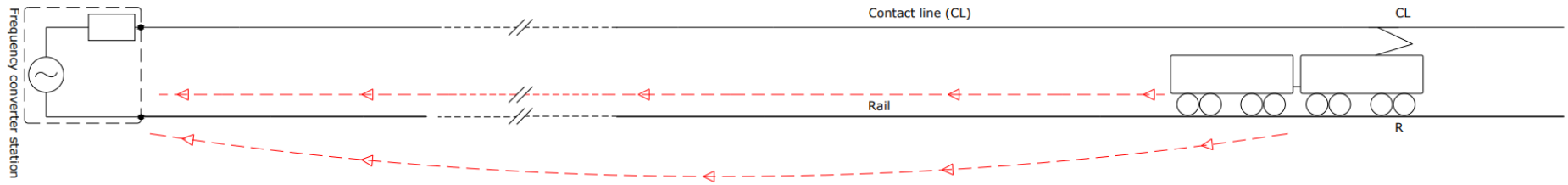

Electric system Design A. Figure adapted from [8].

System B: The overhead contact line with booster transformers and running rails as return conductors. The red arrows in the figure below indicate the path of the return current.

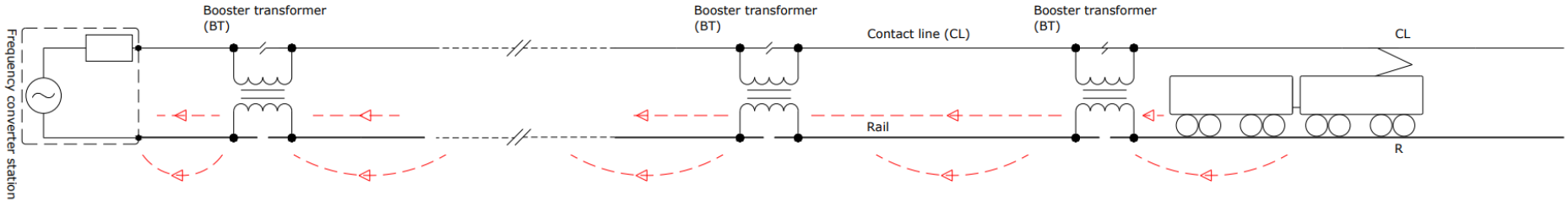

Electric system Design B. Figure adapted from [8].

System D: The overhead contact line with booster transformers with 0-field and return conductor. The red arrows in the figure below indicate the path of the return current.

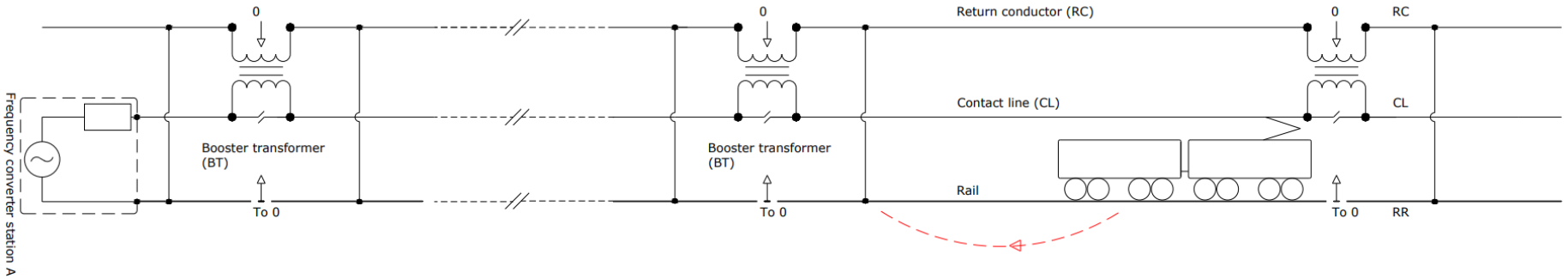

Electric system Design D. Figure adapted from [12].

System F: Autotransformer system with a negative feeder (NF). The red arrows in the figure below indicate the path of the return current.

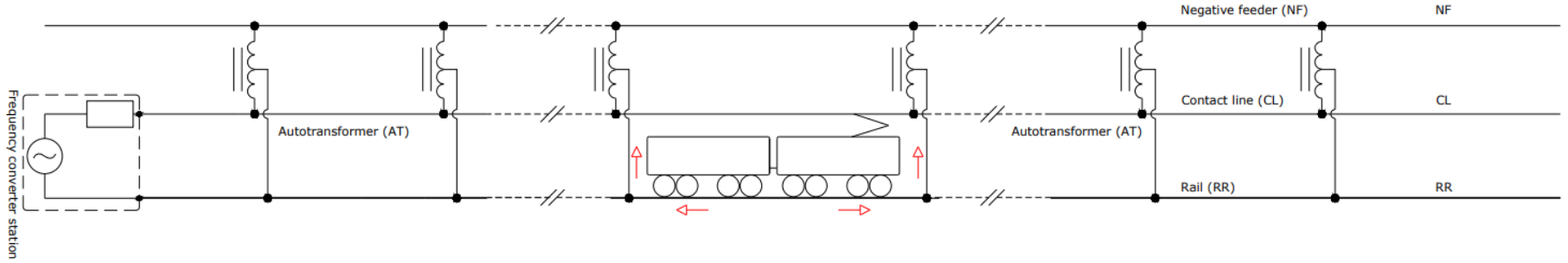

Electric system Design F. Figure adapted from [1].

Appendix 2: Data of booster transformer and autotransformer

Booster transformer (nominal current 800 A)	Autotransformer
Rated power: 95 kVA	Rated power: 5000 KVA (5 MVA)
Primary winding rated voltage:119 V	Primary winding rated voltage: 33000 V
Secondary winding rated voltage: 119 V	Secondary winding rated voltage: 16500 V
Frequency: 16.67 Hz	Frequency: 16.67 Hz
Connection: IIin0	Connection: Ia0
Cooling method: ONAN	Cooling method: ONAN
Load losses P_k: 7012 W	Load losses P_k: 10.6 kW
No-load losses P_0: 40 W	No-load losses P_0: 2.6 kW
Short circuit impedance Z_k: 18.2 %	Short circuit impedance Z_k: 0.4 %

Appendix 3: Parameter arrangement of the BTRC and AT systems

These figures are based on values that are given in the technical report [24].

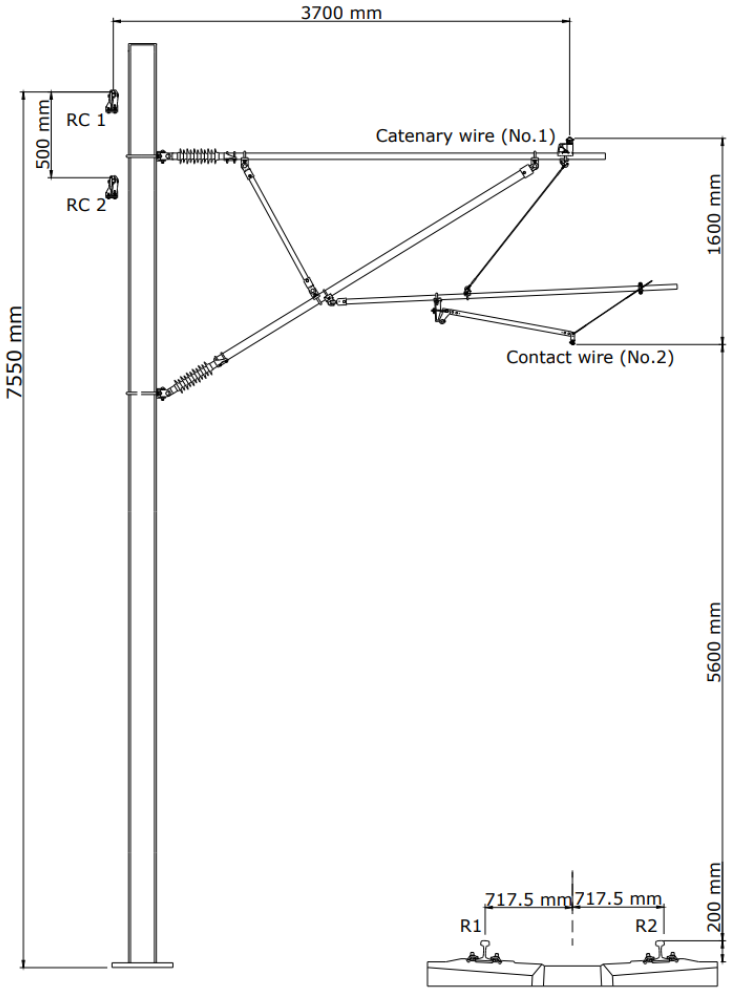

OCL pole of the BTRC system.

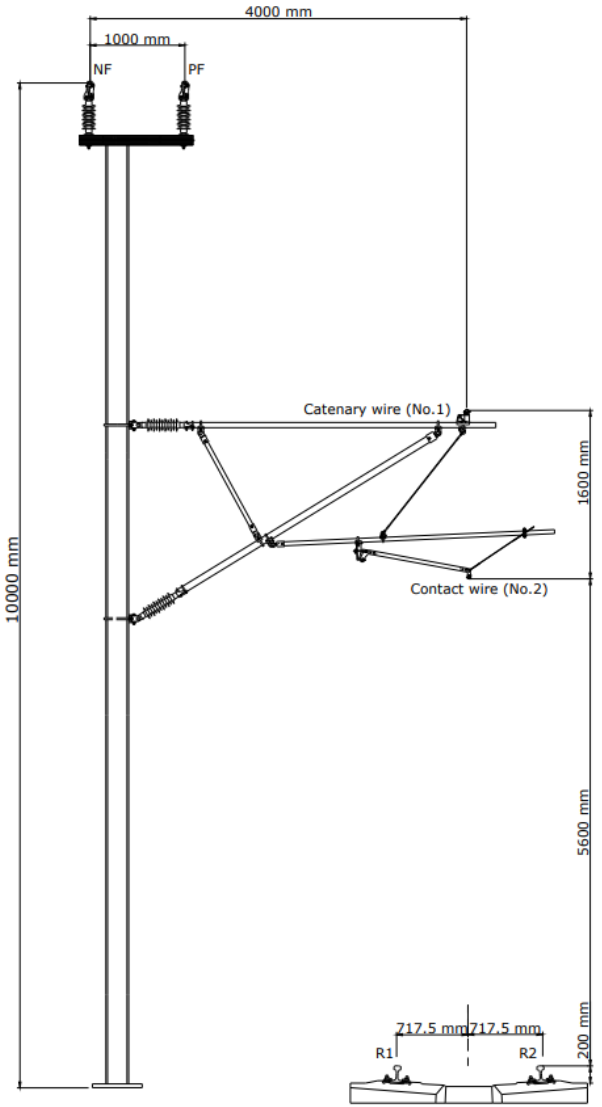

OCL pole of the AT system.

Appendix 4: BTRC system model in ATPDraw

Note: The figure below does not show the entire model that's simulated in ATPDraw. The model is trimmed to fit the page size of the report.

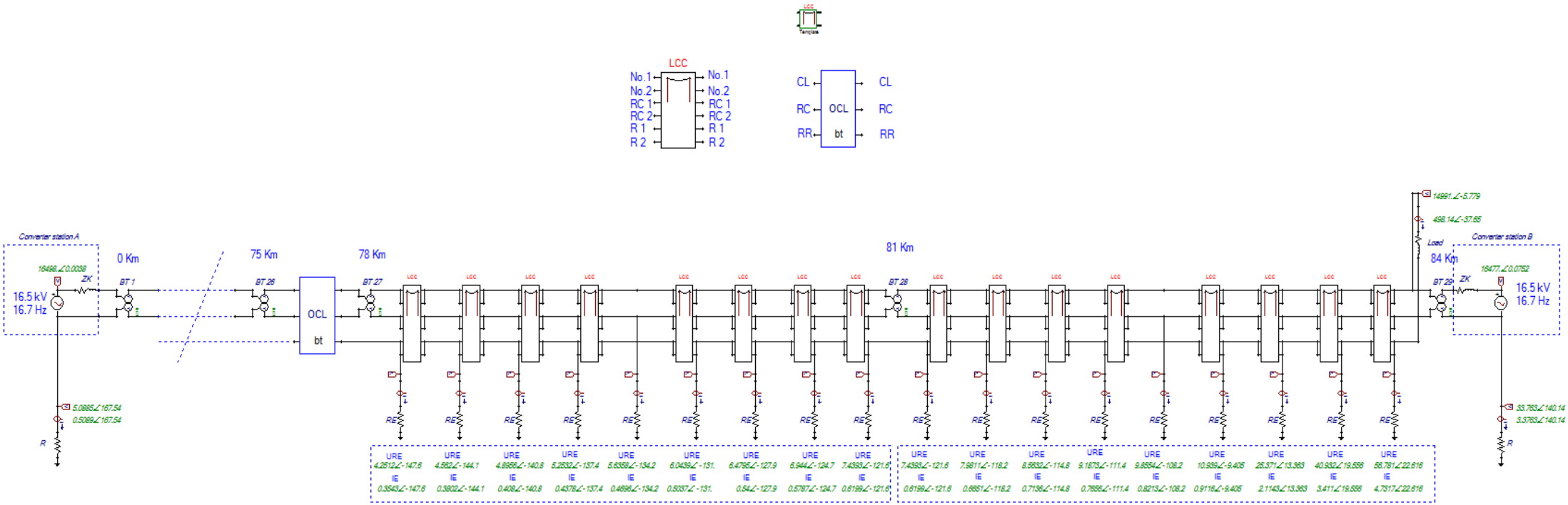

Appendix 5: AT system model in ATPDraw

Note: The figure below does not show the entire model that's simulated in ATPDraw. The model is trimmed to fit the page size of the report.

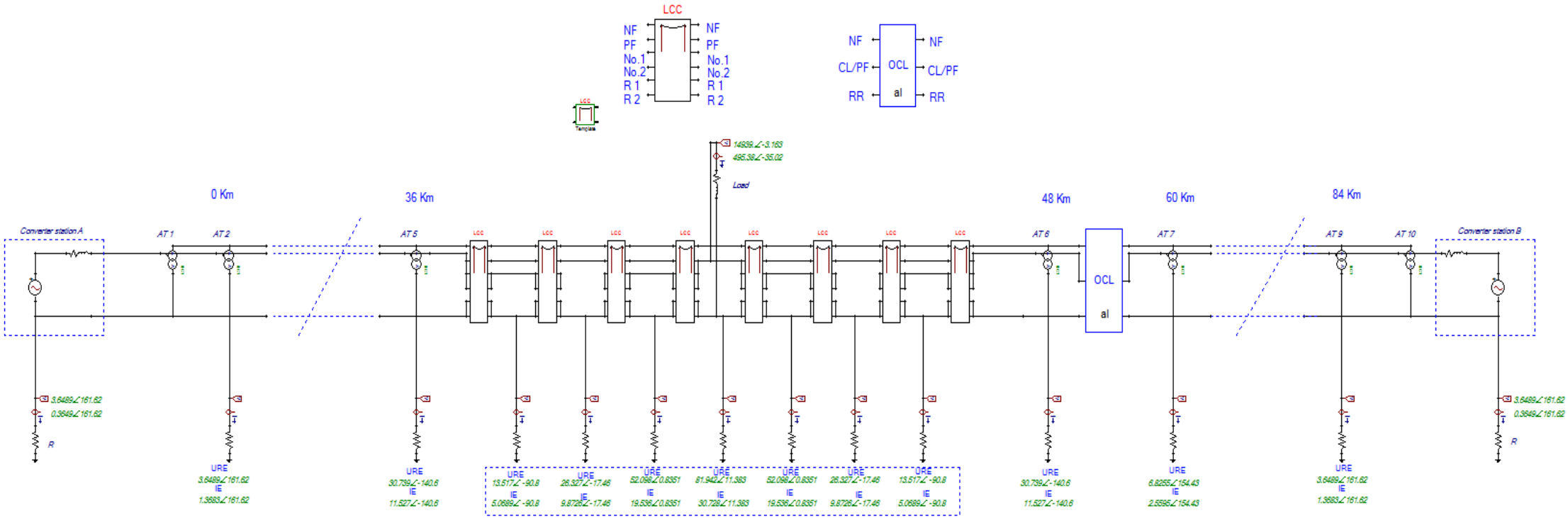

Appendix 6: Data of LCC template for the BTRC and AT systems in ATPDraw

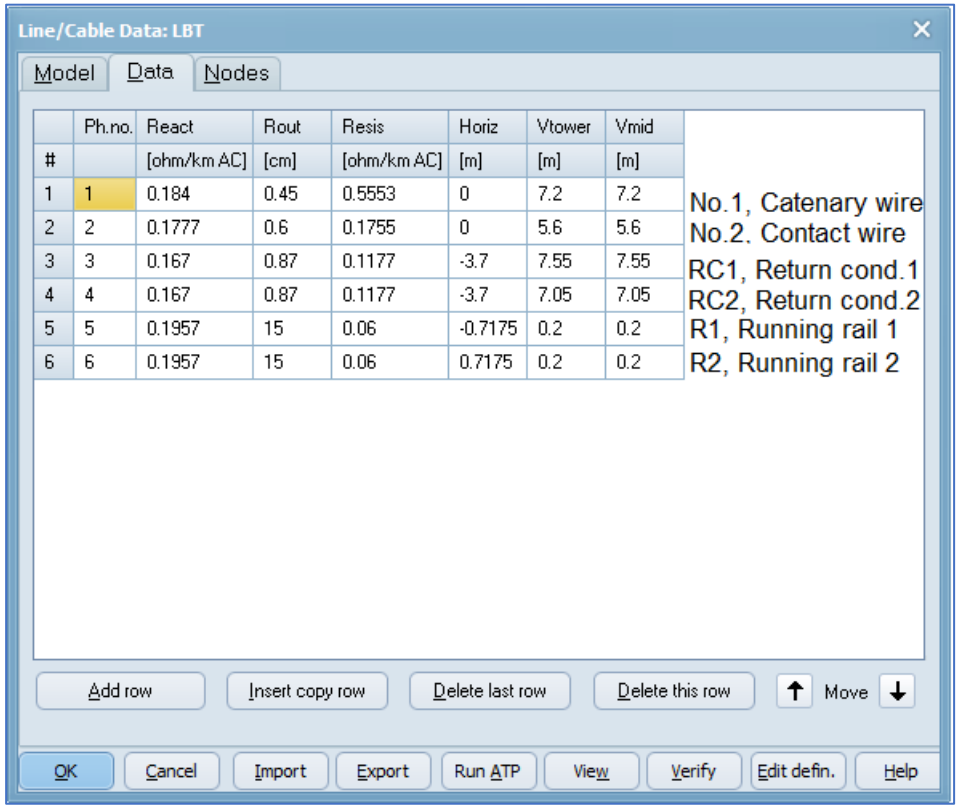

#	Ph.no.	React [ohm/km AC]	Rout [cm]	Resis [ohm/km AC]	Horiz [m]	Vtower [m]	Vmid [m]	
1	1	0.184	0.45	0.5553	0	7.2	7.2	No.1, Catenary wire
2	2	0.1777	0.6	0.1755	0	5.6	5.6	No.2. Contact wire
3	3	0.167	0.87	0.1177	-3.7	7.55	7.55	RC1, Return cond.1
4	4	0.167	0.87	0.1177	-3.7	7.05	7.05	RC2, Return cond.2
5	5	0.1957	15	0.06	-0.7175	0.2	0.2	R1, Running rail 1
6	6	0.1957	15	0.06	0.7175	0.2	0.2	R2, Running rail 2

Data of LCC template for BTRC system.

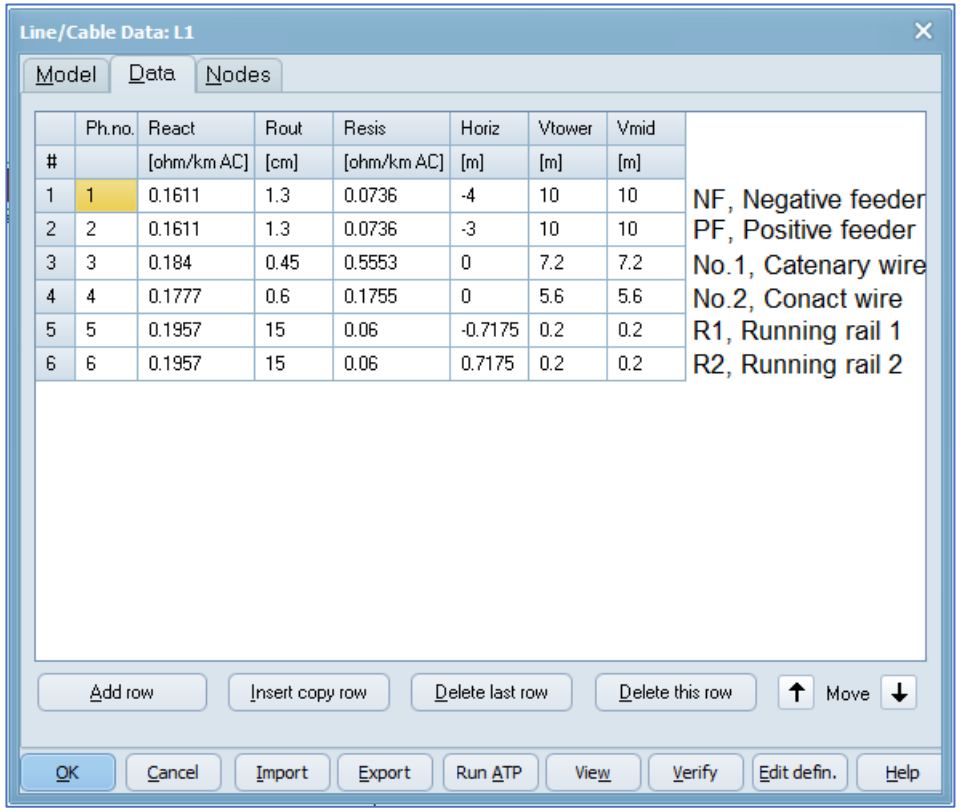

#	Ph.no.	React [ohm/km AC]	Rout [cm]	Resis [ohm/km AC]	Horiz [m]	Vtower [m]	Vmid [m]	
1	1	0.1611	1.3	0.0736	-4	10	10	NF, Negative feeder
2	2	0.1611	1.3	0.0736	-3	10	10	PF, Positive feeder
3	3	0.184	0.45	0.5553	0	7.2	7.2	No.1, Catenary wire
4	4	0.1777	0.6	0.1755	0	5.6	5.6	No.2, Conact wire
5	5	0.1957	15	0.06	-0.7175	0.2	0.2	R1, Running rail 1
6	6	0.1957	15	0.06	0.7175	0.2	0.2	R2, Running rail 2

Data of LCC template for AT system.

Appendix 7: Verification of series impedance of the BTRC and AT systems

The series impedance of OCL parameters are verified in ATPDraw using a *current source, LCC template* component, and *LCC section* component. The applied current from the current source is 1 A. By adjusting the values of *React*, *Rout*, and *Resis* in the *LCC template* component, the simulated results matched the calculated series impedance, as shown in the table below. The calculated equivalent series impedance is calculated by:

$$Z_{eq} = \frac{U_1}{I_1 + I_2} = \frac{Z_{11} \cdot Z_{22} - Z_{12}^2}{Z_{11} + Z_{22} - 2 \cdot Z_{12}} \qquad (10\text{-}1)$$

Z_{eq}: The equivalent impedance

Z_{11}: Self-impedance of the first wire or conductor

Z_{22}: Self-impedance of the second wire or conductor

Z_{12}: The mutual/coupling impedance

Results of calculated and simulated series impedance of OCL parameters.

Parameter	**Calculation [ref. Table 4-5, and equation (10-1)]**		**Simulation [ref. Figures below]**	
	Series self-impedance	**Equivalent impedance**	**Series self-impedance**	**Equivalent impedance**
Catenary wire (No.1)	0.572 + j0.308	0.155 + j0.256	0.5720 + j0.3086	0.15449 + j0.256
Contact wire (No.2)	0.192 + j0.302		0.1919 + j0.3022	
Return conductor (RC1)	0.134 + j0.291	0.0753 +j0.2475	0.1341 + j0.2910	0.0753 + j0.2478
Return conductor (RC2)	0.134 + j0.291		0.1341 + j0.2910	
Positive feeder (PF)	0.0905 + j0.286	0.0535 +j0.2375	0.0902 + j0.2860	0.0532 + j0.2371
Negative feeder (NF)	0.0905 + j0.286		0.0902 + j0.2860	
Running rails (R1)	0.076 + j0.320	0.0464 + j0.251	0.0764 + j0.3200	0.0464 + j0.2507
Running rails (R2)	0.076 + j0.320		0.0764 + j0.3200	

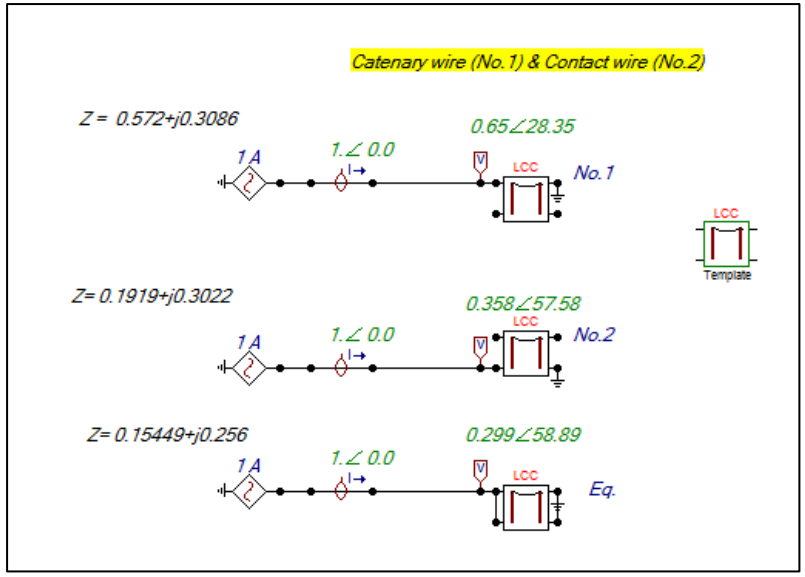
Catenary wire (No.1) & Contact wire (No.2)
Z = 0.572+j0.3086
0.65∠28.35
1 A
1.∠ 0.0
LCC
No.1
LCC
Template
Z= 0.1919+j0.3022
0.358∠57.58
No.2
Z= 0.15449+j0.256
0.299∠58.89
Eq.

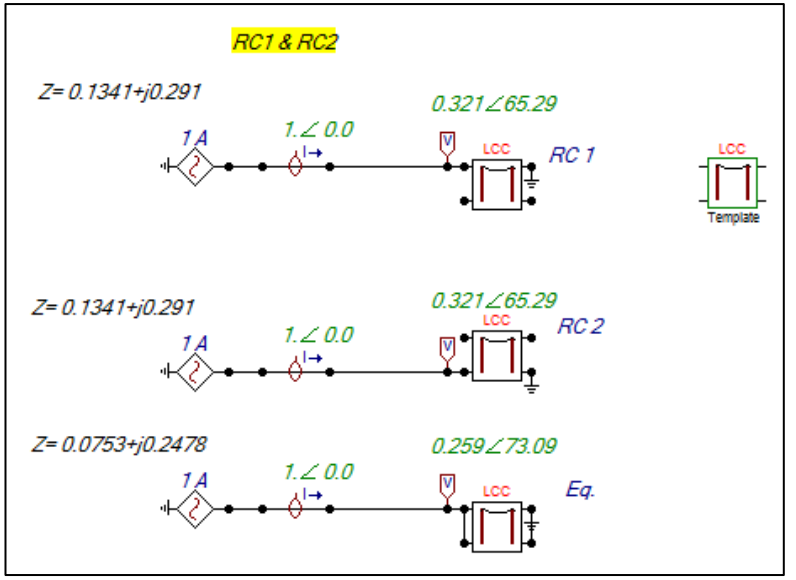
RC1 & RC2
Z= 0.1341+j0.291
0.321∠65.29
RC 1
Template
Z= 0.1341+j0.291
0.321∠65.29
RC 2
Z= 0.0753+j0.2478
0.259∠73.09
Eq.

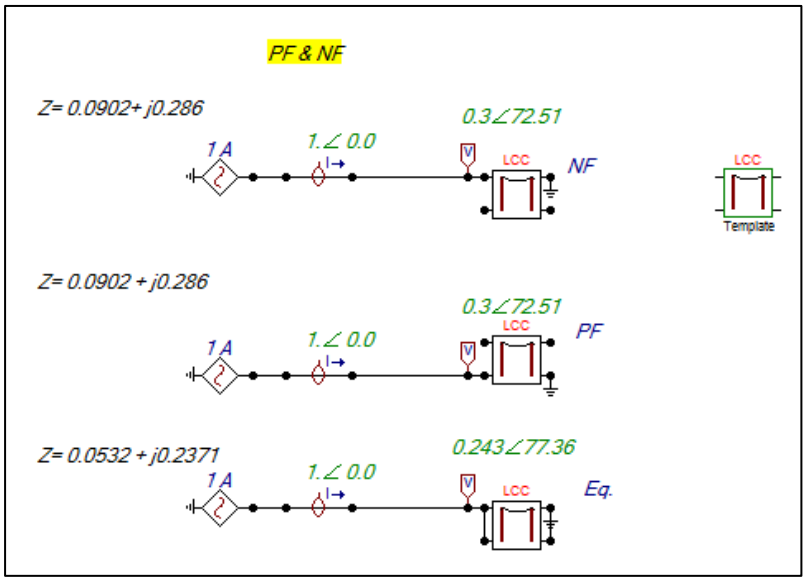
PF & NF
Z= 0.0902+ j0.286
0.3∠72.51
NF
Template
Z= 0.0902 + j0.286
PF
Z= 0.0532 + j0.2371
0.243∠77.36
Eq.

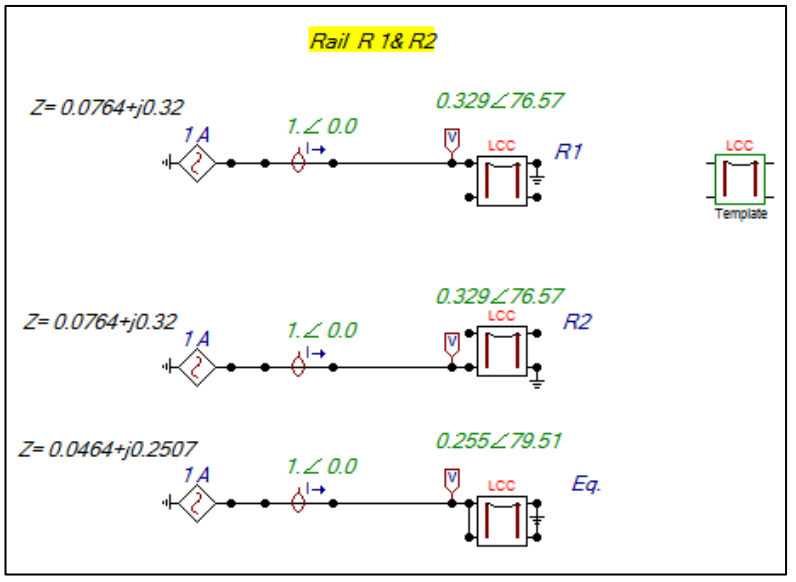
Rail R 1& R2
Z= 0.0764+j0.32
0.329∠76.57
R1
Template
R2
Z= 0.0464+j0.2507
0.255∠79.51
Eq.

Appendix 8: Results for the number of LCC components test

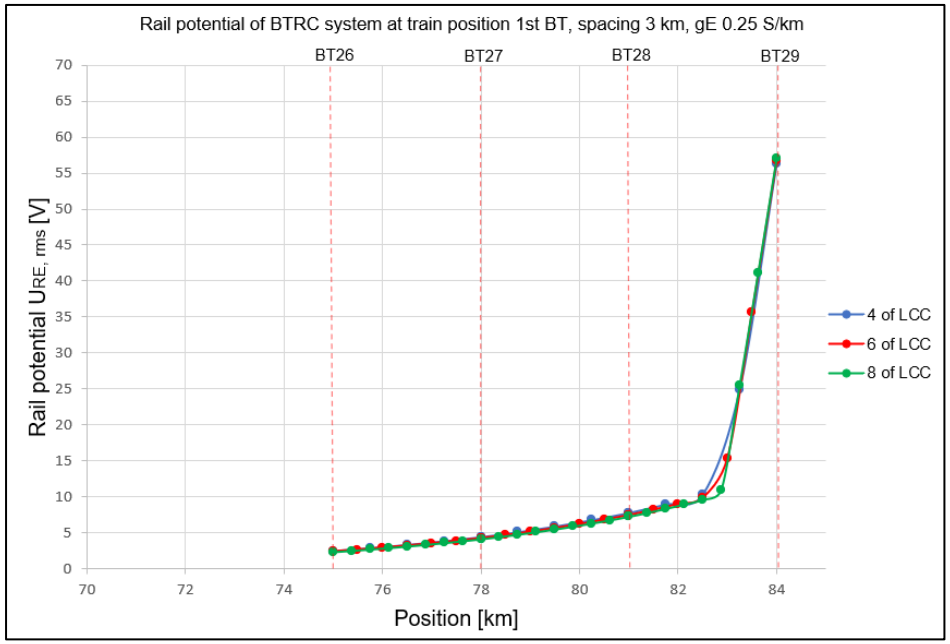

Rail potential of BTRC system for 4, 6, and 8 of LCC.

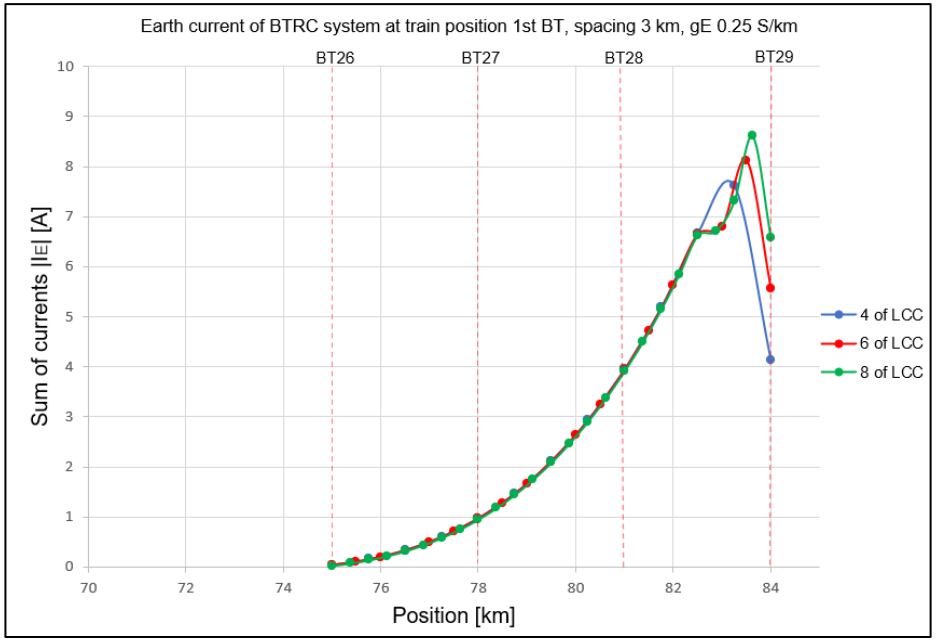

Earth current of BTRC system for 4, 6, and 8 of LCC.

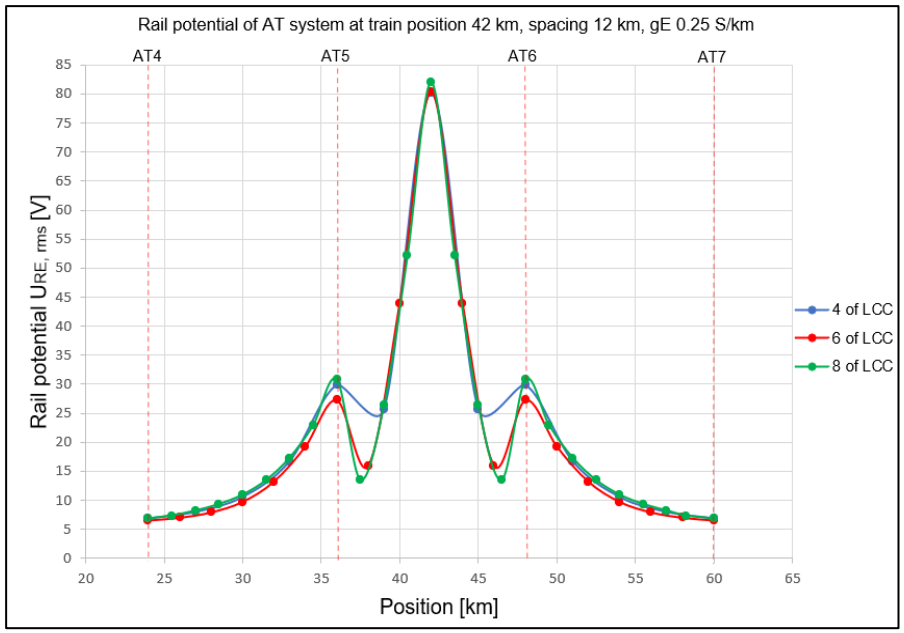

Rail potential of AT system for 4, 6, and 8 of LCC.

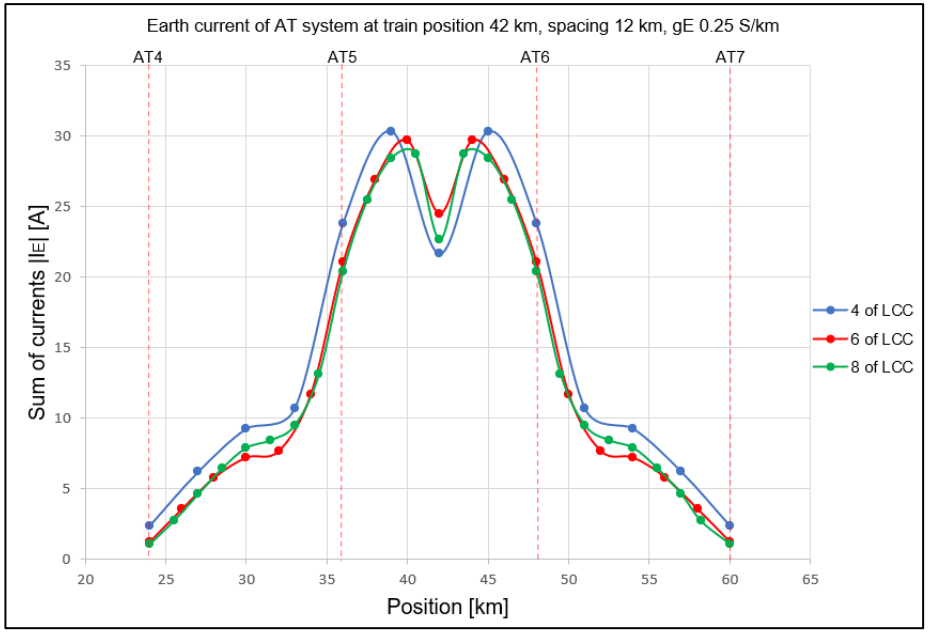

Earth current of AT system for 4, 6, and 8 of LCC.

Appendix 9: Results of Case Study 3 during short circuit (t = 0.3 s)

A9.10.1 Rail potential and Earth current of BTRC system (3 km) during s.c. (t = 0.3 s)

The results of rail potential and earth current for the BTRC system with 3 km spacing during a short circuit (t = 0.3 s) are shown in Figure A9-10-1 and Figure A9-10-2, respectively. The load (short circuit) is at the first or last booster transformer. The levels of rail potential and earth current are studied from 75 km at BT26 to the load (short circuit) location at 84 km at BT29.

The highest rail potential and earth current from 75 km to 81 km are lower than 140 V and 350 A, respectively. The rail potential levels increase at the connection between the contact line and running rails (Bond) at 82,5 km and decrease immediately behind the bond, then become the highest at the load (short circuit) location at 84 km. The rise in rail potential at the bond at 82,5 km can be noticed for g_E levels of 0.75 S/km - 2 S/km. The levels of earth current reach their highest levels in the section between BT28 at 81 km and BT29 at 84 km.

As shown in Table A9-10-1, rail potential levels decrease while earth current levels increase when g_E levels vary from 0.05 S/km to 2 S/km. The $U_{RE,\,max}$ is 1062.8 V and the $I_{E,\,max}$ is 34.89 A at g_E = 0.05 S/km, while the $U_{RE,\,max}$ is 689.8 V and the $I_{E,\,max}$ is 793 A at g_E = 2 S/km.

Table A9-10-1: Maximum rail potential and earth current of BTRC, load at 1st BT for 3 km spacing, s.c. (t = 0.3 s).

Rail-to-earth leakage conductance (g_E) [S/km]	**Maximum rail potential ($U_{RE,\,max}$) [V] at 1st BT**	**Maximum earth current ($I_{E,\,max}$) [A] at 1st BT**
0.05	1062.80	34.89
0.25	943.42	89.48
0.75	830.06	307.98
1	793.20	417.87
2	689.80	793.00

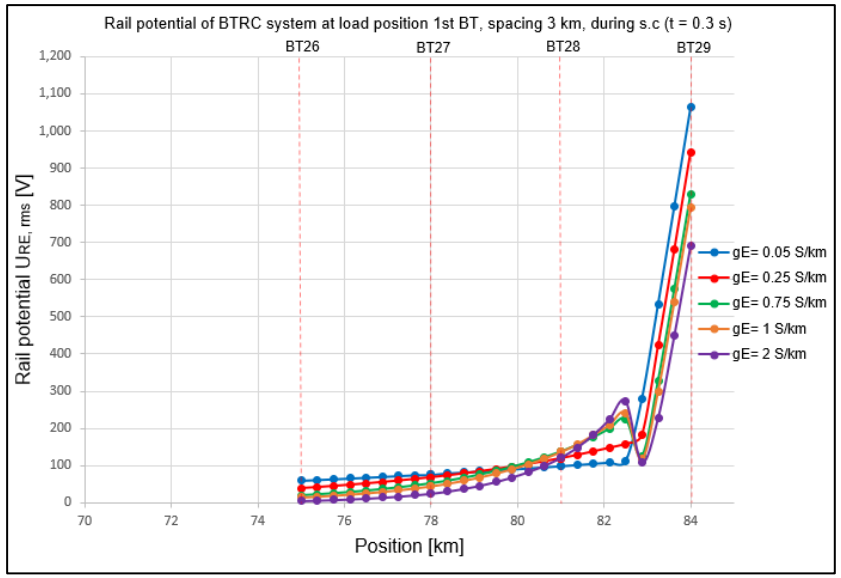

Figure A9-10-1: Rail potential at load position 1st BT, spacing 3 km, during s.c., t = 0.3 s.

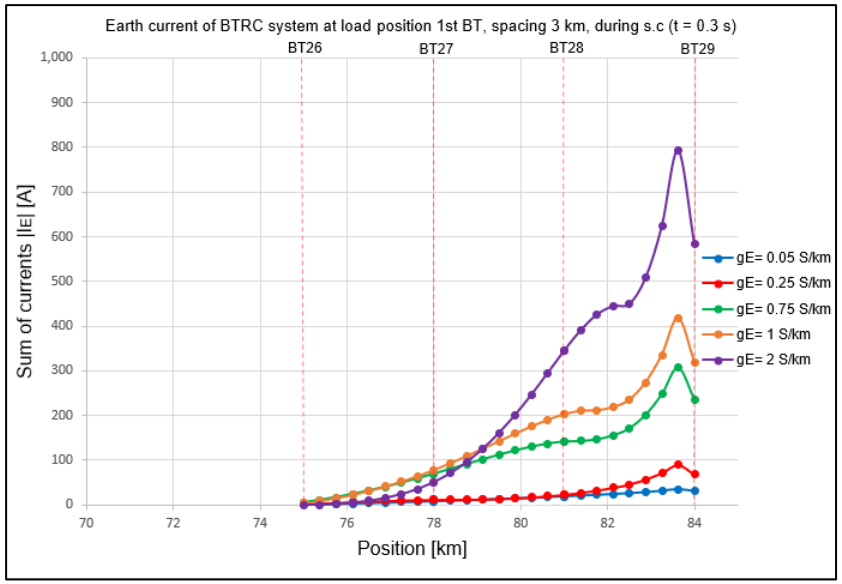

Figure A9-10-2: Earth current at load position 1st BT, spacing 3 km, during s.c., t = 0.3 s.

A9.10.2 Rail potential and Earth current of BTRC system (6 km) during s.c. (t = 0.3 s)

The results of rail potential and earth current for the BTRC system with 6 km spacing during a short circuit (t = 0.3 s) are shown in Figure A9-10-3 and Figure A9-10-4, respectively. The load (short circuit) is at the first or last booster transformer. The levels of rail potential and earth current are studied from 66 km at BT12 to the load (short circuit) location at 84 km at BT15.

The highest levels of rail potential and earth current from 66 km to 78 km are lower than 265 V and 410 A, respectively. The rail potential levels increase at the connection between the contact line and running rails (Bond) at 81 km and decrease immediately behind the bond, then become the highest at the load (short circuit) location at 84 km. The rise in rail potential at the bond at 81 km can be noticed for gE levels of 0.25 S/km - 2 S/km. The levels of earth current reach their highest levels in the section between BT14 at 78 km and BT15 at 84 km.

As shown in Table A9-10-2, rail potential levels decrease while earth current levels increase when gE levels vary from 0.05 S/km to 2 S/km. The $U_{RE,\,max}$ is 2005.5 V and the $I_{E,\,max}$ is 103.16 A at gE = 0.05 S/km, while the $U_{RE,\,max}$ is 897.43 V and the $I_{E,\,max}$ is 2075.36 A at gE = 2 S/km.

Table A9-10-2: Maximum rail potential and earth current of BTRC, load at 1st BT for 6 km spacing, s.c. (t = 0.3 s).

Rail-to-earth leakage conductance (gE) [S/km]	**Maximum rail potential ($U_{RE,\,max}$) [V] at 1st BT**	**Maximum earth current ($I_{E,\,max}$) [A] at 1st BT**
0.05	2005.50	103.16
0.25	1623.40	400.38
0.75	1264.90	1040.18
1	1159.10	1316.16
2	897.43	2075.36

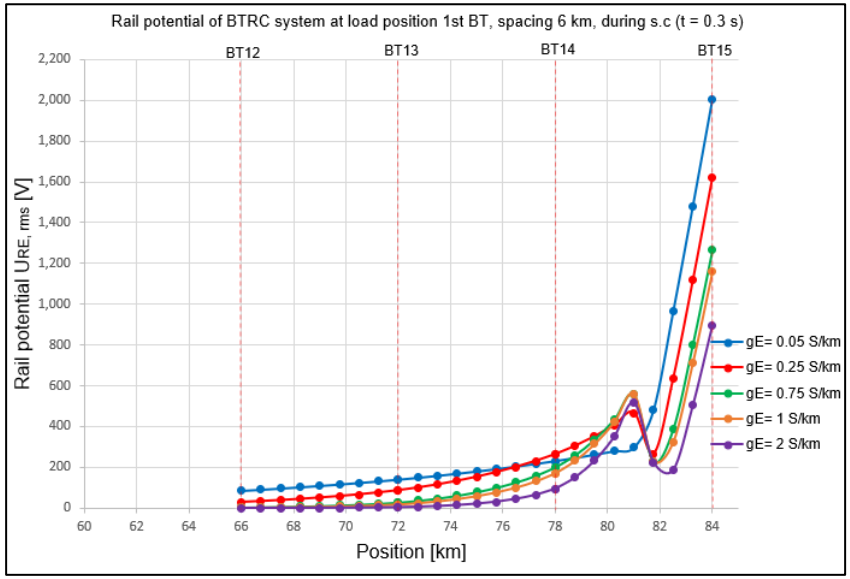

Figure A9-10-3: Rail potential at load position 1st BT, spacing 6 km, during s.c., t =0.3 s.

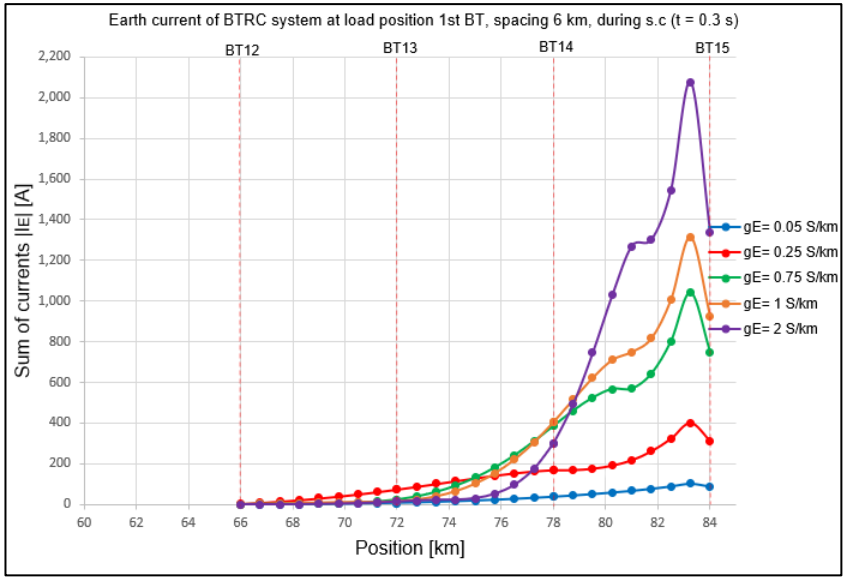

Figure A9-10-4: Earth current at load position 1st BT, spacing 6 km, during s.c., t =0.3 s.

A9.10.3 Rail potential and Earth current of AT system (12 km) during s.c. (t = 0.3 s)

The results of earth current and rail potential for the AT system with 12 km of spacing during a short circuit (t = 0.3 s) are shown in Figure A9-10-5 and Figure A9-10-6, respectively. The load (short circuit) is in the middle of the track line between two ATs at 42 km. The results are studied from 24 km at AT4 to 60 km at AT7.

The peaks of rail potential reach at AT5 and AT6, then become the highest at the load (short circuit) location (42 km). The earth current levels increase from 24 km and reach their highest levels immediately ahead and immediately behind the load (short circuit) location (42 km).

As shown in Table A9-10-3, rail potential levels decrease while earth current levels increase when g_E levels vary from 0.05 S/km to 2 S/km. The $U_{RE,\,max}$ is 1882.5 V and the $I_{E,\,max}$ is 153.6 A at g_E = 0.05 S/km, while the $U_{RE,\,max}$ is 559.08 V and the $I_{E,\,max}$ is 2229.65 A at g_E = 2 S/km.

Table A9-10-3: Maximum rail potential and earth current of AT, load at 42 km for 12 km spacing, s.c. (t = 0.3 s).

Rail-to-earth leakage conductance (g_E) [S/km]	**Maximum rail potential ($U_{RE,\,max}$) [V] at 42 km**	**Maximum earth current ($I_{E,\,max}$) [A] at 42 km**
0.05	1882.50	153.60
0.25	1324.20	740.22
0.75	904.38	1472.97
1	797.39	1724.62
2	559.08	2229.65

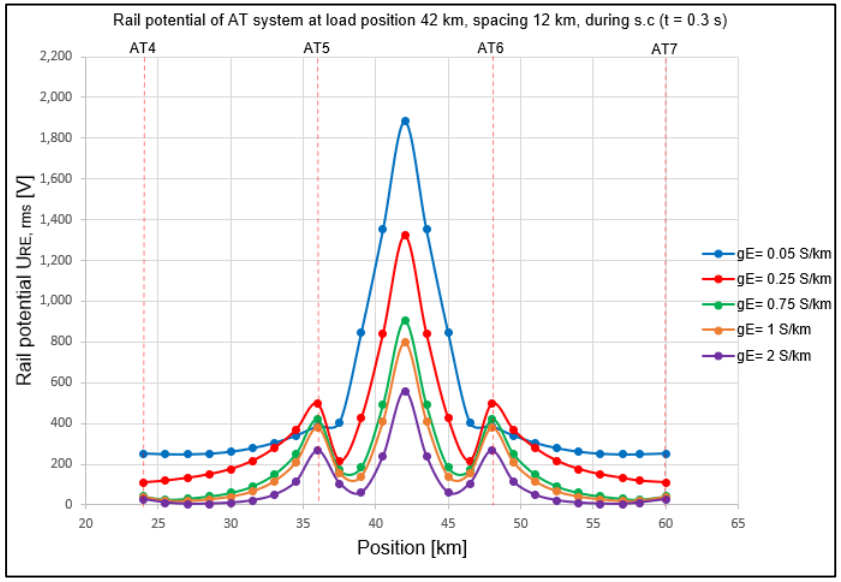

Figure A9-10-6: Rail potential at load position 42 km, spacing 12 km, during s.c., t = 0.3 s.

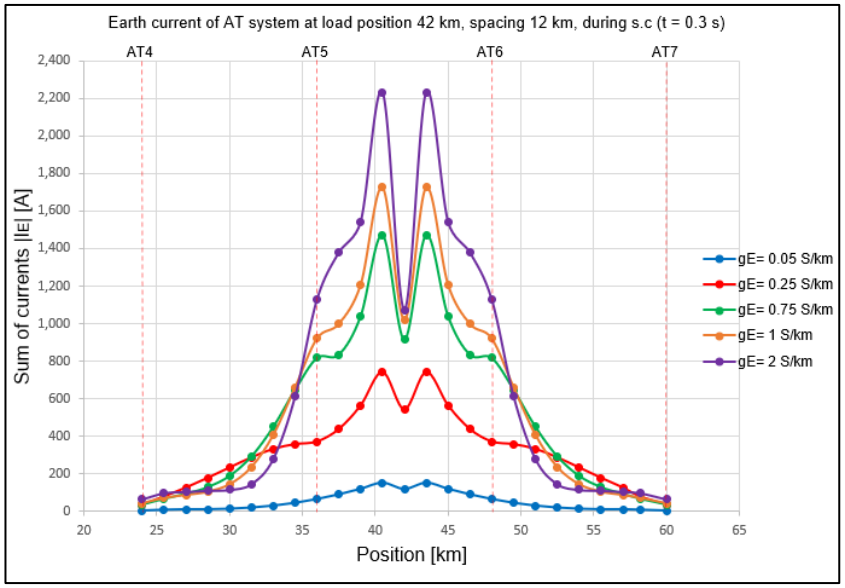

Figure A9-10-5: Earth current at load position 42 km, spacing 12 km, during s.c., t = 0.3 s.

A9.10.4 Rail potential and Earth current of AT system (14 km) during s.c. (t = 0.3 s)

The results of earth current and rail potential for the AT system with 14 km spacing during a short circuit (t = 0.3 s) are shown in Figure A9-10-7 and Figure A9-10-8, respectively. The load (short circuit) is almost in the middle of the track line between two ATs at 35 km. The results are studied from 14 km at AT3 to 56 km at AT6.

The peaks of rail potential reach at AT4 and AT5, then become the highest at the load (short circuit) location (35 km). The earth current levels increase from 14 km and reach their highest levels immediately ahead and immediately behind the load (short circuit) location (35 km).

As shown in Table A9-10-4, rail potential levels decrease while earth current levels increase when gE levels vary from 0.05 S/km to 2 S/km. The $U_{RE,\,max}$ is 2142.4 V and the $I_{E,\,max}$ is 209.74 A at gE = 0.05 S/km, while the $U_{RE,\,max}$ is 553.09 V and the $I_{E,\,max}$ is 2404.51 A at gE = 2 S/km.

Table A9-10-4: Maximum rail potential and earth current of AT, load at 35 km for 14 km spacing, s.c. (t = 0.3 s).

Rail-to-earth leakage conductance (gE) [S/km]	**Maximum rail potential ($U_{RE,\,max}$) [V] at 35 km**	**Maximum earth current ($I_{E,\,max}$) [A] at 35 km**
0.05	2142.40	209.74
0.25	1458.10	920.01
0.75	962.69	1814.26
1	840.31	2039.11
2	553.09	2404.51

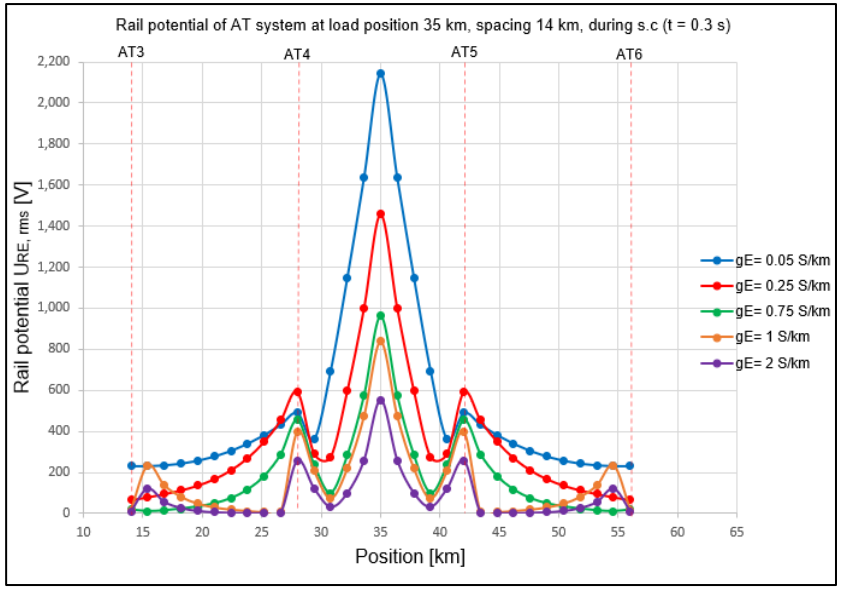

Figure A9-10-8: Rail potential at load position 35 km, spacing 14 km, during s.c., t = 0.3 s.

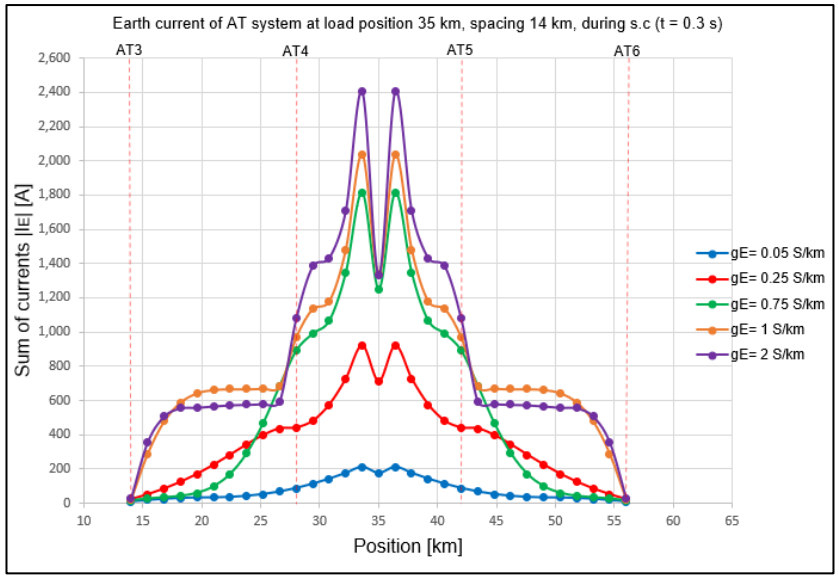

Figure A9-10-7: Earth current at load position 35 km, spacing 14 km, during s.c., t = 0.3 s.

NTNU
Norwegian University of
Science and Technology

BANE NOR